

AD-A051 717

NATIONAL BUREAU OF STANDARDS BOULDER COLO ELECTROMA--ETC F/G 9/1
SURVEYS OF ELECTROMAGNETIC FIELD INTENSITIES NEAR REPRESENTATIV--ETC(U)
DEC 77 E B LARSEN, J F SHAFER DOT-FA73WAI-388

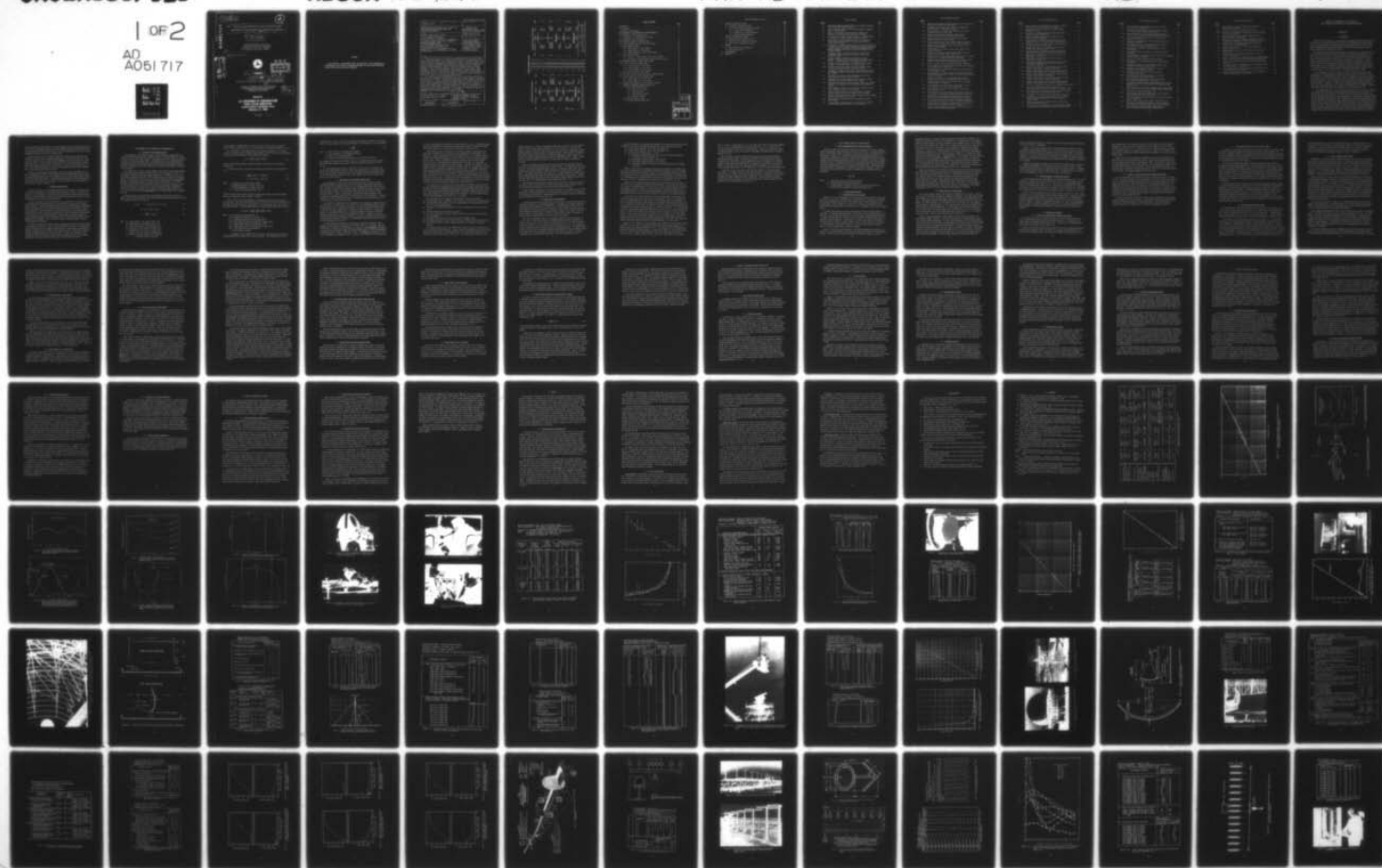
UNCLASSIFIED

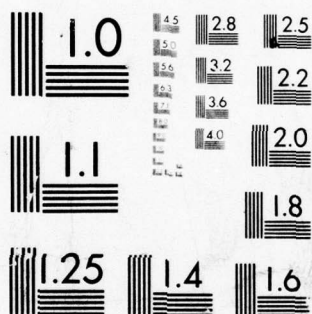
NBSIR-76-849

FAA-RD-77-179

NL

1 OF 2
AD
A051 717





18
19
FAA-RD-77-179

12

AD A051717

6
SURVEYS OF ELECTROMAGNETIC FIELD INTENSITIES NEAR
REPRESENTATIVE HIGHER-POWER FAA TRANSMITTING ANTENNAS

10
Ezra B./Larsen
John F./Shafer

Electromagnetics Division
Institute for Basic Standards
National Bureau of Standards
Boulder, Colorado 80302

14
NBSIR-76-849

AD NO. FILE COPY



DDC
RECEIVED
MAR 24 1978

11
Dec 1977

9
FINAL REPORT, 1974-1976

Under FAA Interagency Agreement DOT-FA73WAI-388

15

Document is available to the U.S. public through
the National Technical Information Service,
Springfield, Virginia 22161.

12
115p.

Prepared for
U.S. DEPARTMENT OF TRANSPORTATION
FEDERAL AVIATION ADMINISTRATION
Systems Research & Development Service
Washington, D.C. 20590

390 891

mt

NOTICE

This document is disseminated under the sponsorship of the Department of Transportation in the interest of information exchange. The United States Government assumes no liability for its contents or use thereof.

Technical Report Documentation Page

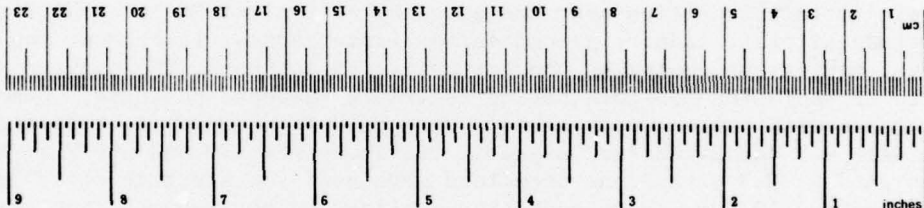
1. Report No. FAA-RD-77-179✓	2. Government Accession No.	3. Recipient's Catalog No.
4. Title and Subtitle SURVEYS OF ELECTROMAGNETIC FIELD INTENSITIES NEAR REPRESENTATIVE HIGHER-POWER FAA TRANSMITTING ANTENNAS	5. Report Date December 1977	6. Performing Organization Code Department of Commerce, NBS
7. Author(s) Ezra B. Larsen, John F. Shafer	8. Performing Organization Report No. NBSIR-76-849✓(12/76)	
9. Performing Organization Name and Address U. S. Department of Commerce National Bureau of Standards, Electromagnetics Division, Institute for Basic Standards Boulder, Colorado 80302	10. Work Unit No. (TRAIS)	11. Contract or Grant No. IAA- DOT-FA73WAI-388 <i>new</i>
12. Sponsoring Agency Name and Address U. S. Department of Transportation Federal Aviation Administration Systems Research and Development Service 2100-2nd St. S. W., Washington, D. C. 20590	13. Type of Report and Period Covered FINAL REPORT - Phase III Work performed during period 1974 to 1976	14. Sponsoring Agency Code FAA/SRDS - ARD-60
15. Supplementary Notes		
<p>16. Abstract</p> <p>The National Bureau of Standards has completed surveys of electromagnetic field intensities near the antennas of typical FAA transmitters. These include aircraft radars, ground surveillance radars, instrument landing systems, navigation equipment and communication antennas. The surveys were made with rf radiation monitors having isotropic response patterns. Commercial monitors with thermocouple sensors were used to measure electric fields between 0.5 and 24 GHz and magnetic fields between 10 and 300 MHz. Probes designed at NBS with diode detectors were used for electric field between 100 kHz and 10 GHz. These radiation monitors cannot measure (accurately) the pulse-peak field of a radar nor the field of a scanning antenna; therefore, most of the radar surveys involved fixed antennas.</p> <p>The intensity in the direct beam of air route surveillance radars was greater than 10 mW/cm² at distances within about 14 meters from the antennas. The intensity of airport surveillance radars was above 10 mW/cm² at distances within 15 meters, except for the newer ASR-8 model. The direct beam of aircraft radars exceeded 10 mW/cm² at distances ranging from 2 to 7 meters. If the time-averaging effect for antenna scanning is taken into consideration, these field values would be greatly reduced. Also, the near-zone beams of FAA antennas are not normally accessible to personnel. In accessible areas the measured fields were generally less than 1 mW/cm².</p>		
17. Key Words Antenna; Calibration; Electromagnetic field intensity; Field strength measurement; Radar; rf probe.	18. Distribution Statement Document is available to the public through the National Technical Information Service, Springfield, Virginia 22161.	
19. Security Classif. (of this report) UNCLASSIFIED	20. Security Classif. (of this page) UNCLASSIFIED	21. No. of Pages 22. Price

METRIC CONVERSION FACTORS

Approximate Conversions to Metric Measures

Symbol	When You Know	Multiply by	To Find	Symbol
LENGTH				
in	inches	2.5	centimeters	cm
ft	feet	30	meters	m
yd	yards	0.9	kilometers	km
mi	miles	1.6		
AREA				
in ²	square inches	6.5	square centimeters	cm ²
ft ²	square feet	0.09	square meters	m ²
yd ²	square yards	0.8	square meters	m ²
mi ²	square miles	2.6	square kilometers	km ²
	acres	0.4	hectares	ha
MASS (weight)				
oz	ounces	28	grams	g
lb	pounds	0.45	kilograms	kg
	short tons (2000 lb)	0.9	tonnes	t
VOLUME				
tsp	teaspoons	5	milliliters	ml
Tbsp	tablespoons	15	milliliters	ml
fl oz	fluid ounces	30	milliliters	ml
c	cups	0.24	liters	l
pt	pints	0.47	liters	l
qt	quarts	0.95	liters	l
gal	gallons	3.8	liters	l
ft ³	cubic feet	0.03	cubic meters	m ³
yd ³	cubic yards	0.76	cubic meters	m ³
TEMPERATURE (exact)				
°F	Fahrenheit temperature	5/9 (after subtracting 32)	Celsius temperature	°C

Symbol	When You Know	Multiply by	To Find	Symbol
LENGTH				
mm	millimeters	0.04	inches	in
cm	centimeters	0.4	inches	in
m	meters	3.3	feet	ft
km	kilometers	1.1	yards	yd
		0.6	miles	mi
AREA				
cm ²	square centimeters	0.16	square inches	in ²
m ²	square meters	1.2	square yards	yd ²
km ²	square kilometers	0.4	square miles	mi ²
ha	hectares (10,000 m ²)	2.5	acres	
MASS (weight)				
g	grams	0.035	ounces	oz
kg	kilograms	2.2	pounds	lb
t	tonnes (1000 kg)	1.1	short tons	
VOLUME				
ml	milliliters	0.03	fluid ounces	fl oz
l	liters	2.1	pints	pt
l	liters	1.06	quarts	qt
m ³	cubic meters	0.26	gallons	gal
m ³	cubic meters	35	cubic feet	ft ³
		1.3	cubic yards	yd ³
TEMPERATURE (exact)				
°C	Celsius temperature	9/5 (then add 32)	Fahrenheit temperature	°F



*1 in. = 2.54 (exactly). For other exact conversions and more detailed tables, see NBS Misc. Publ. 286, Units of Weights and Measures, Price \$2.25, SD Catalog No. C13.10-286.

TABLE OF CONTENTS

	<u>Page</u>
1. INTRODUCTION	1
1.1 Background	1
1.2 Objectives and Approach	2
2. ELECTROMAGNETIC FIELD PARAMETERS AND INSTRUMENTATION	3
2.1 Discussion of Field Strength Units	3
2.2 Description of the Radiation Monitors Used	5
2.3 Calibration of the Instruments	7
3. FIELD INTENSITY SURVEYS OF AIRCRAFT RADARS	10
3.1 Time Averaging Effect Due to Antenna Scanning	10
3.2 X-Band Airborne Radars	10
3.2.1 RDR-1B Radar On a DC-3 Airplane	10
3.2.2 RDR-1E Radar on a DC-9 Airplane	11
3.2.3 RDR-1200 Radar on a Sabre Liner Airplane	12
3.3 C-Band Airborne Radars	12
3.3.1 AVQ-10 on a 720E Airplane, Slotted Array Antenna	12
3.3.2 AVQ-10 on a Turboprop Airplane, Parabolic Dish Antenna	13
4. FIELD INTENSITY SURVEYS OF GROUND RADAR SYSTEMS	14
4.1 Airport Surveillance Radars (ASR)	14
4.1.1 Field Intensity of ASR-4 Radars	15
4.1.2 Field Intensity of ASR-7 Radars	16
4.1.3 Field Intensity of an ASR-8 Radar	16
4.2 Air Route Surveillance Radars (ARSR)	17
4.3 Air Traffic Control Beacon Interrogator (ATCBI) and Omni	19
4.4 Airport Surface Detection Equipment (ASDE)	19
4.4.1 ASDE-1 Radar in the 14 GHz Band	20
4.4.2 ASDE-2 Radars in the 24 GHz Band	20
4.5 Near- Z one Gain Reduction of Large Aperture Antennas	21
5. SURVEYS OF INSTRUMENT LANDING SYSTEMS (ILS)	23
5.1 VHF Localizer Antenna Arrays	23
5.1.1 Eight-loop Localizer	23
5.1.2 V-ring Localizer	24
5.1.3 Traveling-wave Localizer	25
5.1.4 Waveguide Localizer	25
5.2 UHF Glide-slope Antennas	26
5.3 Microwave Landing Systems (MLS)	27

JUSTIFICATION		
BY		
DISTRIBUTION/AVAILABILITY CODES		
Dist.	AVAIL	and/or SPECIAL
A		

TABLE OF CONTENTS (continued)

	<u>Page</u>
6. SURVEYS OF NAVIGATION SYSTEMS	28
6.1 VHF Omnidirectional Range (VOR)	28
6.2 Tactical Air Navigation (TACAN) and VORTAC	29
6.2.1 Ground TACAN Transmissions	30
6.2.2 X-Radiation of a TACAN Transmitter	31
6.2.3 Airborne TACAN Transmissions	31
7. SURVEYS OF COMMUNICATION SYSTEMS	32
7.1 VHF and UHF Fixed Transmitter Sites	32
7.2 VHF/UHF Airborne Communication Antennas	33
7.3 High Frequency (HF) Rhombic Antennas	33
8. SUMMARY	35
8.1 Field Measurement Instrumentation	35
8.2 Field Intensity Data	36
9. ACKNOWLEDGMENTS	39
10. REFERENCES	40

LIST OF FIGURES

<u>Figure</u>		<u>Page</u>
2-1.	Measurement ranges and specifications of the radiation monitors used for the field intensity surveys	41
2-2.	Graph of amplitude ranges of the radiation monitors, comparing units of V/m and mW/cm ²	42
2-3.	Sketch of the standard field setup used to calibrate the radiation monitors and record probe pattern responses	43
2-4.	Calibration of the EDM-1C radiation monitor in a standard field at a frequency of 2 GHz, E-plane and H-plane patterns	43
2-5.	Calibration of the CIM-1 radiation monitor at a frequency of 3 GHz, handle oriented parallel to the propagation vector, axial rotation of probe	44
2-6.	Calibration of the EDM-3 radiation monitor in a 100 nJ/m ³ field at a frequency of 10 MHz, handle oriented at the analytic angle, axial rotation of probe. Comparison of isotropic response (all three dipoles connected) with the meter indications produced by the individual dipoles	44
2-7.	Calibration curves of the EDM-1C monitor at five different frequencies, handle oriented at the analytic angle, axial rotation of probe	45
2-8.	Frequency response calibrations of the CIM-1 and CIM-2 monitors. Comparison of two orientations of the probe handle, parallel to or perpendicular to the propagation vector	45
2-9.	Frequency response calibration of the EDM-1C monitor, handle oriented at the analytic angle, mean axial response	46
2-10.	Frequency response calibration of the EDM-3 monitor, handle oriented at the analytic angle, mean axial response	46
3-1.	Photograph of airplane mechanics and a radar technician raising the radome of an RDR-1B radar antenna mounted in the nose of a DC-3 aircraft	47
3-2.	Photograph of an operator making preliminary checks of the field intensity in front of a DC-3 aircraft	47
3-3.	Photograph of an operator measuring stray fields with a CIM-1 radiation monitor in the cockpit of a DC-3 airplane	48
3-4.	Photograph of an operator measuring leakage fields with an EDM-1C monitor in the fuselage of a DC-3 airplane, Flight Inspector's position	48
3-5.	Field intensity in the center of the beam of an RDR-1B aircraft radar, measured in front of a DC-3 airplane	49
3-6.	Graphs of field intensity in the "pencil" beam of an RDR-1B aircraft radar as a function of distance from the antenna	50
3-7.	Graphs of field intensity versus inverse distance from the antenna, RDR-1B aircraft radar, "pencil" beam	50
3-8.	Leakage fields of an RDR-1B aircraft radar measured inside a DC-3 airplane	51
3-9.	Field intensity versus distance from the antenna of an RDR-1E aircraft radar, measured in front of a DC-9 airplane	52

LIST OF FIGURES (continued)

<u>Figure</u>		<u>Page</u>
3-10.	Graphs of field intensity versus distance from the antenna of an RDR-1E aircraft radar, 180 mile range	52
3-11.	Photograph of the slotted array antenna for the RDR-1200 aircraft radar on a Sabre Liner airplane	53
3-12.	Field intensity in the beam of an RDR-1200 aircraft radar, measured in front of a Sabre Liner	53
3-13.	Graph of field intensity versus the inverse square of distance from the antenna, RDR-1200 aircraft radar	54
3-14.	Field intensity in the beam of an AVQ-10 aircraft radar, measured in front of a 720 E airplane	55
3-15.	Graph of field intensity versus inverse distance from the antenna, AVQ-10 aircraft radar, "pencil" beam, 150 mile range	55
3-16.	Miscellaneous measurements of field of an AVQ-10 aircraft radar in a 720 E airplane	56
3-17.	Field intensity of an AVQ-10 aircraft radar measured near a turboprop airplane	56
3-18.	Graphs of field intensity versus inverse distance from the antenna, AVQ-10 aircraft radar, "pencil" beam	57
4-1.	Photograph of an operator making preliminary checks of the field intensity near an airport surveillance radar (ASR)	57
4-2.	Photograph of measurements being taken in the field of an ASR antenna, closeup view of the feed and reflector screen	58
4-3.	Sketch of an ASR-7 antenna including approximate dimensions	59
4-4.	Field intensity of an ASR-4B airport surveillance radar measured on the antenna tower, Oklahoma City	60
4-5.	Field intensity of an ASR-4B radar measured at several distant locations, Oklahoma City	60
4-6.	Field intensity 3.7 m from an ASR-4B radar antenna; horizontal and vertical cuts through the center of the beam, above the tower railing, Los Angeles	61
4-7.	Graphs of the field 3.7 m from an ASR-4B radar antenna; horizontal and vertical cuts through the center of the beam	61
4-8.	Field intensity of an ASR-7 radar measured near the antenna reflector screen, Los Angeles	62
4-9.	Field intensity 3.7 m from an ASR-7 radar antenna; vertical cut through the center of the beam, Los Angeles	63
4-10.	Field intensity of an ASR-7 radar measured on the antenna tower, Atlantic City	63
4-11.	Field intensity 3.7 m from an ASR-7 radar antenna; horizontal and vertical cuts through the center of the beam, Atlantic City	64
4-12.	Photograph of an ASR-8 antenna (background) and the "cherry picker" used when measuring the field intensity, Oklahoma City	65
4-13.	Field intensity 23 m from an ASR-8 radar antenna; horizontal and vertical cuts through the center of the beam, Oklahoma City	66
4-14.	Field intensity in the beam of an ASR-8 radar as a function of distance from the transmitter antenna, Oklahoma City	66
4-15.	Graph of field intensity in the beam of an ASR-8 radar versus distance from the transmitting antenna	67

LIST OF FIGURES (continued)

<u>Figure</u>		<u>Page</u>
4-16.	Graph of electric field strength in the beam of an ASR-8 radar versus inverse distance from the antenna	67
4-17.	Photograph of an Air Route Surveillance Radar (ARSR) installation, Denver	68
4-18.	Photograph of an ARSR transmitter building and antenna mounted on a tower, Oklahoma City	68
4-19.	Sketch of an ARSR-1D antenna, type CA-4000 reflector, giving approximate dimensions	69
4-20.	Leakage fields of an ARSR-1D radar measured in the area below the top deck of the antenna tower, Oklahoma City	70
4-21.	Photograph of the setup used to measure field intensity in the near-zone beam of an ARSR radar	70
4-22.	Average field intensity of three ARSR radars tested at Oklahoma City, Denver and Atlantic City	71
4-23.	Field intensity of an ARSR-1D radar measured at several distant locations, below the direct beam, Oklahoma City	72
4-24.	Measurements of field intensity near the antenna of an ASDE-1 radar, Los Angeles	73
4-25.	Measurements of field intensity near the antenna of an ASDE-2 radar, Atlantic City	73
4-26.	Computed field intensity in the near-zone beam of an ASR radar antenna, assuming uniform phase and amplitude in the aperture illumination	74
4-27.	Computed field intensity in the near-zone beam of an ASR antenna, cosine taper of aperture illumination	74
4-28.	Computed field intensity in the near-zone beam of an ASR antenna, cosine-squared taper of aperture illumination	75
4-29.	Computed field intensity in the near-zone beam of an ARSR antenna, uniform aperture illumination	75
4-30.	Computed field intensity in the near-zone beam of an ARSR antenna, cosine taper of aperture illumination	76
4-31.	Computed field intensity in the near-zone beam of an ARSR antenna, cosine-squared taper of aperture illumination	76
5-1.	View of the components and layout of an instrument landing system . .	77
5-2.	Sketch of an eight-loop localizer antenna array, top view (above) and side view of one element in the array (left)	78
5-3.	Field intensity at the radome surface of each antenna element in an eight-loop localizer array, Oklahoma City	78
5-4.	Photograph of a V-ring localizer antenna array, ILS, Denver	79
5-5.	Photograph of an operator using the EDM-1C field strength meter on the metal counterpoise of a V-ring localizer antenna, Denver	79
5-6.	Sketch of one element in a V-ring localizer antenna array giving approximate dimensions	80
5-7.	Top view of a V-ring localizer antenna, including mean values of the measured field intensity at several positions, Denver	80

LIST OF FIGURES (continued)

<u>Figure</u>		<u>Page</u>
5-8.	Field intensity at antenna height in front of a V-ring localizer array, Oklahoma City	81
5-9.	Profile of field intensity in front of the center element of a V-ring localizer antenna, Oklahoma City	81
5-10.	Graph showing profile of the electric field strength in front of a V-ring localizer antenna, data given in figure 5-9 . . .	82
5-11.	Field intensity near the antenna of a V-ring localizer, south site, Oklahoma City	83
5-12.	Top view of a traveling-wave localizer antenna array, with approximate dimensions	84
5-13.	Field intensity 30 cm in front of each antenna element of a traveling-wave localizer, Oklahoma City	85
5-14.	Photograph of a waveguide localizer showing one of the slot antennas	85
5-15.	Field intensity near the antenna of a waveguide localizer, Los Angeles	86
5-16.	Field intensity as a function of distance in front of a waveguide localizer antenna, Los Angeles	86
5-17.	Photograph of a UHF localizer antenna installation	87
5-18.	Photograph of the lower antenna element in one glide-slope array surveyed	87
5-19.	Photograph of another type of glide-slope antenna, being surveyed with an EDM-3 radiation monitor	88
5-20.	Photograph of the "elevation" antenna for a Ku band microwave landing system, El-2 site	88
5-21.	Photograph of the "azimuth" antenna for an S band microwave landing system	89
5-22.	Field intensity at the antenna aperture of a Ku band microwave landing system, Atlantic City	89
5-23.	Field intensity at the aperture of two S band antennas for a microwave landing system, Atlantic City	90
6-1.	Photograph of a VORTAC transmitter building with circular roof, showing the conical tower with enclosed VOR antenna and TACAN radome on top	90
6-2.	Field intensity of the VOR signal measured at the antenna height, about 1.2 m above the roof of the VORTAC building, Oklahoma City. .	91
6.3.	Photograph of a Doppler VOR antenna array	91
6.4.	Field intensity near the 50 radomes on the outer perimeter of a Doppler VOR antenna array, Los Angeles	92
6.5.	Field intensity near the center radome of a Doppler VOR antenna array, Los Angeles	93
6.6.	Magnetic field intensity near a Doppler VOR antenna array	93
6.7.	Photograph of a TACAN antenna mounted on a tower, showing an operator making preliminary checks at the side of the radome. . . .	94
6.8.	Field intensity of the ground TACAN signal measured on a tower by the TACAN Academy building, Oklahoma City.	94

LIST OF FIGURES (Continued)

<u>Figure</u>		<u>Page</u>
6-9.	Field intensity of a ground TACAN signal measured near the antenna, Los Angeles	95
6-10.	Intensity of X-rays near a TACAN transmitter rack	95
6-11.	Locations of the navigation, communication and radar antennas on a Sabre 75A aircraft	96
6-12.	Field intensities near the airborne TACAN antennas on a Sabre Jet aircraft, Oklahoma City	96
7-1.	Photograph of VHF antenna towers and transmitter building at a communication antenna site, NAFEC, near Atlantic City.	97
7-2.	Closer view of a VHF communication antenna showing the "Swastika" type of antenna surveyed.	97
7-3.	Field intensity in the vicinity of a VHF communication antenna, Atlantic City	98
7-4.	Magnetic field intensity near a VHF communication antenna, Atlantic City	99
7-5.	Field intensity near the VHF/UHF antennas on a Sabre 75A aircraft, Oklahoma City	99
7-6.	Sketch of a portion of the transmitting site and rhombic antenna layout on Long Island, used for HF transoceanic transmissions . . .	100
7-7.	Intensity of stray fields inside the HF transmitter building, Long Island	101
7-8.	Field intensity near the rhombic antenna and transmission line for antenna number 14, Long Island	102
7-9.	Field intensity near the rhombic antenna and transmission line for antenna number 2, Long Island.	103
7-10.	Magnetic field intensity near the transmitter, transmission line and antenna number 2, Long Island	104

SURVEYS OF ELECTROMAGNETIC FIELD INTENSITIES
NEAR REPRESENTATIVE HIGHER-POWER FAA TRANSMITTING ANTENNAS

1. INTRODUCTION

1.1 Background

This report is in response to a Federal Aviation Administration (FAA) request that the National Bureau of Standards (NBS) perform surveys of electromagnetic (EM) field intensities near the antennas of typical higher-power FAA transmitting systems. These include ground "surveillance" radars, airborne "weather" radars, instrument landing systems, and various navigation and communication radiators.

The measurements reported herein should serve as a major input to a data base on radiation levels in the vicinity of various representative higher-power transmitters used by FAA. The data will be useful in connection with the reassessment and validation or updating of existing standards and procedures for the protection of personnel. However, it should be pointed out that this report by itself should not be construed or used as an official FAA directive pertaining to protection of personnel from radiation. Another important purpose of the electromagnetic measurement survey data reported in this document is to support the work of the Electromagnetic Radiation Advisory Council (ERMAC), which is an advisory group for the Executive Office of Telecommunications Policy (OTP).

For electromagnetic energy from 10 MHz to 100 GHz, the radiation protection guide recommended by the American National Standards Institute (ANSI) is 10 mW/cm^2 for continuous exposure, or the equivalent free-space electric and magnetic field strengths of approximately 200 V/m and 0.5 A/m respectively [1] and [2]. Higher field levels are allowable for short durations of time if the power density averaged over any 6-minute period does not exceed 10 mW/cm^2 . According to the ANSI C95.1 standard, "Radiation characterized by a power level tenfold smaller will not result in any noticeable effect on mankind. Radiation levels which are tenfold larger than recommended are certainly dangerous" [1].

The instrumentation used for the field intensity surveys had to be capable of accurate measurement of very complicated EM fields ranging from levels less than 0.1 mW/cm^2 up to field levels greater than 10 mW/cm^2 . Recently, instruments employing "isotropic" probes have been developed which permit practical measurement of complex fields, including the near zone of complicated antenna arrays. Some of these meters are available commercially in the frequency range of 10 to 300 MHz for magnetic (H) fields, and 0.3 to 18 GHz for electric (E) fields. Other instruments were developed by NBS for measuring E fields at frequencies from 100 kHz to 10 GHz. Prior field intensity meters (FIM's) with directive antennas would not reliably measure complicated EM fields such as those with reactive near-field components, multipath reflections, arbitrary polarization, multiple frequency components, complicated

modulations and large field gradients. The term modulation used here includes characteristics of radar and navigation pulses such as pulse duration, repetition rate and duty factor. Antennas which employ a rotating or sector scan cause an additional type of duty factor and measurement difficulty which will be discussed later.

The only practical way to accomplish the FAA field intensity surveys was with radio frequency (rf) probes that are essentially independent of orientation in the field. Such probes are isotropic rather than merely being independent of the arrival angle for single plane-wave fields. It is also important that the probe be small and thus able to resolve fine-structure spatial variations in field intensity. Further, it is important that the field is not seriously perturbed by the operator or equipment associated with the measurement, such as probe, cables, meter case, etc.

Presently no radiation monitors completely satisfy all of these requirements for all types of transmissions; however, three commercial and three NBS-developed probes satisfied the requirements sufficiently well that reasonably accurate field strength surveys could be made for the present FAA systems. The description and calibration of these instruments are covered briefly in section 2 of this report. The field intensity data and description of the surveys are covered in sections 3 to 7.

1.2 Objectives and Approach

The overall objective of this FAA/NBS program was to make accurate field intensity surveys at several representative, transmitting sites operated by the FAA. To satisfy this objective, it was necessary to check the accuracy and adequacy of existing field intensity meters and develop satisfactory procedures for measuring high-intensity near-zone EM fields of antennas which are often not easily accessible.

In order to estimate the field levels likely to be encountered in our surveys, a compilation was made of transmitter power levels and modulation characteristics of higher-power FAA emitters. This included computer printouts from the Electromagnetic Compatibility Analysis Center (ECAC) of all the fixed transmitters operating within 25 miles of the airports surveyed [3]. Wherever feasible, this information was used to make calculations of expected EM field levels, taking into consideration the gain and electrical characteristics of the antennas. Sufficient measurements were then performed to adequately define the spatial radiation patterns of the FAA antennas, down to the lowest levels capable of being measured by the instruments in use. During the surveys an attempt was made to develop optimum measurement techniques.

The first work phase was to modify existing instrumentation and (where required) design new instruments to measure the types of fields encountered at FAA sites. The second phase involved calibration of the rf probes by inserting them in known fields, and verifying the adequacy by making several "exploratory" field intensity surveys. These first two phases have been reported previously in FAA Letter Reports. The third and final phase of the program was to make more extensive surveys at several selected FAA facilities, choosing transmitters and antennas which were most likely to produce high level fields.

2. ELECTROMAGNETIC FIELD PARAMETERS AND INSTRUMENTATION

2.1 Discussion of Field Strength Units

If electromagnetic fields always occurred in simple plane-wave configurations, the question of which physical quantity to measure and how to relate this quantity to biological effects would be more easily answered. The regions very close to radiating systems are most likely to approach hazardous levels. Unfortunately they are also characterized by complicated field structure including reactive (stored) and real (propagated) energies, multipath reflections, standing and traveling waves, irregular phase surfaces, and unknown field polarization.

It is assumed that for linear isotropic materials, such as most types of human tissue, the heating and potential damage are proportional to the time-average value of $\bar{\mathbf{E}} \cdot \bar{\mathbf{E}}^* = |\mathbf{E}|^2$, where the asterisk denotes the complex conjugate [4]. The quantity $|\mathbf{E}|$ is called the Hermitian magnitude of the field. It is closely related to the electric field energy density, a scalar quantity which involves $|\mathbf{E}|$ and the complex permittivity of the medium. Similarly, the Hermitian magnitude of a magnetic field is defined as $|\mathbf{H}| = \sqrt{\bar{\mathbf{H}} \cdot \bar{\mathbf{H}}^*}$. The familiar power density or Poynting vector, however, is not directly relatable except when the field structure is quite simple, as with a single plane wave. Taking some liberties with technical exactness, it is possible to convert a measured field in $|\mathbf{E}|$ or $|\mathbf{H}|$ to an "equivalent" plane-wave power density, but this common practice is not necessarily valid.

The above expressions for generalized field strength are valid for an electric or magnetic field in any configuration. The pertinent relationships between the units involved here (using RMS values for E and H) are:

$$U_E = \frac{1}{2} \epsilon_0 |\mathbf{E}|^2, \quad U_H = \frac{1}{2} \mu_0 |\mathbf{H}|^2, \quad U_T = U_E + U_H, \quad (1)$$

$$S = c U_T = 2 c U_E = 2 c U_H, \quad (2)$$

$$S = \frac{|\mathbf{E}|^2}{Z_0} = Z_0 |\mathbf{H}|^2, \quad (3)$$

where: U_E = energy density of the electric field, J/m³,
 U_H = energy density of the magnetic field, J/m³,
 U_T = total energy density of the EM Field, J/m³,
 ϵ_0 = permittivity of free space $\approx 8.854 \times 10^{-12}$ F/m,
 μ_0 = permeability of free space $\approx 1.257 \times 10^{-6}$ H/m,
 c = speed of light in free space $\approx 2.998 \times 10^8$ m/s,
 $Z_0 = \sqrt{\mu_0 / \epsilon_0}$ = intrinsic free-space wave impedance
 = free-space $|\mathbf{E}/\mathbf{H}| \approx 376.7$ ohms.

It is important to remember that eqs. (2) and (3) above are valid only for plane-wave fields. However, those given by eq. (1) are general for the Hermitian magnitudes of E and H.

For an isotropic E field radiation monitor, the Hermitian magnitude of the electric field at a measurement point is defined by (and measured in terms of) the root-sum-of-squares (RSS) value of three orthogonal E field components, as follows:

$$|E| = \sqrt{|E_x|^2 + |E_y|^2 + |E_z|^2} . \quad (4)$$

For an H field isotropic monitor, a similar expression can be given for the Hermitian magnitude $|H|$.

For plane-wave fields, the pertinent conversion factors between the field parameters are:

$$S = \frac{E^2}{3767} = 3767 H^2 = 0.05996 U_E , \quad (5)$$

$$E = 15.03 \sqrt{U_E} = 61.38 \sqrt{S} , \quad (6)$$

where: S = magnitude of the power density, mW/cm^2 ,
 E = Hermitian magnitude of electric field, V/m ,
 H = Hermitian magnitude of magnetic field, A/m ,
 U_E = electric field energy density, nJ/m^3 .

The above "mixed" units are used in order to express power density in the units commonly used for rf hazards work, where $10 \text{ mW}/\text{cm}^2 = 100 \text{ W}/\text{m}^2$.

The duty factor of a pulsed transmitter is defined as the ratio of pulse on-time to the total time. For typical FAA radars this factor is the order of 0.001. The indication on most types of radiation monitors is proportional to the time-average field level and not to the pulse-peak value. The relationship between the average field and peak field is given by:

$$\text{Duty factor} = \frac{P_{av}}{P_{pk}} = \frac{S_{av}}{S_{pk}} = \frac{U_{av}}{U_{pk}} = (\text{PRR})(\tau) \quad (7)$$

where: P_{av} = transmitter time-average power, W ,
 P_{pk} = transmitter power during the rf pulse, W ,
 S_{av} = average power density of the EM field, mW/cm^2 ,
 S_{pk} = power density of the field during the rf pulse, mW/cm^2 ,
 U_{av} = average energy density of the EM field, nJ/m^3 ,
 U_{pk} = energy density of the field during the rf pulse, nJ/m^3 ,
 PRR = pulse repetition rate, pulses/second,
 τ = pulse duration, seconds.

A knowledge of the transmitter power, duty factor, and antenna gain is useful for estimating the peak and average field levels of FAA radars. The following formula (with

mixed units) can be used to calculate the average field intensity at distances on the order of $2D^2/\lambda$ or greater, where D is the largest dimension of the antenna and λ is the wavelength.

$$S = \frac{PG}{40\pi d^2} \quad (8)$$

where: S = power density of the radiated field, mW/cm^2 ,
 P = power delivered to the transmitting antenna, W ,
 G = gain of the transmitting antenna,
 d = distance from the transmitting antenna to the field point, meters.

For computation of power density at points closer to the antenna (within the near field) more complicated techniques are required. These are discussed in section 4.5 of this report.

For radar antennas which rotate, or oscillate in a sector scan, an additional duty factor can be defined which relates the overall time average level to the boresight value. The so-called "rotational duty factor" of a fully rotating antenna is given approximately by the 3 dB beam width, in degrees, divided by 360 degrees. For typical FAA radars this factor is the order of 0.01.

2.2 Description of the Radiation Monitors Used

The instrumentation used for the FAA field intensity surveys consisted of three commercially-available radiation monitors and three monitors designed and fabricated at NBS. The meters are identified in this report by the nomenclature CIM-1, CIM-2 and CIM-3 (for commercial isotropic meter) and EDM-1C, EDM-3, and EDM-4A (for energy density meter). Figure 2-1 gives a summary of the measurement ranges and basic capabilities of these radiation monitors. Figure 2-2 shows some of the amplitude ranges in graphical form, including the relationship between the field intensity units of V/m and mW/cm^2 . A detailed description of some rf radiation monitors and a discussion of the characterization of EM fields are given in references [5] and [6].

Unfortunately the readout unit on the commercial CIM's is mW/cm^2 , a power density unit, for either the E or H field probes. The readout unit for the NBS-designed EDM's is nJ/m^3 , an energy density unit. As mentioned previously, the relations between the power density, S , and the other field parameters are not necessarily valid. However, it is often convenient, for comparison purposes only, to express the intensity in terms of "equivalent plane-wave power density," even for non-plane-wave situations. Therefore, the fields measured with the CIM's are generally reported in V/m or A/m , in addition to the free-space equivalent mW/cm^2 indicated on the meter. The measurements made with the EDM's are given in V/m and generally also in nJ/m^3 .

The EDM instruments incorporate some features not commercially available, such as peaking circuits with switch-selectable time constants from 0.1 to 30 seconds. When the metering unit is switched to the peak mode, it is possible to make approximate measurements of the peak value of modulated signals (including scanning radars), using an experimentally determined correction factor for each type of radar. The additional uncertainty for this type of measurement is estimated to be up to 3 dB due to the relatively slow response time

(~ 1 ms) of the instrument with respect to the pulse duration (~ 1 μ s). The diode detectors have a fast risetime but the overall meter response time is limited by the high-resistance line (filter) between the rf detectors and the electronic shaping circuitry.

The EDM monitors have on-off switches for selecting a single E field component for measurement, in addition to the RSS value of three orthogonal E field components. The EDM-1C has a sizable temperature coefficient of roughly 2% per $^{\circ}$ C. Its use was therefore restricted to a temperature range of 10° to 40° C in order to avoid using large correction factors. There is also a considerable frequency correction factor for this instrument (see section 2.3). The measured field values reported in sections 3 to 7 have been adjusted according to the applicable correction factors. The EDM-3 is an improved, lower-frequency version of the EDM-1C, having greater dynamic range, less susceptibility to static fields, and a lower temperature coefficient of about 0.5% per $^{\circ}$ C. The EDM-4 sensors have longer antenna elements than the EDM-3, with selectable dipole lengths of 5, 10 or 20 cm each. The EDM-4A version, with 5 cm dipoles, is useful at frequencies down to 300 kHz and signal levels down to 1 V/m. However, it has not been calibrated extensively and was seldom needed for the FAA surveys. One limitation of all the EDM sensors is the erroneous increase in indication when measuring multifrequency fields. The error may be as great as 3 dB when measuring a field with two frequency components of equal amplitude [5].

The capabilities of the commercial and the NBS meters are somewhat different, making the CIM's more useful for measuring average field levels of high-power pulsed radars, while the EDM's are better for measuring the lower-frequency nonpulsed signals radiated by navigation, communication and instrument landing systems. Both types of monitors employ an isotropic sensor embedded in a styrofoam sphere of 10 cm diameter. Thus the minimum distance for which field measurements can be made is 5 cm (2 inches).

Some characteristics of an ideal rf radiation monitor are listed as follows:

- (a) The instrument (probe, case, cables, etc.) should not perturb the field being measured;
- (b) The probe should have capability for direct measurement of the pulse-peak field value as well as the time average value;
- (c) The sensor size should be small enough to resolve the spatial fine structure of the field;
- (d) The probe response pattern should be isotropic;
- (e) The sensor should have no resonant-frequency effects and (for most purposes) should be very broadband;
- (f) The dynamic range should be at least 30 dB without changing probes;
- (g) Measurements should not require calibration charts, nulling or frequent rezeroing; and
- (h) The instrument should be stable, rugged, lightweight, well shielded, and battery operated.

The radiation monitors used in the FAA/NBS field intensity surveys do not possess all of the above desirable characteristics. The most serious shortcoming was the relatively long response time of the probes. The 90% response time of the three EDM instruments to an instantaneous change in field level is about 0.2 ms. The response time of the CIM-1 sensor

element is about 35 ms. However, the overall response time for the three CIM instruments is about 0.75s with the time constant switch set to the "fast" position. It was thus not possible to measure directly the peak intensity of radar pulses nor the (momentary) maximum-envelope intensity in the beam center of a scanning antenna. Another problem in measuring radar beams is that the peak intensity may exceed the saturation or burnout level of the sensor, even though the indicated value remains below measurable levels. It might be noted that the rf sensor is subject to burnout in a strong field even when the instrument is turned off.

There is a considerable perturbation error when the probes are hand held, caused by the operator and/or cable between the probe and metering unit. The measured field distortion was up to ± 0.5 dB when taking measurements close to a transmitting antenna where the field gradient was high and the operator could place himself in a weaker field than the probe sensor. The operator perturbation was as great as ± 2 dB when measuring at a large distance from a transmitting antenna, where the probe and operator were in equal fields. The EDM-3 probe has a relatively long handle (1 meter) which permits greater operator separation than the other probes. For this instrument the perturbation was within ± 1 dB.

When using radiation monitors with isotropic probes it is easy to search for and locate "hot spots." These are local regions of higher field intensity (fine structure) created by the constructive interference of multiple signals and their reflections.

To zero the meter indication of the radiation monitors prior to making a field strength measurement, the probe was inserted into a closed metal tube 40 cm long by 11 cm diameter. This "zeroing can" functioned as a waveguide-below-cutoff attenuator to provide a zero-power-density environment for setting the meter zero.

2.3 Calibration of the Instruments

The radiation monitors used to make the FAA field intensity surveys were calibrated for response with respect to the following parameters: (a) frequency, (b) ambient temperature, (c) linearity of dial indication vs. field level, (d) imperfect probe isotropy, that is, probe directivity and field polarization sensitivity, and (e) (EDM-1C only) peak response vs. pulse duration and repetition rate for radar signals. Figure 2-3 is a sketch of the setup used to produce a standard (known) rf field in a small anechoic chamber to calibrate the radiation monitors and determine the various probe pattern responses.

Some typical calibration curves for the radiation monitors are given in figures 2-4 to 2-10. Above 2.5 GHz the accuracy of the standard field used for the calibrations is estimated to be within ± 0.5 dB. Between the frequencies of 0.5 and 2.5 GHz the estimated field uncertainty is ± 0.7 dB. Below 0.5 GHz the uncertainty is ± 1 dB. The calibrating field at frequencies above 2.5 GHz was produced by standard-gain horns. The standard field between 0.5 and 2.5 GHz was produced by open-ended waveguides which were calibrated at NBS [7]. The standard field setup at frequencies below 0.5 GHz consists of a series of "coaxial" transmission lines of rectangular cross section, called TEM transmission cells [8].

Pattern responses of all the probes were measured for several configurations at several frequencies. Six types of amplitude-vs-angle patterns can be identified as follows:

- (1) E-plane pattern response, -90° to $+90^\circ$ (see figure 2-4),
- (2) H-plane pattern response, -90° to $+90^\circ$ (see figure 2-4),
- (3) Axial rotation of probe handle, 0° to 360° ,
 - (a) Probe handle oriented parallel to the direction of energy propagation, \bar{S} , where $\bar{S} = \bar{E} \times \bar{H}$ (see figure 2-5),
 - (b) Probe handle oriented parallel to the \bar{E} vector,
 - (c) Probe handle oriented parallel to the \bar{H} vector,
 - (d) Probe handle oriented at the analytic angle as defined later (see figures 2-6 and 2-7).

Figure 2-4 shows both the E-plane and H-plane patterns recorded for the EDM-1C probe. This type of response pattern is obtained by rotating the horizontal probe in a horizontal plane around a vertical axis through the sensor, using a horizontally polarized field for the E-plane pattern and a vertical polarization for the H-plane pattern. A direction angle of 0° corresponds to the orientation shown in figure 2-3, with the sensor end of the probe toward the rf source. The maximum error in this case for the EDM-1C was $\pm 3/4$ dB.

Figure 2-5 is the pattern response recorded for axial rotation of the CIM-1 probe. It can be seen that the response is essentially correct (within $\pm 1/2$ dB) when the sensor end of the probe is oriented toward the rf source, that is, when the probe handle is parallel to the propagation vector \bar{S} . However, the error was found to be generally greater with the probe handle parallel to the \bar{E} or \bar{H} vector (perpendicular to \bar{S}), such as would be the case when holding the probe vertically upward to measure the intensity of an elevated antenna.

One critical test of probe directivity is to record, separately, the response of each of the three field sensors as a function of field orientation. This can be accomplished only for the EDM probes, which feature switches for selecting separate dipole outputs. The test is performed by fixing the probe handle at the "analytic" angle and rotating the probe on its own axis in the test field. The "analytic" angle is the angle which the diagonal of a cube makes with the three intersecting edges at one corner of the cube. It is also the angle at which the probe handle makes equal angles with the E field vector, H vector, and Poynting vector. At certain 120° intervals in the handle rotation, one dipole of the probe will be parallel to the E vector and the other two dipoles will be orthogonal to it. For example, figure 2-6 shows the separate dipole responses, each of which should ideally peak at the standard field value but be zero when oriented orthogonally to the E field. The figure also shows the RSS output (upper dashed line) for normal operation of the EDM-3 meter.

Figure 2-7 is a composite of five calibrations for the EDM-1C at five different frequencies from 2 to 6 GHz. All of the curves were made with the probe handle mounted at the analytic angle, at an ambient temperature of 25° C. The increase in probe sensitivity with increase in frequency is readily apparent. The mean axial response of the EDM-1C was about 4% low (-0.2 dB) at 2 GHz and about 4% high at 3 GHz. (The 3 GHz curve is not shown in figure 2-7 since it nearly coincides with the 2 GHz curve.) The response at 6 GHz varied

from + 3.3 dB at a rotation angle of 0° , to + 3.9 dB at 100° , which is a mean axial response of $+ 3.6 \pm 0.3$ dB, corresponding to a calibration factor of 2.3, or a correction factor (required multiplying factor) of 0.43 at this frequency. Graphs of the correction factors vs. signal frequency, for use with the CIM-1, CIM-2, EDM-1C, and EDM-3 meters, are given in figures 2-8 to 2-10.

The rf sensors of the CIM-1 and CIM-2 probes consist of three mutually-orthogonal thin-film thermocouple arrays. The sensor of the CIM-3 H-field probe consists of three orthogonal coils, each having two turns approximately nine cm in diameter. The frequency response of this probe was not calibrated but is specified by the manufacturer to be flat within ± 0.5 dB from 10 to 200 MHz. The meter indication increases 1 to 1.5 dB between 200 and 300 MHz, due possibly to E field response of the relatively large loop antennas used.

In general, the only correction factors which were applied to the meter-indicated values were: (1) frequency correction factor when applicable, (2) slight correction factor for probe angle with respect to the field orientation, and (3) a temperature correction for the EDM-1C for ambient temperatures below or above 25°C . These corrections (and pulse calibration factors which apply only to the EDM-1C when used to measure radars) have been applied to all the data reported in sections 3 to 7.

3. FIELD INTENSITY SURVEYS OF AIRCRAFT RADARS

3.1 Time Averaging Effect Due to Antenna Scanning

Surveys were made for five different aircraft, each parked near a hangar. Airborne radars use high-gain antennas mounted in the nose of the aircraft. In the normal operating mode of these "weather" radars the antenna is continuously rotating through 360° or is oscillating in a sector scan. During the field intensity measurements reported here the transmitter was generally operated with a fixed antenna orientation, obtained by a special procedure such as disconnecting the power cable to the scanner motor and tying the antenna reflector in place. It should be noted that the time-average field strength under normal operating conditions would be much less than these bore-sight values. The measured power density could then be multiplied by a rotational duty factor as described in section 2.1. The scanning factor used by the FAA is given in paragraph 26c of reference [9] by the expression:

$$\frac{S}{S_0} = \frac{D}{2d} \quad (9)$$

where: S = time-average value of scanned power density,
S₀ = stationary-antenna value of power density,
D = antenna diameter or dimension parallel to the path of rotation, and
d = distance from the antenna to the field measurement point.

3.2 X-Band Airborne Radars

3.2.1 RDR-1B Radar On a DC-3 Airplane

Figures 3-1 to 3-4 are photographs of field intensity surveys being made for the radar system of a DC-3 aircraft. The RDR-1B type of radar operates at a frequency of 9.375 GHz. The nominal pulse-peak power is 40 kW, pulse duration is 1.5 μs and the repetition rate 400 per second. This corresponds to a duty factor of 0.0006 and average power of 24 W. The pulse duration measured with an oscilloscope was 1.4 μs between the (0.7 x peak) voltage points.

A cockpit switch permits a choice of the narrowest "pencil" beam (search mode) or a "map" beam. The measured beam width between the half-power points was approximately 4° for the pencil beam. The map beam is broader in a vertical plane, illuminating the ground with a "cosecant squared" pattern. This mode is used to enhance the surface signal return as a guide for terrain avoidance (at low altitude) or to check if the radar set is operating (at high altitude). There is a cockpit control to tilt the radar reflector up or down, to ± 15°, with respect to the airplane center line. The DC-3 tilts upward at an angle of about 11° above horizontal when it is parked or taxiing.

Figure 3-5 lists the field intensities of the pencil beam measured with the CIM-1 directly in front of the airplane. For this test the antenna was locked in a forward-pointing position. In the first set of data the reflector was tilted 11° downward. At each

measurement distance the CIM probe height was adjusted for maximum meter indication. The second set of data was taken with a 5.5° downward tilt of the antenna dish, in an attempt to produce a horizontal beam. The antenna "elevation" control changes the tilt of the reflector only, but the feed remains fixed. Figure 3-6 is a graph of both sets of data. The third set of data was taken with a 0° tilt angle of the dish, producing a beam along the airplane center line. In this case the maximum field was generally at a height above the highest attainable probe height of 4m. The power density in the center of the pencil beam exceeded 10 mW/cm^2 for distances less than 3 m from the antenna. Figure 3-7 is a graph of the same data plotted to show field strength vs. inverse distance. For free-space, far-zone conditions this type of plot is theoretically a straight line. As seen in the figure, the graph is linear except at small distances (right side of graph), indicating that ground reflections and near-zone antenna gain reduction were small. Additional data were taken in front of the DC-3 airplane with the radar switched to the "map" beam. In this mode of operation the power density was above 10 mW/cm^2 for distances within 2.5 m of the antenna.

Figure 3-8 gives data for fields measured inside the aircraft with the more sensitive EDM-1C instrument. These fields, while low, were nevertheless much stronger than any found later inside the other (newer) types of aircraft. This may have been due to a partially torn "radiation shield" on the bulkhead between the cockpit and nose compartment. The fields inside the DC-3 were very weak, even with the radar antenna fixed and pointing directly back into the cockpit. The maximum hot spot found was near the pilot's right rudder control or copilot's left rudder control, which is very close to the radar antenna. The maximum measured pulse-peak E field was about 800 V/m, corresponding to a calculated time-average E field of 19 V/m or an equivalent power density of 0.1 mW/cm^2 .

3.2.2 RDR-1E Radar on a DC-9 Airplane

This survey involved a similar type of radar but different type of aircraft. The DC-9 has a tricycle landing gear and thus the fuselage was horizontal. The antenna had a measured center height of 2 m above the parking apron, which is slightly above the head height of an adult. The peak-power rating of the RDR-1E transmitter is 50 kW, compared with 40 kW for the RDR-1B. The center frequency of this transmitter was also 9.375 GHz. The 75 cm diameter antenna produced a -3dB beam width of 3° for the pencil beam. The plastic radome was kept in place during all the field measurements. The radar "range" switch had three positions, for 30, 80, and 180 miles. The closest range uses a pulse duration of $2.5 \mu\text{s}$ at a repetition rate of 400 per second, and the two longer ranges use a pulse duration of $5 \mu\text{s}$ at a repetition rate of 200/s. The duty factor was thus 0.001 in both cases.

Figure 3-9 gives measurements of power density in front of the DC-9 airplane. The radar antenna normally rotates in a 360° scan but was fixed in a forward-looking direction for the field strength measurements. The CIM-1 probe was mounted on a plastic pole with the sensor end toward the aircraft and at the same height as the radar antenna. The probe handle was horizontal, with its identification mark upward. The radar dish elevation angle was adjusted for maximum indication on the CIM-1 meter, at a distance of 15 meters. This maximum reading occurred for an indicated elevation angle of $+0.5^\circ$. For each data point the beam center was located by moving the probe laterally (at a given horizontal distance) until the meter indication was maximum. An initial check was made near the antenna height for a

possible standing-wave pattern (fine structure in the field caused by ground reflections) but this was found to be negligible.

Figure 3-10 is a graph of the data from the last two columns of figure 3-9, after converting to electric field strength in V/m. The pencil beam was more intense than the map beam and exceeded 10 mW/cm^2 for distances within 1.8 m of the antenna. At distances beyond 5 m, the E field decreased linearly with reciprocal distance, denoting far-field conditions. A comparison with figure 3-6 indicates that the RDR-1E has a more noticeable near-zone gain reduction than the RDR-1B, and a weaker field, due presumably to attenuation by the radome.

Additional measurements were made using the EDM-1C probe inside the DC-9 cockpit, but all readings were negligible. The antenna was then set into normal rotation. A small indication was observed whenever the antenna pointed back toward the cockpit. The maximum hot spot found was near the pilot's right rudder pedal. The measured value of (E pk) was 66 V/m, corresponding to an (E av) of 2.1 V/m or (S av) of 0.001 mW/cm^2 .

3.2.3 RDR-1200 Radar on a Sabre Liner Airplane

The next radar tested was a type RDR-1200 on a Model 80 twin-jet aircraft. This radar operates at a frequency of 9.345 GHz and peak power of 12 kW. The pulse repetition rate was 99 per second and pulse duration 3.5 μs . The duty factor of approximately 0.00035 results in an average carrier power of 4.2W. The antenna on this aircraft was a waveguide slotted array in a flat dish of about 30 cm diameter, as shown in figure 3-11. The antenna has a nominal gain of 28.5 dB and a sector scan which can be set to either $\pm 30^\circ$ or $\pm 60^\circ$.

One set of field intensity data for this radar is given in figure 3-12. All of these readings are for the 25 mile range, "weather" position, pencil beam, 0° antenna tilt angle, and with the antenna azimuth fixed in a forward-pointing direction. The maximum field intensity measured with the CIM-1 sensor sphere touching the front tip of the radar nose cone was 10 mW/cm^2 . A graph of the measured power density vs. inverse distance squared is given in figure 3-13, where the straight line portion at a 45° slope corresponds to far-zone conditions. The near-zone gain reduction on the right side of the graph is quite apparent.

3.3 C-Band Airborne Radars

3.3.1 AVQ-10 on a 720E Airplane, Slotted Array Antenna

This radar set operates at a nominal frequency of 5.4 GHz and pulse-peak power of 75 kW. The repetition rate was 400/s and the pulse duration 2 μs . The duty factor of 0.0008 results in an average carrier power of 60 W. The antenna was a waveguide slotted array similar in appearance to that of figure 3-11.

The four sets of field intensity data in figure 3-14 are for a fixed antenna pointing forward, with the radome in place. The height of the antenna above ground was 3.2 m. The CIM-1 probe was mounted on a plastic pole with the handle vertical and sensor at the

radar antenna height. This radar has a choice of "pencil" beam or "contour" (cosecant squared) beam. The pencil beam was strongest (at a 15 m distance) with the reflector "elevation" control set at -1.5° . As seen in figure 3-14, the power density in the beam center exceeded 10 mW/cm^2 for distances less than 6.1 m. Figure 3-15 is a graph of the measured field strength versus inverse distance from the antenna, for the pencil beam and 150-mile range.

Figure 3-16 lists some miscellaneous measurements of field strength made with the EDM-1C probe while the radar antenna was rotating. As seen, there was a measurable but very weak leakage field of about 3 V/m inside the cockpit. The third set of data is for the radar signal reflected from a nearby building. For this measurement the EDM-1C probe was held upward outside the copilot's window, at arms' length above the fuselage. The reflected signal corresponded in azimuth direction with the side of a three-story building about 100 m away. The measured average field was about 4 V/m.

3.3.2 AVQ-10 on a Turboprop Airplane, Parabolic Dish Antenna

The final measurements of aircraft radars were of an AVQ-10 mounted in a turboprop airplane. The circular parabolic dish had a diameter of 76 cm and a height above ground of 2.6 m. The stationary antenna was pointed forward, at an elevation angle of $+0.5^\circ$ (for maximum horizontal beam). The field intensity of the pencil beam was measured at two heights above the concrete apron. The data are given in figure 3-17, which show that a 10 mW/cm^2 level occurred for distances within 4.6 m of the antenna. A graph of the data plotted versus inverse distance is given in figure 3-18, both for antenna height and for head height (1.7m). The intensity at head height never exceeded 39 V/m, even directly beneath the forward-looking radar dish.

A search was also made for possible hot spots inside this aircraft, with the radar antenna rotating, using the EDM-1C probe. No measurable field was found anywhere inside the cockpit, except that caused by a distant ARSR antenna. Checks made inside the fuselage revealed only one location with a readable (but negligible) indication.

4. FIELD INTENSITY SURVEYS OF GROUND RADAR SYSTEMS

In addition to the aircraft radars reported in section 3, several types of FAA "ground" surveillance radars are capable of producing near-field power densities greater than 10 mW/cm^2 . Mitigating factors for these high-power rf sources are the general inaccessibility of the antennas to personnel (locked towers and safety interlock switches) and the fact that the radars operate in a scanning mode. A discussion of the time-averaging duty factor for scanning antennas is given in section 3.1.

The airport surveillance radar (ASR) represents the highest power radar unit in operation at most FAA airport installations. A higher power "long range" radar, called an air route surveillance radar (ARSR), is used for each "regional" air route traffic control center, but these radars are not normally located at an airport. Our measurements confirm that the highest fields for the large aperture FAA antennas are found between the feed point and reflector screen. When the probe of a radiation monitor is moved (in the direct beam) from the center of the reflector toward the feed, the indicated power density varies up and down in a standing wave interference pattern, increasing in value as the feed point is approached.

The field intensity data in this section of the report are generally stated in terms of the indicated power density in mW/cm^2 and the electric field strength in V/m (Hermitian magnitude). The fields were measured with isotropic probes having sensors imbedded in polyfoam spheres of 10 cm diameter. The minimum measurement distance was thus 5 cm, with the probe sensor touching the rf source. It is not possible to obtain accurate field strength measurements of scanning antennas with the CIM and EDM monitors. A few (approximate) measurements of rotating radars were made using the EDM-1C probe switched to the "peak" mode. However, most of the data pertain to measurements of fixed (non-rotating) antennas taken with the CIM probes.

4.1 Airport Surveillance Radars (ASR)

The FAA maintains an airport surveillance radar at each major airport to aid in air traffic control. These radars operate in the 2.7 to 2.9 GHz band with a magnetron power of 425 to 550 kW during the pulses, or about 375 to 475 W average power. The nominal half-power (-3dB) pulse duration (τ) is $0.833 \mu\text{s}$ and the pulse repetition rate (PRR) is 800 to 1200 pulses per second. This results in a duty factor (τ)(PRR) range of 0.0007 to 0.001.

A photograph of a typical ASR installation is given in figure 4-1. The transmitter building is in the foreground and the antenna with near-rectangular reflecting screen is in the background. The paraboloidal reflector is approximately 2.6 m high x 5.5 m wide (8.5 x 18 ft.). Either vertical or circular polarization may be selected. The antenna has a specified minimum far-field gain of 34 dB with respect to an isotropic radiator. Its nominal -3 dB beam width in the far zone is 1.5° horizontally and 5° vertically. The rotation rate is 13 to 15 RPM. The antenna is mounted on a metal tower having a square 7.4 m x 7.4 m (approximately 24 ft. x 24 ft.) cross section. The narrow "beacon" antenna (ATCBI) seen

above the main reflector is used for identification signals, as discussed in section 4.3. A closeup view of the feed (left edge of picture) and reflector for an ASR antenna is shown in figure 4-2. The sensor sphere of the CIM-1 probe, mounted on a dielectric extension pole, is being held near the focusing "dot" at the "center" of the antenna reflector. A sketch of the antenna, with approximate dimensions, is given in figure 4-3.

4.1.1 Field Intensity of ASR-4 Radars

Measurements of time-average field strength were made in the vicinity of a non-rotating ASR-4B antenna, using the CIM-2 radiation monitor. The intensity between the antenna feed and reflector screen was generally greater than 10 mW/cm^2 . The measured values at several points on the antenna tower are given in figure 4-4. As shown, a field of 10 mW/cm^2 occurred at a point below the beam center, 60 cm from the reflector, at a height of 1.8 m above the tower deck. This is near head height. However, it should be emphasized that the tower and approach stairway are enclosed, locked, and protected by safety interlock switches to the transmitter. These interlock switches were defeated during measurements on the tower.

Figure 4-5 gives field intensity data for the ASR-4B radar measured on a distant tower at about the same height above ground as the transmitting antenna. The field at a distance of 84 m was about 0.6 mW/cm^2 . A comparison was made between two types of radiation monitors, the CIM-1 and the EDM-1C. In one case (row 2 of the data table) the antenna was fixed and a field intensity of 0.6 mW/cm^2 was read on the CIM-1. In another case (row 4) the antenna was rotating and a pulse-peak field of 1700 V/m was measured with the EDM-1C. This corresponds to a calculated free-space power density of 0.73 mW/cm^2 , which is 0.9 dB higher than the CIM-1 value. This discrepancy is not considered excessive because (a) the temperature coefficient of the EDM-1C was not calibrated for short-pulse fields, and (b) several calibration factors are involved in obtaining the approximate peak field value from the value indicated on the EDM-1C meter.

As seen from the third row of figure 4-5, the commercial radiation monitor does not respond to the narrow beam of a rotating antenna due to its lack of peak reading capability. The last two measurements given in the figure were taken at greater distances, below the center of the beam, using the more sensitive EDM-1C monitor.

Field intensity measurements were made of another ASR-4B radar, located at a commercial airport. The height of the tower deck for this particular antenna was 5.2 m (17 ft.) above ground. This is the lowest height normally used for an ASR antenna. An attempt was made to measure the field intensity at head height (1.7 m) in the vicinity of the tower base. However, the field was too weak to produce an indication on the CIM-1 meter, even with the antenna rotation disengaged. One measurement at a horizontal distance of 15 m from the tower, at a height above ground equal to the bottom of the antenna reflector, produced an indication of 0.04 mW/cm^2 .

A series of measurements was taken to determine the field in the very near zone of the antenna. Figure 4-6 gives the values for vertical and horizontal cuts through the center of the direct beam, at a horizontal distance of 3.66 m (12 ft.) from the center of the tower.

The axis of antenna rotation (vertical line through the center of the tower) is considered to intersect the phase center of the antenna. The distance from the antenna to the middle measurement point was thus 3.66 m (12 ft.). The distance between the center of the reflector and the nearest point above the middle of the tower railing, inside edge, was 3.96 m (13 ft.). The maximum intensity found in the beam center at this distance was 49 mW/cm^2 (430 V/m).

Figure 4-7 is a graph of the data given in figure 4-6. It is evident that the near-zone beam is narrower in the vertical plane than in the horizontal. This contrasts with the far-zone antenna pattern, specified as 1.5° horizontally and 5° vertically. Also noticeable in the figure is the relatively large lobe in the near-zone vertical pattern, about 3 dB weaker than the main beam, which is at an angle of about 5° above the horizontal.

4.1.2 Field Intensity of ASR-7 Radars

Two series of measurements were made to obtain additional data for determining the profile of the aperture illumination of an ASR antenna. Figure 4-8 gives data for the field very near the reflector screen or aperture of an ASR-7 antenna at Los Angeles. These data were used in an attempt to calculate the intensity of the on-axis beam at various distances from the antenna, including the far zone, as discussed in section 4.5. The tower height for this antenna was 14.3 m (47 ft.). Figure 4-9 gives data for a series of measurements at a distance of 3.66 m, similar to that of figure 4-6. As can be seen, the intensity for the ASR-7 radar was slightly less than that of the ASR-4B. The ASR-7 transmitter is a newer solid-state version of the ASR-4, using the same type of antenna at both installations. The desired coverage at this location was 60 miles (97 km) for the ASR-7 radar and 70 miles (113 km) for the ASR-4.

An attempt was made to measure the field intensity of the ASR-4B and ASR-7 radars while standing on the roof of the airport control tower, which is between the two ASR antennas. However, the time-average field of the rotating antennas was too weak to cause any measurable indication on the commercial CIM radiation monitors.

Field intensity data for another ASR-7 radar were obtained at the National Aviation Facilities Experimental Center (NAFEC) near Atlantic City, New Jersey. Figure 4-10 gives field intensity data for the center of the beam between the antenna feed point and the center of the reflector screen, and also some miscellaneous readings taken near the reflector. Figure 4-11 gives the measured field values for vertical and horizontal cuts through the center of the beam, above the tower railing, at a horizontal distance of 3.66 m. These data are similar to those given in figures 4-6 and 4-9 for other ASR antennas.

4.1.3 Field Intensity of an ASR-8 Radar

Two series of measurements were made of a newer and more powerful type of ASR radar, at the Aeronautical Center in Oklahoma City. Measurements in the direct beam of the ASR-8 antenna at a height of 15 meters (49.2 ft.) above ground were accomplished with the aid of a "cherry picker". A photograph of the operation, with the antenna visible in the background, is shown in figure 4-12. Figure 4-13 gives the measured field values for vertical

and horizontal cuts through the center of the near-zone beam at a distance of 23.1 m. The field in the center of the beam was 20 mW/cm^2 (274 V/m). The radar transmitter was operating at full power, with both channels turned on, producing a total average power of 1537 watts. This power level is about five times greater than that of the ASR radars previously tested. The pulses of one transmitter channel were keyed $1.4 \mu\text{s}$ behind that of the other (slave) channel. The transmitter was set to produce circular polarization. All of the data reported here were taken with the antenna rotation disengaged.

The field intensity in the center of the ASR-8 beam was also measured as a function of distance from the antenna. These measurements at a height of 15 m were made possible by the availability of a mobile "cherry picker." The field values ranged from 20 mW/cm^2 at a distance of 23.1 m, down to 0.1 mW/cm^2 at 397 m. The measurements were made with the antenna tilt angle and azimuth angle adjusted (at each location) for maximum indication on the radiation monitor. A table of the data is given in figure 4-14 and graphs of the field strength versus distance and inverse distance are shown in figures 4-15 and 4-16. It can be seen that the ASR-8 radar produced a field of 10 mW/cm^2 at a distance of 35.7 m (117 ft.) from the antenna.

4.2 Air Route Surveillance Radars (ARSR)

The FAA operates and maintains nearly 50 ARSR-1 and -2 type "long-range" radars in the continental United States (CONUS) for air route traffic control, which were installed prior to FY-74. In addition, a quantity of ARSR-3's are being implemented in FY-75 and later. Also, the FAA maintains a number of military types of long-range radar in the CONUS, under a joint civil/military program. These radars operate in the 1.25 to 1.35 GHz band with a nominal peak power of 4 MW during the $2 \mu\text{s}$ pulses. A photograph of an ARSR-1E installation is given in figure 4-17, showing a plastic radome on the antenna tower and transmitter building on the left. Figure 4-18 shows an ARSR-1D installation in which the antenna is visible (background) since no radome is employed. As seen, the type CA-4000 reflector of this antenna is somewhat elliptical in cross section. The main deck of this tower is 15.8 m (52 ft.) above ground. The height of the center of the reflector is 20.2 m (about 66 ft.) above ground.

Figure 4-19 is a sketch of an ARSR antenna installation giving approximate dimensions. The antenna reflector is approximately 5.5 m high by 12.2 m wide (18 x 40 ft.). The antenna has a specified far-field -3 dB beam width (horizontally) of 1.4° and rotates at three to ten RPM. The nominal gain along the axis of maximum radiation is 34.2 dB. Either horizontal or circular polarization may be selected. The nominal peak power of an ARSR transmitter is 4 MW with the "amplitron" (rf amplifier) turned on, but may be operated at 500 kW or less with the magnetron only. The pulse duration (τ) is 1.8 to $2 \mu\text{s}$ and pulse repetition rate (PRR) is 350 to 370 per second, resulting in a duty factor (τ)(PRR) of about 0.0007. The average power of the transmitter is thus 2.8 kW with the amplitron on and 350 W for the magnetron only. The ARSR at the Aeronautical Center in Oklahoma City is used mainly for training purposes and is often operated with the magnetron only in order to reduce possible rf interference.

A field intensity survey was made inside the ARSR transmitter building for leakage fields, especially from the amplatron rack and rf transmission lines, but the measured levels were negligible. After defeating the safety interlock switch on the door of the amplatron cabinet, it was possible to obtain readable indications at several locations. The largest value was 0.4 mW/cm^2 , found inside the transmitter cabinet.

Figure 4-20 gives data for a survey made in the "mezzanine" area just below the top deck of the ARSR-1D antenna tower. The mezzanine area is the highest deck normally accessible to personnel. The transmitter was operated at its full power of 4 MW and the antenna was rotating in the usual search mode. Field intensities were measured with the EDM-1C radiation monitor, which had been calibrated previously in an anechoic chamber for making approximate measurements in this type of pulsed field. The last data point in figure 4-20 gives the maximum hot spot found at head height (1.7 m) on the mezzanine deck. The measured (E pk) value of 1220 V/m corresponds to an average Hermitian magnitude of 33 V/m, or an equivalent plane-wave power density of 0.29 mW/cm^2 . Even though the average field level is low, the peak field of 1220 V/m is high. It was stated that an ordinary flash bulb attached to a camera was fired by the rf field in this location.

The next measurements were made of the field on the upper deck of the ARSR-1D tower. It was necessary to defeat safety interlock switches at the locked gate between the mezzanine deck and upper deck of the antenna tower. The interlock switches disconnect the power to the transmitter and antenna rotator motor. The time-average value of field in the vicinity of the non-rotating ARSR antenna was measured with the CIM-1 monitor. Figure 4-21 is a photograph of measurements being taken at antenna height on the upper deck of the ARSR antenna tower. The antenna feed and lower portion of the reflector are visible in the foreground of the picture, and the CIM-1 sensor mounted on a polyfoam tower is seen at the far edge of the tower deck. The maximum intensity measured in the center of the beam at this distance of 9.5 m, above the deck railing, was 15 mW/cm^2 (238 V/m).

Field intensity data for three different ARSR transmitters were taken at the following antenna sites: (1) ARSR-1D at Oklahoma City, (2) ARSR-1E at Parker, Colorado near Denver, and (3) ARSR-2 at Elwood City, New Jersey near Atlantic City. The transmitter power levels used and the measured fields for these three installations were very similar. Consequently the fields reported here represent the average value of the three locations tested. Figure 4-22 is a summary of the data obtained with the CIM-1 and CIM-2 monitors. The four reported field values above 60 mW/cm^2 were actually taken at 1/8 the power level, transmitting with the magnetron only, and the values shown have been multiplied by a factor of eight. As seen in the first set of data, the maximum intensity measured at head height on the tower deck was 1 mW/cm^2 . Very intense fields were measured between the antenna feed horn and the reflector screen. The maximum field above the antenna rotator pedestal, in the center of the beam, was 48 mW/cm^2 . The level increased as the feed point was approached, reaching 600 mW/cm^2 at a distance of 60 cm from the feed. The final measurement in the beam center was at a distance of about 83 m (275 ft.) from the antenna, where the field was 1.2 mW/cm^2 (67 V/m).

Figure 4-23 gives additional data on ARSR fields measured with the EDM-1C monitor below the center of the beam at various locations in the FAA Aeronautical Center. The ARSR antenna was rotating so there was no indication on the commercial monitors. The first measurement location was on the roof of the VORTAC building, 310 m from the transmitting antenna. The next measurements were made in the top floor rooms of the CAMI building at a distance of 560 m. There was no measurable field penetrating the wall of the building but weak fields were noted at the windows facing the ARSR antenna tower. The average field intensity of 0.02 mW/cm^2 , registered momentarily during each rotation of the ARSR antenna, is nearly three orders of magnitude below the level generally considered hazardous. However, the pulse-peak level may be sufficient to cause interference problems. As shown in the third set of data, a search was also made near Hanger No. 9. The average fields of the ARSR (and ASR) antennas were very weak at this location ($< 0.01 \text{ mW/cm}^2$), but the peak amplitudes were high enough to produce a meter indication during each antenna rotation.

4.3 Air Traffic Control Beacon Interrogator (ATCBI) and Omni

In order to identify an individual radar echo picked up on an ASR or ARSR radar, a pulse-coded system is used in which a ground "beacon" interrogates the airplane on 1.03 GHz and receives a coded reply from the aircraft transponder on 1.09 GHz. The transponded reply contains an "IFF" type of identification, radar target reinforcement, and other information such as the airplane altitude. The ATCBI antenna is generally co-sited with the primary radar antenna. For example, the narrow beacon antenna is visible above the large radar reflector in figures 4-1 and 4-18. This phased-array antenna has a nominal gain of 21 dB. However, the transmitter average power output is only 1.2 W and the field intensity of the radiated pulse signals is very low. The beacon antennas produced no measurable contribution to the existing ASR or ARSR fields. In fact, the intensity measured 5 cm from the antenna, with the primary radar turned off, was below the minimum measurable level of 0.02 mW/cm^2 .

Another antenna usually co-sited with the ATCBI is a stationary whip called the "omni" antenna, used for achieving "effective" side-lobe suppression of the beacon signal. This non-directional antenna has low gain but is fed a higher-power pulsed signal than the beacon, also at a frequency of 1.03 GHz. The maximum intensity of the field measured with the CIM sensor touching the side of the whip (5 cm spacing) was 0.04 mW/cm^2 .

4.4 Airport Surface Detection Equipment (ASDE)

This recent type of primary radar is utilized at several major airports to detect the presence of aircraft and vehicles on the runways and taxiways, or aircraft at an altitude below about 30 meters. The ASDE radars are similar to the ASR but use shorter pulses and much lower power, for observing close-in targets. The ASDE readout oscilloscopes are located in the control tower as an aid to visual observation by the controllers. The rotating antenna is generally located above the control tower but may be mounted on a separate tower. This type of radar is used only on demand, for example when visibility is poor or at night.

The CIM-1 and CIM-2 radiation monitors were calibrated to measure the intensity of ASDE radars, both at 14 GHz and at 24 GHz. These calibrations were accomplished by placing the probes in the calculated field of pyramidal horns calibrated previously at NBS. The appropriate correction factors have been applied to all the ASDE field intensity measurements reported in this section.

4.4.1 ASDE-1 Radar in the 14 GHz Band

The CIM-1 radiation monitor was used to measure the field intensity of an ASDE-1 radar at Los Angeles International Airport. This facility has the only 14 GHz ASDE radar in the country. The measurement was considered important because the ASDE radars at 24 GHz are scheduled to be phased out and replaced gradually by new equipment operating at a frequency near 16 GHz. The FAA plans to install these radars at about 35 airports over the next 10 year period.

The radar transmitter has a nominal pulse power output of 25 kW at a frequency of 14.1 to 14.3 GHz. With a nominal pulse duration of 35 ns and repetition rate of 15 khz, this represents an average power output of 13 W. The ASDE transmitter in use had a pulse duration of 30 ns and a measured average power of 11.3 W. Because of the 5 dB loss in the 18 m length of WR-75 waveguide feedline between the transmitter/receiver and the antenna, this resulted in a delivered power of 3.6 W.

The ASDE antenna at Los Angeles is mounted on the roof of the control tower about 37 m above ground level. The blade-shaped antenna is similar in appearance and sound to a helicopter rotor, having a scan rate of 150 RPM. It consists of a waveguide slotted array approximately 4.4 m long, a horizontal width of about 0.5 m, and a maximum thickness (vertically) of about 0.2 m. The circularly polarized beam has a specified width of 1/3 degree horizontally and 10° vertically. The nominal antenna gain is 35 dB.

The average field produced by an ASDE radar is relatively weak and no measurable intensity was detected in the control tower, either when the antenna was scanning or stationary. The field at the radiating edge of the antenna was greatest near the axis of rotation. The maximum value, with the CIM-1 sensor touching the antenna "radome", was 0.59 mW/cm². Figure 4-24 gives measurements of the time-average field strength for the non-rotating ASDE antenna.

4.4.2 ASDE-2 Radars in the 24 GHz Band

This type of radar transmitter has a nominal pulse power output of 36 to 50 kw at a frequency of 23.6 to 24.5 GHz. With a pulse duration of 20 ns (0.02 μ s) and a repetition rate of 14.4 kHz, this represents a duty factor of 0.00029. The rated average power is thus 11 to 14 W. The measured power for the installation in Atlantic City was 14 W at the directional coupler near the transmitter, resulting in about 7 W delivered to the antenna. The shape of the pulses is roughly a narrow isosceles triangle.

In contrast with the ASDE-1 slot antenna, the ASDE-2 radar uses a feed horn and rectangular reflector which is 3.7 m wide and 1.2 m high. The specified 3 dB beam width is 0.25° horizontally and 1° vertically. The nominal gain is 45 dB and the scan rate is 60 RPM. There is a choice of vertical or circular polarization. The distance between the antenna feed point and center of the reflector is 1.5 m. The height of the antenna tested was about 30 m above ground.

The maximum field intensity measured for an ASDE-2 radar was 80 mW/cm^2 , with the CIM-2 sensor sphere touching the antenna feed horn. Figure 4-25 gives measurements taken on the tower for the case of a non-rotating antenna. A search was made for rf leaks in the waveguide feeder between the transmitter and antenna but no measurable fields were located.

4.5 Near-Zone Gain Reduction of Large Aperture Antennas

As stated in section 2.1, power density in the far zone of a transmitting antenna may be calculated accurately from the simple expression given in eq. (8). However, computation of near-zone intensity requires more complicated techniques. Several theoretical approaches which have been used are discussed in references [11] to [17]. The value of gain for any given antenna, G in eq. (8), is a constant which applies to far-field conditions. As a first approximation for determining the possibility of hazard-level fields, the intensity calculated from eq. (8) may be considered as a "worst-case" value for near-zone situations. However, the "effective" gain generally decreases for distances less than about $2 D^2/\lambda$, where D is the largest dimension of the antenna. For smaller distances the equation may be modified to read:

$$S = \frac{PG}{4\pi d^2} [F(d)] \quad (10)$$

In the above equation, $F(d)$ is a near-zone correction factor which is a function of distance, varying from unity at a large distance, down to 0.01 or less at points very close to the antenna.

A small effort was undertaken at NBS to calculate $F(d)$ and the theoretical field intensity in the direct beam of ASR and ARSR radar antennas. Computer programs were written and graphs plotted for the on-axis power density and antenna gain reduction factor for distances out to $D^2/2\lambda$, where D is the width of the reflector. These programs were used to calculate the on-axis near-zone field intensities for several aperture illumination functions, including uniform illumination, cosine, cosine squared, and cosine cubed illumination tapers. Various combinations of these taper functions in the horizontal and vertical directions were also analyzed. The main purpose of this study was to compare the calculated field with measured values to see if near-field intensities can be predicted analytically. However, it appears that before a good comparison can be made between the computed and measured fields, it would be necessary to measure the illumination function more accurately and then test these values in the present computer program.

Figures 4-26 to 4-31 are graphs of computed fields for the ASR and ARSR radars as a function of distance from the antenna. The theoretical derivation involves inserting an assumed aperture illumination into the power density integral and then solving for the on-axis field intensity. The illumination function must specify both amplitude and phase at each point of the aperture plane. The integration (computer summation) can then predict field values at any distance, from the aperture out to infinity. The curves shown in the figures are actually calculations using the Fresnel approximation. This approximation was checked against the direct numerical integration (which requires more computer time) and the difference in the final answer was found to be insignificant. Thus the main source of inaccuracy stems from the uncertainty in the aperture illumination function. Perturbations caused by the feed and mounting assembly were also neglected but these were relatively minor.

An attempt was made during the field intensity surveys to determine an aperture field distribution experimentally, for example in the plane above the ASR tower railing. However, due to the difficulty of precise near-zone measurements and the complicated structure of the antenna reflector (not a simple paraboloid producing constant phase) this was not possible. Agreement with experiment has thus only been qualitative and not precise, but the theoretical model used here is nevertheless considered to be the best which is presently available.

5. SURVEYS OF INSTRUMENT LANDING SYSTEMS (ILS)

The FAA maintains over 500 ILS installations which use runway "localizer" antennas in the 100 MHz band and "glide-slope" transmissions in the 300 MHz band. The localizer provides horizontal (lateral) guidance and the glide-slope provides vertical (descent angle) guidance for aircraft approaching a runway during the last few miles prior to landing. A sketch of the components and layout used for the instrument landing system is given in figure 5-1.

A new and improved type of instrument landing system referred to as the microwave landing system (MLS) has been developed during the past several years. It is presently anticipated that this new system will be implemented gradually to augment the present ILS system and that it may eventually replace existing ILS facilities. The MLS has components which transmit in the 5 GHz region.

5.1 VHF Localizer Antenna Arrays

A localizer antenna array is situated about 300 m from the end of a runway, on the runway centerline. The antenna radiates a horizontally polarized signal with modulation frequencies of 90 Hz and 150 Hz. There are 20 available channels, with assigned frequencies on the odd-tenth MHz values between 108.1 and 111.9 MHz. The even-tenth MHz frequencies are used for VOR navigation aids. Most of the localizer transmitters have a power output up to 200 W.

5.1.1 Eight-loop Localizer

This older type of runway localizer consists of eight antenna "elements" in a straight-line array, as shown in the sketch of figure 5-2. Each element is covered by a plastic mushroom-shaped radome. The figure shows a top view of the array and a side view of one element in the array, giving approximate dimensions. This antenna is also called an Alford Loop array. The nominal power output of the transmitter is 200 W, but the measured power during our test was 135W for the carrier and 2.75 W in the sidebands. The power actually delivered to the antenna, situated 150 m from the transmitter building, was reduced by loss in the No. 217 coaxial transmission line. Most of the power delivered to the antenna is fed to the two inner elements of the array.

Part I of figure 5-3 gives the measured electric field at the indicated locations. The actual measurements were of the energy density in nJ/m^3 , which have been converted to the Hermitian magnitude of E , in V/m. The maximum intensity 5 cm from the side of each radome occurred at a height 25 cm above the bottom of the radome, which is 1.3 m above ground level. The highest field measured was 255 V/m, an equivalent plane-wave power density of 17.3 mW/cm^2 . The field intensity decreases at greater distances in front of the antenna array. The intensity in front of the array also varies with height above ground. At a distance of 4.6 m in front of the antenna, the height having maximum field strength was 2.1 m above ground level. The field at this point was 15 V/m. At a distance of 15 m the intensity increased with increasing probe height, from ground level up to the maximum height tested of 2.7 m.

Measurements were also taken of the magnetic field produced by the eight-loop antenna, using the (uncalibrated) CIM-3 monitor. As shown in Part II of figure 5-3, the H field had a maximum value at a height about 15 cm above the point where the E field maximum occurred. This highest indication was 18 mW/cm^2 , an equivalent plane-wave H field of 0.69 A/m .

5.1.2 V-ring Localizer

The V-ring localizer is an improved type of antenna which permits reduced transmitter power compared with the eight-loop array. This antenna consists of 15 V-ring elements which (in Denver) are mounted 2.3 m above a metal counterpoise measuring $6 \text{ m} \times 33 \text{ m}$. The total length of the antenna array is approximately 32 m. Each element consists of a driven elliptical ring fed across a teflon-spaced "gap", and a V-shaped reflector. Greater power is fed to the center element, with power per element decreasing toward the outside of the array. The EM field pattern in the near zone above the metal counterpoise is quite complex and would be difficult to measure except with an isotropic probe.

Figure 5-4 is a photograph of one antenna which was surveyed and figure 5-5 is a closer view showing an operator near the EDM-1C radiation monitor. In this photograph the probe is attached to the metering unit (no intervening cable) and both are supported on a plastic pole. The sensor end of the probe is nearest to the radiating element. Figure 5-6 is a sketch of one V-ring element showing the shape and approximate dimensions.

Figure 5-7 is a top view of half of the localizer array, with dimensions and locations of the field measurement points. The figure includes values of field intensity at some of these positions. The rf field was essentially symmetric with respect to the center element, so numbers on the figure represent mean values for the left and right sides. The "hottest" point for each V-ring element was at the electrical gap in the ring. As seen, all the field values were below 194 V/m (10 mW/cm^2) except at the gap of the center element and each adjacent element. The field strength 2.3 m above the front edge of the counterpoise (antenna height) varied from 34 V/m in front of the center element to less than 2 V/m at the left or right edge of the array. The intensity at head height (1.7 m) above the metal counterpoise, directly beneath the center ring gap, was about 30 V/m (0.24 mW/cm^2).

A "leakage" field was discovered near the cable junction box mounted on the counterpoise behind the center V-ring element. The maximum hot spot was at the right front corner, having an intensity of 66 V/m . The largest leakage field found inside the localizer transmitter building was near the sliding short of the tuner used to adjust antenna phasing. The measured field here was 62 V/m at a 5 cm spacing from the tuner, and 39 V/m at a 10 cm distance.

Measurements of another V-ring localizer were made at the Aeronautical Center in Oklahoma City. The nominal transmitter power of 100 W was less than that maintained in Denver. Figure 5-8 gives the measured values of field strength 5 cm and also 33 cm from each ring gap. The field at the 5 cm spacing varied from about 100 V/m at the center element gap to about 10 V/m at the two outer elements. Figure 5-9 gives data for a profile of field intensity at several distances in front of the center V-ring element and at

several heights above the ground-level counterpoise. A graph of this data is given in figure 5-10. It can be seen from the graph that the field strength at head height (1.7 m above ground) varied from 14 V/m at the center antenna element to 7 V/m at a distance 3.7 m in front of the center element.

The measured field intensities of a third V-ring localizer antenna installation are given in figure 5-11. This site in Oklahoma City has no ground screen or elevated counterpoise. The newer EDM-3 radiation monitor was used to make this survey. In spite of the close measurement distances involved, the maximum field intensity found was 136 V/m, which occurred at the gap in the ring of the center V-ring element.

5.1.3 Traveling-wave Localizer

Another type of runway localizer array surveyed is shown in figure 5-12. This D6 traveling-wave antenna has 14 elements, each made of 15 overlapping circular rings. The length of each element in the array is 4.6 m. Each ring has a diameter of approximately 54 cm, thus being about 1/2 wavelength in circumference. The average spacing between adjacent elements was approximately 2.0 m except for the two center elements which were spaced 1.6 m apart. The height of the antenna array was 2.2 m above the ground. The transmitter has a nominal power of 100 W. The measured carrier power output was approximately 25 W and the power delivered to the "cable distribution box" at the antenna would be about half this amount. The power leaving the output (front) end of each antenna element and returned to the junction box through a coaxial cable is nominally 40% of the power entering the input (back) end of the element.

Field intensity measurements were made in the near zone of the "course" beam (front array), which has a narrow pattern and is normally fed about 3/4 of the total transmitter power. The "clearance" beam (back array) has a broader pattern but was turned off during this survey. Figure 5-13 gives the field intensity data. Measurements were made 30 cm in front of the center of each antenna element. The highest intensity was 7.4 V/m directly in front of the second element on either side of center. The two outer elements produced a field of only 1.5 V/m at the 30 cm distance, which is the minimum discernible level for the EDM-1C monitor. No hot spots or areas of high intensity were located. This contrasts with the higher levels measured previously at the gaps in the rings of the V-ring localizers.

5.1.4 Waveguide Localizer

A waveguide type of localizer with an improved radiation pattern is used at certain sites. When this antenna is used, the transmitter for the waveguide "course" array is set a few kilohertz above the assigned channel frequency and the regular "clearance" array transmitter is set a few kilohertz below. The site surveyed, in Los Angeles, employs an 8-loop antenna for the clearance array, which is situated about 15 m behind the waveguide course array. The transmitter operated at a carrier power of 150 W and sideband power of 4.7 W. The power delivered to the antenna was less because of loss in the 100 m length of coaxial transmission line.

The waveguide localizer tested consists of a slotted array with 18 feed slots spaced $5/8$ wavelength apart. The antenna is mounted on pedestals about 0.6 m above ground level. The metal enclosure for the array is 1.65 m high and is composed of 20 sections, each 1.8 m long. The total length of the antenna enclosure is approximately 36 m. Figure 5-14 is a photograph showing the plastic radome in front of one of the slot radiators. The CIM-3 probe is being held at the position of maximum H field. The E field is maximum near the center of the protruding radome.

Figure 5-15 gives data for two types of measurements, one of electric field intensity and the other of magnetic field. Measurements were made in front of each of the 18 slot radiators. In the first set of E field data (5 cm spacing) the EDM-3 probe sensor was touching the front-center of each radome. In all three sets of E field data the probe handle was held horizontal and parallel to the front surface of the localizer, that is, perpendicular to the direction of propagation. The highest readings observed were at the inner two radomes, with an average value of 144 V/m. This is equivalent to a plane-wave power density of 5.5 mW/cm^2 . The H field reading was maximum with the sensor sphere touching the slanted front surface near the top or bottom of the radome. Each number shown in the first set of data (5 cm spacing) is the average of two readings, one at the top and one at the bottom of the radome. The highest reading observed was 45 mW/cm^2 , which corresponds to an H field of 1.1 A/m, or an equivalent E field of 412 V/m.

Measurements of field intensity were also made as a function of distance in front of the waveguide localizer. These data are given in figure 5-16. The readings were taken on a line perpendicular to the front surface of the localizer, midway between the No. 8 and No. 9 slot radiators, at the same height as the center of the radomes (1.4 m). For these measurements the operator was kneeling on the ground, holding the probe handle upward (45° above horizontal) and to one side (perpendicular to the direction of propagation). The E field values shown decrease from 24 V/m at a distance of 1 m to 4.5 V/m at a 12 m distance.

5.2 UHF Glide-slope Antennas

Vertical guidance during instrument landing is provided by glide-slope transmissions in the 328.6 to 335.4 MHz frequency range. Twenty channels are assigned at 0.3 MHz intervals which are paired one-for-one with the 20 localizer channels. Figure 5-17 is a photograph of a glide-slope antenna installation showing the two antenna elements. The radiated emissions from a glide-slope antenna produce a series of vertical lobes in the far-zone pattern with a null on the desired descent angle of 2.5 to 3 degrees. The aircraft receiver detects a 90 Hz modulation signal when it is above the assigned glide path and a 150 Hz modulation when it is below the path.

Field intensities were measured in the near zone of a glide-slope ILS antenna at the Aeronautical Center in Oklahoma City. This installation has three antenna elements in a vertical array. Figure 5-18 is a photograph of the lower element in the "two-lambda" array. Each rectangular element is protected by a plastic radome approximately 0.9 m high by 1.8 m wide. The transmitter had a nominal power of 10 W at a frequency of 331.7 MHz.

The measured power delivered to the element surveyed was only about 1 W. The polyfoam sphere of the EDM sensor was held against the radome, which bulges out about 30 cm toward the front. The field intensity at the center of the radome was 20 V/m. Two hot spots were found about 18 cm to either side of the radome center, each with a field strength of 42 V/m.

Another type of glide-slope antenna was surveyed for comparison purposes, as shown in figure 5-19. This transmitter was operating at a frequency of 333.5 MHz and a delivered power to the antenna element of about 1 W. The field intensity measured 1 m in front of the center of this antenna element was 6.7 V/m. The maximum intensity found along the front of the radome (see figure 5-19) was 21 V/m.

5.3 Microwave Landing Systems (MLS)

The present type of VHF/UHF system used by the FAA for instrument landing is often difficult or expensive to implement at certain sites. This is due mainly to the varying effect of rf ground reflections at these frequencies. Shifting to microwave frequencies would theoretically permit smaller antennas with beams that are independent of the local site conditions. Therefore various types of microwave landing guidance system (LGS) were tested at the National Aviation Facilities Experimental Center (NAFEC) near Atlantic City, New Jersey. The types undergoing tests operate in the Ku band at 15.4 to 15.7 GHz or in C band at 5 to 5.25 GHz.

The field intensity surveys made by NBS involved only the ground facilities of MLS; no tests were made of airborne equipment. The types of MLS transmitters surveyed employ a rather complicated switching and modulation, producing a combination of pulsed and non-pulsed signals. The transmitter power level of about 20 W is relatively low and the transmitting antenna arrays have relatively extended source areas. Consequently, there were no local regions of extremely high power density such as the feed/reflector type of antennas measured for some of the radar systems.

Figure 5-20 is a photograph of an operator measuring field intensity at the aperture of an MLS "elevation" antenna and figure 5-21 shows an MLS "azimuth" antenna. The aperture height of the 15 GHz EL-2 antenna is 2.44 m (8 ft.) while the aperture height of the 5 GHz EL-1 antenna is 3.66 m (12 ft.). The specified beam width is 0.5° for the EL-2 antenna, which has 139 elements, while the beam width is 1° for the EL-1 antenna, which uses 81 elements. The electrical scanning rate is 10,000 degrees per second for the EL-2 antenna and 20,000 degrees per second for the EL-1 antenna. All of the radiated MLS fields are vertically polarized.

Figure 5-22 gives measured fields for the elevation antenna of the Ku band system at the EL-2 site. Figure 5-23 gives similar data for both the elevation and azimuth antennas of the C band system. It can be seen that all of the measured fields were quite low. The maximum intensity observed at the antenna aperture was 0.15 mW/cm^2 .

6. SURVEYS OF NAVIGATION SYSTEMS

Radio navigation systems that determine the position of an aircraft by measuring the bearing angle θ and distance from a fixed station are known as rho-theta systems. One method for measuring the bearing angle, θ , is VHF omnidirectional range (VOR) in which a pilot or navigator can obtain the azimuth reading of a transmitting VOR "beacon" antenna, regardless of the heading of the airplane. A conventional VOR operates in the 108 to 118 MHz frequency range. The distance measuring equipment (DME) of the ρ - θ navigation system is a pulsed type of transmission in which each channel of the DME is associated with a particular VOR channel. Tactical air navigation (TACAN) is a polar-coordinate radio navigation system that provides an airplane with both azimuth bearing and range from the ground station. The pilot can tune the airborne TACAN transponder to any desired channel. Commercial airlines generally use only the DME portion of TACAN, obtaining the bearing portion from VOR. A ground station with VOR transmissions and only the DME portion of TACAN is known as VOR/DME. A station equipped with both VOR and TACAN transmitters at the same site (co-sited) is called a VORTAC station. The DME interrogator in an airplane transmits on a channel in the frequency range 1025 to 1150 MHz. It receives a reply from the ground TACAN transponder on a frequency in the range 962 to 1024 MHz or 1151 to 1213 MHz.

6.1 VHF Omnidirectional Range (VOR)

A VOR transmitting antenna radiates an FM/AM multiplexed signal on one of 80 available channels. A cardioid antenna pattern is generated which rotates 30 times per second, resulting in a 30 Hz amplitude modulation in the airborne receiver. The bearing information is obtained from the phase difference between the FM and AM 30 Hz modulations. The 200 W transmitters are assigned to one of 20 even-tenth-MHz channels between 108 and 112 MHz (interleaved with the ILS localizer channels) or one of 60 tenth-MHz channels between 112 and 118 MHz. The VOR signal is fed to four Alford Loop antenna elements to provide an omnidirectional radiation pattern. By tuning to two different VOR stations, it is possible for a pilot to locate his position on a map by means of triangulation.

Figure 6-1 is a photograph of a VORTAC transmitter building in Oklahoma City. The conical tower on the roof houses the VOR antenna in the base and the cylindrical TACAN antenna on top. The circular metal roof of the building has a diameter of 15.8 m (52 ft) and serves as the counterpoise for the VOR antenna. The base of the plastic conical tower has a diameter of 3.4 m (11 ft) and the height of the tower is about 6 m from roof level to the base of the TACAN radome.

The data reported in figure 6-2 pertain to the 110 MHz VOR signal only, with the TACAN transmitter turned off. In the first series of measurements, the field strength at antenna height (1.2 m) above the outer edge of the building roof was 16 to 18 V/m. The next two sets of data in the figure are measurements taken with the EDM-1C sensor sphere touching the outside of the conical tower at a height equal to the center of the VOR antenna. The probe handle was held perpendicular to the side of the cone. The VOR signal has a 30 Hz modulation produced

by an electrical rotation of the cardioid-shaped beam. The measured average field strength with the beam rotating was essentially the same for any azimuth angle, at a level of about 68 V/m. With the beam rotation turned off, the level in the direction of maximum field was about 79 V/m. The field inside the plastic tower reached very high values when the probe sensor was brought close to the transmitting antenna, having a value of 194 V/m (10 mW/cm²) at a distance of 20 cm.

A "Doppler VOR" or "Mountain-Top VOR" site was also surveyed. This type of antenna has 50 "loop" elements in a circular array of 13.4 m (44 ft) diameter, plus one antenna element at the center of the circle. A Doppler VOR is used at locations which have an adverse terrain, such as the sand dune site in Los Angeles. A distributor feeds the 50 antenna elements consecutively around the circle at a rate of 30 revolutions per second, thus achieving a 30 Hz modulation. Figure 6-3 is a photograph showing the 51 mushroom-shaped radomes of the antenna array.

Figure 6-4 gives data on the measured time-average field intensity near each antenna element on the outer perimeter of the Doppler VOR antenna array. The nominal power of the VOR transmitter is 200 W. The power delivered to the 50 outer elements is approximately 10 W. Each radome had a base diameter of 80 cm, a base height 110 cm above ground, and a height of 70 cm between the radome base and top. The spacing between the radome centers was 85 cm and the separation between radomes (nearest point) was 4 cm. The measured field strength at the radome surface (5 cm distance), on the outer edge of the circular array, was greatest at a height about 13 cm above the radome base. The average value was about 11.5 V/m. The intensity between two adjacent radomes was greatest at a height of 7 to 9 cm above the base, having an average value of about 16 V/m.

The center radome of the antenna array was about 15 cm higher than those on the outer perimeter and the field intensity was much greater near this element. The carrier power delivered to the center element was 55 W. Figure 6-5 gives the measured field strength near the center "mushroom" element and also on a north-south line across the center of the circular antenna array. The readings were taken at a height above ground having the maximum field, which was about 12 cm above the base of the radomes. Figure 6-6 gives some measurements of magnetic field near the Doppler VOR antenna. Field intensities up to 60 mW/cm² were found near the center antenna element at locations 5 cm beneath the bottom of the radome surface.

6.2 Tactical Air Navigation (TACAN) and VORTAC

The standard ρ - θ system of airline navigation is obtained from the DME portion of TACAN plus VOR. When both ground station antennas are co-sited, the combination is known as VORTAC. By tuning to two or three different DME stations, it is possible to use a map and compass construction to determine the airplane's location. The military version of TACAN includes both the DME and azimuth information in a single transmission. An airborne TACAN interrogator transmits about 30 pulse-pairs per second on one of 126 channels between 1025 and 1150 MHz. A ground TACAN transponder replies on one of 126 channels between 962 and 1024 MHz or between 1151 and 1213 MHz, each channel occupying a 1 MHz band.

6.2.1 Ground TACAN Transmissions

A ground TACAN antenna radiates a vertically-polarized nine-lobed pattern which rotates at a rate of 15 times per second. The distance measuring function is achieved by measuring the round-trip transmission time of pulses from the airborne interrogator to the ground transponder. TACAN pulses are cosine-squared in shape, nominally 3.5 μ s wide, generated at a maximum repetition rate of 3600 pulse pairs per second. The spacing between the pulses in each pair is 12 μ s but the spacing between pulse pairs is random, with a minimum value of 60 μ s. A TACAN signal is mechanically modulated by a rotating director at a rate of 15 revolutions per second.

TACAN transmitters operate at a nominal pulse-peak power of 10 kW and average power of about 200 W. The measured field strength on the roof of a VORTAC building (see figure 6-1) is quite low because the antenna is mounted on top of a tower 6 m high, and the beam is directed slightly above the horizontal. No significant field could be found on the building roof except above the outside edge, with the probe held high above head level. A search was then made for leakage fields inside the transmitter room, but none could be found except inside the transmitter cabinet after defeating the safety interlock switch. The near-zone field of a TACAN transmitting antenna was measured at the TACAN Academy in Oklahoma City and at the Los Angeles airport. In both cases an RTB-2 transmitter was operated at a frequency near 1 GHz into a Type FA-6239 antenna. Checks were made inside the transmitter rooms for stray EM fields, such as leakage from equipment racks, but no hot spots were found. The highest reading noted was near the transmitter exciter amplifier stage, at a level of 0.05 mW/cm².

Figure 6-7 is a photograph of measurements being taken on a 3.7 m square (12 ft x 12 ft) TACAN tower in Oklahoma City. The plastic radome shown on top has a height of 1.4 m and diameter of 1.1 m. The top of the radome is 3.3 m above the tower deck level. Figure 6-8 gives measurements of the field taken with the commercial CIM-1 monitor at points near the TACAN radome. The location of highest field strength at the radome surface was 46 cm below the top. The maximum intensity found at this height, searching around the entire periphery of the radome, was 4.5 mW/cm² (130 V/m).

Measurements of TACAN fields were also made on the sand-dune site in Los Angeles, which is adjacent to the Doppler VOR antenna site. The measured levels (figure 6-9) are much lower than those obtained on a similar survey in Oklahoma City (figure 6-8). The first set of readings in figure 6-9 was taken on a vertical line at the side of the radome (5 cm distance), with the probe handle horizontal and perpendicular to the radome surface. A second set of readings was taken as a function of distance from the side of the radome, at the height of maximum field. The highest indication at the surface of this TACAN antenna was 0.18 mW/cm² (26 V/m).

6.2.2 X-Radiation of a TACAN Transmitter

The Klyston Tube used in a ground TACAN transmitter operates at a cathode potential of 24,000 volts. It was thus suggested that a few measurements be made to check for possible x-rays emanating from the equipment racks in the TACAN transmitter building. A battery-operated x-ray monitor was used which has full-scale meter readings of 3, 10, 30, 100 and 300 mR/hr. This commercial radiation monitor was calibrated with a known x-ray source by the Physics Department of the University of Colorado. The upper limit generally adopted for this type of radiation is 1.25 R per calendar quarter, which is equivalent to about 1.75 mR per hour for a person exposed continuously for eight hours each working day.

Figure 6-10 gives the data taken on a survey for x-rays in the transmitter room of a ground TACAN. The probe of the x-ray monitor was held 2.5 cm (1 inch) from the ventilator screen or other measurement points as indicated in the figure. The only high readings obtained were with the metal cabinet doors open, which required defeating the safety interlock switches. The maximum reading found during normal operation with the cabinet doors closed was 0.2 mR/hr, which is less than one-tenth of full scale reading on the instrument's most sensitive range.

6.2.3 Airborne TACAN Transmissions

Field intensities were measured in the very near zone of several antennas on a Sabre jet aircraft. Figure 6-11 is a sketch showing locations of the navigation, communication and radar antennas on this type of airplane. The frequency band used for airborne TACANS covers 1025 to 1150 MHz. The transmitter power rating is 500 W minimum, pulse-peak value. Even at the close measurement distances tested, the average field strength did not exceed 1.3 mW/cm^2 (70 V/m). The measured field levels are given in figure 6-12.

7. SURVEYS OF COMMUNICATION SYSTEMS

The earliest air/ground radio communications were accomplished by means of telegraphy but voice equipment became reliable by about 1930. Before 1940 most of the communication transmissions were in the LF and HF bands. Later, when good VHF equipment became available, the lower bands were essentially abandoned for airborne communications. The present VHF aviation band is used mainly for civilian air/ground transmissions while the UHF band is used mainly for military aircraft. However, the 3 to 30 MHz HF band is still used, especially for long range transmissions of data and weather information.

7.1 VHF and UHF Fixed Transmitter Sites

Civilian aviation communication is assigned to the 118 to 136 MHz VHF band, generally employing 50 kHz channels. The FAA also provides communication service to military aircraft on 94 channels in the 225 to 400 MHz UHF band. Both the VHF and UHF transmissions are essentially line of sight. The VHF ground transmitters generally have a power output between 10 and 50 W while the power output of the UHF transmitters is generally 25 to 100 W.

A survey of field intensities produced in the near zone of VHF communication equipment was performed at the National Aviation Facilities Experimental Center (NAFEC) near Atlantic City, New Jersey. The transmitters in use had a maximum power output of 50 W but VHF field sites are generally operated with a power of about 30 W. Some of our tests were made with only the 10 W exciter turned on in order to determine the field level to be expected for lower power operation. A Type T-1108/GRT-21 transmitter was used as the exciter to drive an AM-6154/GRT-21 linear amplifier. Tests were made with two different transmitters, both of them tone modulated at 1 kHz with 90% amplitude modulation. One transmitter was tuned to 118 MHz and the other to 133 MHz.

The VHF antennas in use radiate a circularly polarized field and were identified as "Swastika" type because of their appearance. Figure 7-1 is a photograph showing the four 15 m (50 ft) high antenna towers located at the corners of a square 24 m (80 ft) on each side, with the transmitter building between the towers. Figure 7-2 is a closer view of one tower showing an operator on the center of the upper platform and the antenna mounted near one corner of the triangular tower. The coaxial transmission lines to the antennas have a diameter of 2.2 cm (7/8 inch) and length of about 30 m, with a line attenuation of about 2 dB.

A search was made for leakage radiation from the coaxial cables and equipment racks in the transmitter room but all the readings were below 2.6 V/m, the minimum measurable level of the EDM-3 radiation monitor. Figure 7-3 gives data on measured fields near the north antenna tower, at two different transmitter power levels, with the transmitter tuned to 118 MHz. Measurements were then made on the same tower with another transmitter, tuned to 133 MHz, but the data are similar and are not included here. Also, measurements were made of magnetic fields using the commercial H field monitor. These data are given in figure 7-4.

7.2 VHF/UHF Airborne Communication Antennas

Field intensity measurements were made near the antennas on a Sabre Jet aircraft. The locations of these antennas are shown in figure 6-11. The blade antennas used for communications are larger than the TACAN antennas and are sufficiently broadband to tune either the VHF or UHF frequency bands. The number 17 antenna, which is beneath the cockpit and behind the nose wheel, extended about 35 cm below the fuselage. It had a length of 18 cm at the tip and 25 cm at the fuselage. The VHF transceivers were tunable over a 116 to 152 MHz range and were operated at an estimated power output of 25 W. The UHF transceivers were tunable over 225 to 399 MHz and had an estimated power output of 5 W.

The field levels of the communication signals were much greater than the average fields of the pulsed TACAN signals. Intensities exceeding the maximum measurable level of the EDM-3 instrument (3000 nJ/m^3 or 823 V/m) were found at locations within a few centimeters of the antenna surface. Figure 7-5 gives the measured fields near the VHF/UHF antennas used for airborne communications on a Sabre Jet aircraft.

7.3 High Frequency (HF) Rhombic Antennas

Field intensity surveys were made near several of the transmitters, transmission lines, and beneath the large HF rhombic antennas in West Sayville, New York, on Long Island. These antennas are used for long range communications and transmission of weather data or weather forecasts. The transmissions are beamed toward Europe, Iceland, the Azores and North Africa. Several transmitters are operated simultaneously at power levels up to 50 kW each, using relatively close-spaced antennas in the frequency range 3 to 25 MHz. The antennas surveyed were all wire rhombics strung on 30 m high wooden poles. Figure 7-6 is a sketch of this transmitter site showing part of the rhombic antenna layout.

The measured electric field at head height (1.7 m above ground) beneath the transmitting rhombic antennas was rather low, ranging from 1 to 10 V/m. However, very intense fields were found at some locations near the open-wire transmission lines and near the transmitter cabinets. Parallel-wire lines are used between the transmitter building and rhombic antenna input, and also at the grounding end of each antenna. The two-wire lines had a spacing of about 33 cm and a characteristic impedance of about 660Ω . The electric field at a distance of 33 cm out from the center of the open-wire line was as high as 3000 nJ/m^3 (823 V/m), which is the maximum measurable level of the EDM-3 radiation monitor used. The magnetic field was also very intense near the transmission lines, with readings up to the maximum measurable level of 100 mW/cm^2 (1.63 A/m). A search was made for x-radiation near the cabinets of the high-power transmitters and near the neutralizing capacitor mounted above the transmitter, but all the readings on the commercial x-ray monitor were below the minimum measurable level of 0.3 mR/hr .

Figure 7-7 gives data on some miscellaneous measurements of stray E fields in the transmitter building. Figure 7-8 gives some values of E field measured outdoors near the open-wire transmission line for antenna number 14, beneath the rhombic antenna, and near the guy

wires of the wooden poles supporting the antenna and transmission lines. The open-wire line leaves the building at a height about 5 m above ground. The line is strung on wooden poles to antenna number 14 as shown in figure 7-6. The line height gradually decreases as the antenna is approached, having a height of about 3.5 m at the final transmission line pole. The line then ascends to the rhombic antenna input at point A in figure 7-6. The height of the antenna is about 30 m. There were two rhombic wires for this antenna, one of them below and inside the other. The antenna wires are tensioned by concrete weights which hang at the D and F corners of the rhombus. The bottom end of each counter weight is about 1.5 m above ground. An open-wire line descends vertically beside the pole at the far end of the rhombic antenna (point E in figure 7-6) to a height about 1 m above ground. The terminating resistance for each antenna is furnished by the ground loss of a horizontal "terminating" line which is strung near the ground between points E and B. This pair of wires gradually approaches ground level and increases in spacing until point B is reached, which is about 9 m from point A. The spacing of the two wires at the grounded end is about 1.8 m.

Figure 7-9 gives data on the electric field for rhombic antenna number 2, similar to that discussed in the previous paragraph for antenna 14. Figure 7-10 gives the measured values of magnetic field near the transmitter cabinet, transmission lines, and beneath antenna number 2.

8. SUMMARY

This project was sponsored by the FAA under an interagency agreement with the National Bureau of Standards. The objective was to survey electromagnetic fields near transmitting antennas at representative sites operated by the FAA. These sites include fixed air traffic control facilities, airborne equipment, or any system likely to produce an equivalent free-space power density exceeding 0.1 mW/cm^2 , or electric field magnitude above 20 V/m . Initial attention was given to identifying the probable sources of higher-level radiations and determining the adequacy of existing measurement instrumentation. The next step included calibration and modification (if necessary) of existing radiation monitors to achieve capability for measuring the complicated types of fields involved. The instrument calibrations required for measuring CW or pulse-modulated fields are covered in a Phase I letter report to the sponsor. A Phase II letter report discussed the measurement techniques used and data obtained in some "exploratory" field intensity surveys. Phase III of this project consisted of more extensive measurements of rf radiation levels at typical FAA sites. Results of the third phase are presented in this final report.

8.1 Field Measurement Instrumentation

The high level fields of interest in this contract generally occur close to the transmitting antennas (or a reflecting surface) and are likely to have a complicated EM field structure. Therefore, the most practical way to make field intensity surveys is with an isotropic probe, preferably one which does not perturb the field being measured. Suitable probes which meet the desired qualifications (in most respects) became available recently and were evaluated at NBS. The instruments utilized for the FAA surveys consist of three commercially-available radiation monitors and three NBS-developed monitors which all feature isotropic probes. The commercial instruments use thermocouple rf sensors and are designated CIM-1, CIM-2 and CIM-3 in this report (for commercial isotropic meter). The NBS-designed instruments use diode rf detectors and are designated EDM-1C, EDM-3 and EDM-4A in this report (for energy density meters). In addition, a commercial x-ray monitor was used for a few incidental measurements of x radiation.

The capabilities of the commercial and the NBS instruments are somewhat different, making the CIM's more useful for measuring the average fields of high-power microwave radars, while the EDM's are better for measuring the lower-frequency, lower-level, non-pulsed signals of navigation, communication and instrument landing systems. The three commercial monitors proved to be quite accurate for measuring the time-average value of either CW or pulsed fields, but cannot measure pulse-peak field values nor the intensity of a rotating radar antenna. The three EDM monitors can measure (within $\pm 3 \text{ dB}$) the "momentary" field of a scanning radar antenna by switching the metering unit to the "peak" mode. However, the EDM's then require the use of large calibrating factors which differ for each frequency and type of radar being tested. Consequently, only a few of these pulse-peak field readings are included in this report. The EDM's also incorporate some other features not commercially available, such as switches for selecting either a single E field component or the RSS value of three orthogonal components.

Both types of radiation monitors (CIM and EDM) employ an isotropic sensor embedded in a styrofoam sphere 10 cm in diameter. Thus the minimum measurement distance to an rf source is 5 cm (2 inches). All of the monitors except the EDM-3 use short-handled probes which make them susceptible to perturbation by the operator when the probe is hand-held. This field perturbation was found to be generally within ± 1 dB. The EDM-3 has a longer probe handle (1 m) which reduces the operator perturbation.

The five E-field monitors (CIM-3 measures H field) were calibrated by immersing them in standard (known) fields in the NBS laboratories. The CW calibrations are described briefly in section 2.3 of this report. They were performed as a function of ambient temperature, signal frequency, field amplitude, polarization, and orientation angle of the probe. Also, special calibrations of pulse-peak fields were made for the EDM-1C as a function of pulse duration, repetition rate and duty factor. However, most of the radar data were obtained with the CIM-1 and CIM-2 monitors, after stopping the antenna scanner. The magnitude of the standard field used for calibrating the E-field probes was known to within ± 0.5 dB for signal frequencies above 2.5 GHz. Between 0.5 and 2.5 GHz the field uncertainty was ± 0.7 dB, and below 0.5 GHz the uncertainty was ± 1 dB. The measured deviation from perfect isotropic response was less than ± 1 dB for all the probes, for fields incident in any direction other than through the handle.

The measuring range of the CIM-1 and CIM-2 E-field monitors is approximately 0.02 to 100 mW/cm² (9 to 600 V/m). The frequency range for response within ± 1 dB is 0.8 to 15 GHz, and for ± 3 dB response it is 0.3 to 20 GHz. The CIM-3 H-field monitor has a measuring range of 0.1 to 100 mW/cm² (0.05 to 1.6 A/m) over a specified frequency range of 10 to 250 MHz for ± 1 dB response. No corrections for ambient temperature are required when using the commercial instruments, providing the meters are re-zeroed frequently in a field-free environment.

The measuring range of the EDM-1C monitor is approximately 0.03 to 300 nJ/m³ (2.6 to 260 V/m). The frequency range for response within ± 1 dB is 10 to 4000 MHz. The measuring range of the EDM-3 is 0.03 to 3000 nJ/m³ (2.6 to 820 V/m) and the frequency range for ± 1 dB response is 3 to 2000 MHz. However, frequency correction factors for both instruments have been determined up to 10 GHz. The EDM-1C requires the use of a correction factor for ambient temperatures below or above 25°C. The EDM-3 has built-in temperature compensation and the error is less than 0.5 dB for temperatures between 15°C and 35°C. The EDM-4A employs longer dipole antennas, for use at lower frequencies and lower signal levels, but this instrument was seldom needed for the FAA field surveys. It has a measuring range of 1 to 200 V/m for signal frequencies from 300 kHz to 300 MHz.

8.2 Field Intensity Data

Aircraft radars. Field intensity surveys were made of five different aircraft radar sets. The fields in the beam center, with the antennas fixed in direction, were greater than 10 mW/cm² at the following distances: less than 3.0 m for an RDR-1B radar with radome removed, less than 1.8 m for an RDR-1E, less than 0.3 m for an RDR-1200, less than 6.1 m for an AVQ-10 with a slotted-array antenna, and less than 4.6 m for an AVQ-10 radar with a para-

bolic dish antenna. Thus, for all the aircraft radars checked, no intensity exceeding 10 mW/cm^2 was found at a distance beyond 6 m. In general, for distances greater than two or three meters from the antenna, the power density decreased proportionally to the inverse square of the distance. In other words, the E field decreased proportionally to the inverse distance. Section 3.1 discusses the additional time-average reduction of field intensity for a scanning radar antenna.

The largest "leakage" field observed inside an airplane due to the aircraft radar was that of an RDR-1B installed in a DC-3 airplane. The maximum "hot spot" found was in the cockpit near the rudder controls, which was just above the antenna. The measured pulse-peak E field was 800 V/m (170 mW/cm^2) but the calculated average E field of 19 V/m (0.1 mW/cm^2) was rather weak. Reference [10] recommends some radiation safety precautions for ground operation of aircraft weather radars.

Ground radar systems. The measured fields in the beam center of the ASR, ARSR and ASDE radars were generally less than the far-zone values calculated from equation (8) because of near-field antenna gain reduction. An ASR transmitter has a nominal peak power output of 500 kW (average power about 425 W), except for the newer ASR-8 model which has a peak power level of 2.5 MW. The measured power density in the beam center of an ASR-4B or ASR-7 radar, with antenna fixed, was about 40 mW/cm^2 at a distance of 3.7 m from the antenna. It was about 0.7 mW/cm^2 at a distance of 85 m. A 10 mW/cm^2 field occurred at a point 60 cm in front of the reflector screen and 60 cm above the bottom edge of the reflector. This point is about 1.8 m above the tower deck and thus near head height. The intensity midway between the feed and reflector was 90 mW/cm^2 . The field of the higher-power ASR-8 radar was 10 mW/cm^2 at a distance of 36 m and 0.1 mW/cm^2 at 397 m.

An ARSR transmitter has a nominal peak power output of 4 MW and average power of about 2.8 kW. A field intensity of 15 mW/cm^2 was measured in the beam above the tower railing at a distance of 9.5 m, and 1.2 mW/cm^2 at a distance of 83 m. The intensity was 65 mW/cm^2 at a point midway between the antenna feed and reflector, increasing above this value when the CIM-2 probe was moved toward the feed point, and reaching 600 mW/cm^2 at a point 60 cm from the antenna feed. The ARSR field was also measured on the "mezzanine" deck just below the top deck of the antenna tower, which is the highest area normally accessible when the antenna is transmitting. The maximum hot spot found at head height (1.7 m) in this area had a measured pulse-peak E field value of 1220 V/m (395 mW/cm^2), which corresponds to a calculated average intensity of 33 V/m (0.29 mW/cm^2), during each short interval of time that the rotating beam is directed toward the fixed measurement point.

The intensity of field produced by two types of ASDE radars was measured near the transmitting antennas, one of these in Ku band and the other in K band. The transmitters had average power levels less than 15 W. The maximum field of the 14 GHz ASDE, with the CIM-1 monitor touching the center of the slot-antenna radome, was 0.6 mW/cm^2 . The 24 GHz ASDE radar uses a feed horn with parabolic reflector. The maximum field at the aperture of the feed was 80 mW/cm^2 , and the intensity midway between the feed and reflector was 2.4 mW/cm^2 .

ILS systems. The maximum field intensity observed for any ILS system was near the center antenna element of a VHF V-ring localizer array at the Denver airport. Fields exceeding 194 V/m (10 mW/cm^2) occurred only at distances less than 13 cm from the "gap" in the center element. The intensity at head height (1.7 m) above the metal counterpoise, directly beneath the antenna "gap", was about 30 V/m (0.24 mW/cm^2). The greatest field found for a UHF glide-slope antenna was 42 V/m (0.47 mW/cm^2) near the center of the plastic radome. The maximum field measured near the antennas of a microwave landing system was 0.05 mW/cm^2 (14 V/m) at the center of a 15.5 GHz antenna aperture, and 0.15 mW/cm^2 (24 V/m) at the center of a 5.2 GHz antenna aperture.

VOR and TACAN systems. The highest field intensity measured near a VOR antenna was on the roof of a VORTAC building. The field inside the conical plastic tower exceeded 194 V/m (10 mW/cm^2) at distances less than 20 cm from the antenna. The greatest VOR field at the outside surface of the conical tower was 70 V/m (1.3 mW/cm^2). The TACAN field strength at the VORTAC site was quite low because of the inaccessible antenna height. The maximum field measured with the EDM-3 probe touching the side of the center radome of a doppler VOR array was 235 V/m (14.7 mW/cm^2). The largest average intensity measured at the surface of a TACAN radome was 4.5 mW/cm^2 (130 V/m). The largest field measured for an aircraft TACAN, with the probe sensor touching the side of a blade-type antenna, was 1.3 mW/cm^2 (70 V/m).

Communication systems. High level fields were measured near the "Swastika" type antenna of a VHF ground communication transceiver. The E field was 67 V/m at the top of the antenna array and 207 V/m with the probe sensor touching one end of a dipole element. The indicated value of H field at the center of this dipole was 15 mW/cm^2 (0.63 A/m). The VHF and UHF aircraft transceivers produced very intense fields at the surface of the transmitting antennas. An intensity equal to the maximum measurable level of 3000 nJ/m^3 (823 V/m) for the EDM-3 instrument was recorded when the front surface of the sensor sphere was 7.5 cm from one side of the blade-type antenna.

Field intensity surveys were also made at an HF transmitting site on Long Island. The electric field at head height beneath the large rhombic antennas was only 1 to 5 V/m. However, intense fields were found near the transmitter cabinets and transmission lines. The E field measured 1000 nJ/m^3 (475 V/m) near the neutralizing capacitor above the transmitter cabinet and 3000 nJ/m^3 (823 V/m) at a distance of 30 cm from the center of the open-wire transmission line. The indicated H field was 100 mW/cm^2 (1.63 A/m) at a hot spot a few centimeters from the side of a coaxial transmission line.

9. ACKNOWLEDGMENTS

The authors wish to express their appreciation to all who contributed time and interest during this FAA/NBS project. First, we are grateful for the suggestions and patience of the three FAA project monitors during the period of this contract, all from the Systems Research and Development Service in Washington, D.C. They are:

1. Roger Hunter -- Original project monitor;
2. Isadore Goldman -- Principal project monitor; and
3. Robert Lorenz -- Final project monitor and reader for the final report.

We are grateful to the FAA staff and supporting personnel at several transmitting sites for expediting and helping with the field intensity surveys. These include, especially:

1. John Pritchett, FAA Aeronautical Center, Oklahoma City, OK;
2. Jim Loughheed, Airway Facilities Sector Manager, Los Angeles, CA;
3. Reginald Bishop, Western Region Office, Los Angeles, CA;
4. Charles Makey and Albert Hankenson, Frequency Management Office, Denver, CO;
5. John Williamson and Marty Bifson, NAFEC, Atlantic City, NJ;
6. Charles Thuma, HF Rhombic Antenna Site, Sayville, NY; and
7. Many others who worked and cooperated with us during the field surveys by furnishing equipment, aircraft, and operators for the radars and other transmitters.

The authors also acknowledge the assistance of several NBS staff members at the Boulder Laboratories, particularly the following:

1. Dr. Ramon Baird, Chief of the Fields and Antennas Section, in which this project was carried out;
2. Charles Miller, Chief of the present Radiation Hazards and Electromagnetic Compatibility Section;
3. Ronald Bowman, former project leader at NBS, for instrumentation design and cogent analysis of measurement techniques;
4. Francis Ries, present project leader at NBS, for helpful advice and comments during preparation of this report;
5. William Jessen, for instrument calibrations and gathering of data during the early stages of this program;
6. Ramon Jesch, for data analysis and preparation of calibration curves; and
7. Dr. Arthur Yaghjian, for theoretical near-field analysis and computer programming.

10. REFERENCES

- [1] ANSI C95.1 - 1974, An American National Standard, "Safety level of electromagnetic radiation with respect to personnel," IEEE, November 15, 1974.
- [2] W. W. Mumford, "Some technical aspects of microwave radiation hazards," Proc. IRE, 49, pp. 427-447, Feb. 1961.
- [3] Electromagnetic Compatibility Analysis Center, Annapolis, Maryland, FAA E-File Listing, data base request number DB-1955, Mar. 1974.
- [4] P. F. Wacker and R. R. Bowman, "Quantifying hazardous electromagnetic fields: scientific basis and practical considerations, IEEE Trans. Microwave Theory & Techniques, MTT-19, pp. 178-187, Feb. 1971.
- [5] R. R. Bowman, "Some recent developments in the characterization and measurement of hazardous electromagnetic fields," Proc. of Intl. Symposium on Biologic Effects and Health Hazards of Microwave Radiation, Warsaw, Poland, October 15-18, 1973, pp. 217-227.
- [6] E. Aslan, "Broad-band isotropic electromagnetic radiation monitor," IEEE Trans. Inst., & Meas., IM-21, pp. 421-424, Nov. 1972.
- [7] R. R. Bowman, "Calibration techniques for electromagnetic hazard meters: 500 MHz to 20 GHz," Nat. Bur. Stand. (U.S.), Inter-Agency Report 75-805, Apr. 1976.
- [8] M. L. Crawford, "Generation of standard EM fields using TEM transmission cells," IEEE Trans. Elec. Comp., EMC-16, No. 4, pp. 189-195, Nov. 1974.
- [9] Federal Aviation Administration, "Radiation health hazards and protection," FAA Handbook No. 3910.3, February 12, 1970.
- [10] Federal Aviation Administration, "Recommended radiation safety precautions for airborne weather radar," FAA Advisory Circular No. 20-68A, April 11, 1975.
- [11] C. Polk, "Prediction of power densities in the vicinity of large antennas," Proc. of third conference on radio interference reduction, Chicago, Illinois, Feb. 1957, pp. 453-474.
- [12] See latter portion of reference [2], pp. 436-447, Feb. 1961.
- [13] S. Soejima, "Fresnel gain of aperture aerials," Proc. IEE, 110, No. 6, pp. 1021-1027, June 1963.
- [14] Federal Aviation Administration, I. Goldman, "Calculation of power densities in the near and far fields of large round and rectangular antennas," Working paper on project No. 511-2, Aug. 1965.
- [15] W. R. Lind, "Fresnel zone theory," Rome Air Development Center Technical Report No. RADC-TR-66-66, Griffiss Air Force Base, New York, March 1966.
- [16] U. S. Air Force Communications Service, "Electromagnetic Radiation Hazards," Technical Manual T.O. 31Z-10-4, Chap. 2, Sec. 1 and Chap. 4, Sec. 2, Aug. 1966, revised June 1971.
- [17] R. C. Hansen, "Circular-aperture axial power density," Microwave Journal, pp. 50-52, Feb. 1976.

Instrument Nomenclature	Commercial CIM-1	Commercial CIM-2	Commercial CIM-3	NBS Model EDM-1C	NBS Model EDM-3	NBS Model EDM-4A
Field parameter measured	E-field	E-field	H-field	E-field	E-field	E-field
Meter readout unit	mW/cm ²	mW/cm ²	mW/cm ²	nJ/m ³	nJ/m ³	V/m
Meter full scale values	0.2, 2, 20	1, 10, 100	1, 10, 100	0.3, 1, 3, 10, 30, 100, 300	0.3, 1, 3, 10, 30, 300, 1000, 3000	(calibration curve required)
Type of field sensor	Three orthogonal dipole arrays	Three orthogonal dipole arrays	Three orthogonal loops	Three orthogonal dipoles	Three orthogonal dipoles	Three orthogonal dipoles
Type of field detector	Thermocouples	Thermocouples	Thermocouples	Diodes	Diodes	Diodes
Size of each sensor	~ 3 cm	~ 3 cm	9 cm diameter	0.8 cm long	2 cm long	5 cm long
Overall probe length	35 cm	35 cm	40 cm	52 cm	120 cm	54 cm
Frequency range:	0.8 to 15 GHz	0.8 to 15 GHz	10 to 250 MHz	10 to 4000 MHz	3 to 2000 MHz	300 kHz to 300 MHz
for ± 1 dB response	0.3 to 20 GHz	0.3 to 20 GHz	8 to 350 MHz	3 to 6000 MHz	1 to 3000 MHz	---
for ± 3 dB response						
Dynamic range:						
indicated	0.02 to 20 mW/cm ²	0.1 to 100 mW/cm ²	0.1 to 100 mW/cm ²	0.03 to 300 nJ/m ³	0.03 to 3000 nJ/m ³	1 to 200 V/m
equivalent	8.7 to 275 V/m	19.4 to 614 V/m	0.05 to 1.63 A/m	2.6 to 260 V/m	2.6 to 823 V/m	---
Overload level:				(estimated)	(estimated)	(estimated)
cw field	100 mW/cm ²	300 mW/cm ²	300 mW/cm ²	3000 V/m	3000 V/m	1000 V/m
pulsed field	60 W/cm ²	300 W/cm ²	300 W/cm ²	3000 V/m	3000 V/m	1000 V/m
Peak-average capability	average only	average only	average only	Peak or average (Calibration curve required for peak)	Peak or average (Not calibrated for peak)	Peak or average (Not calibrated for peak)
90% response time	1 second (fast)	1 second (fast)	1 second (fast)	0.2 millisecond	0.2 millisecond	0.2 millisecond
Isotropic response, except through handle	± 1 dB	± 1 dB	± 1 dB	± 1 dB	± 1 dB	--
Instrument weight	4.7 lb	4.7 lb	5.8 lb	3 lb	3 lb	4 lb
Battery type	15 V Nickel-cadmium	15 V Nickel-cadmium	25 V Nickel-cadmium	9 V transistor types	9 V transistor types	9 V transistor types
Battery use time	20 hours	20 hours	40 hours	40 hours	40 hours	40 hours

Figure 2-1. Measurement ranges and specifications of the radiation monitors used for the field intensity surveys.

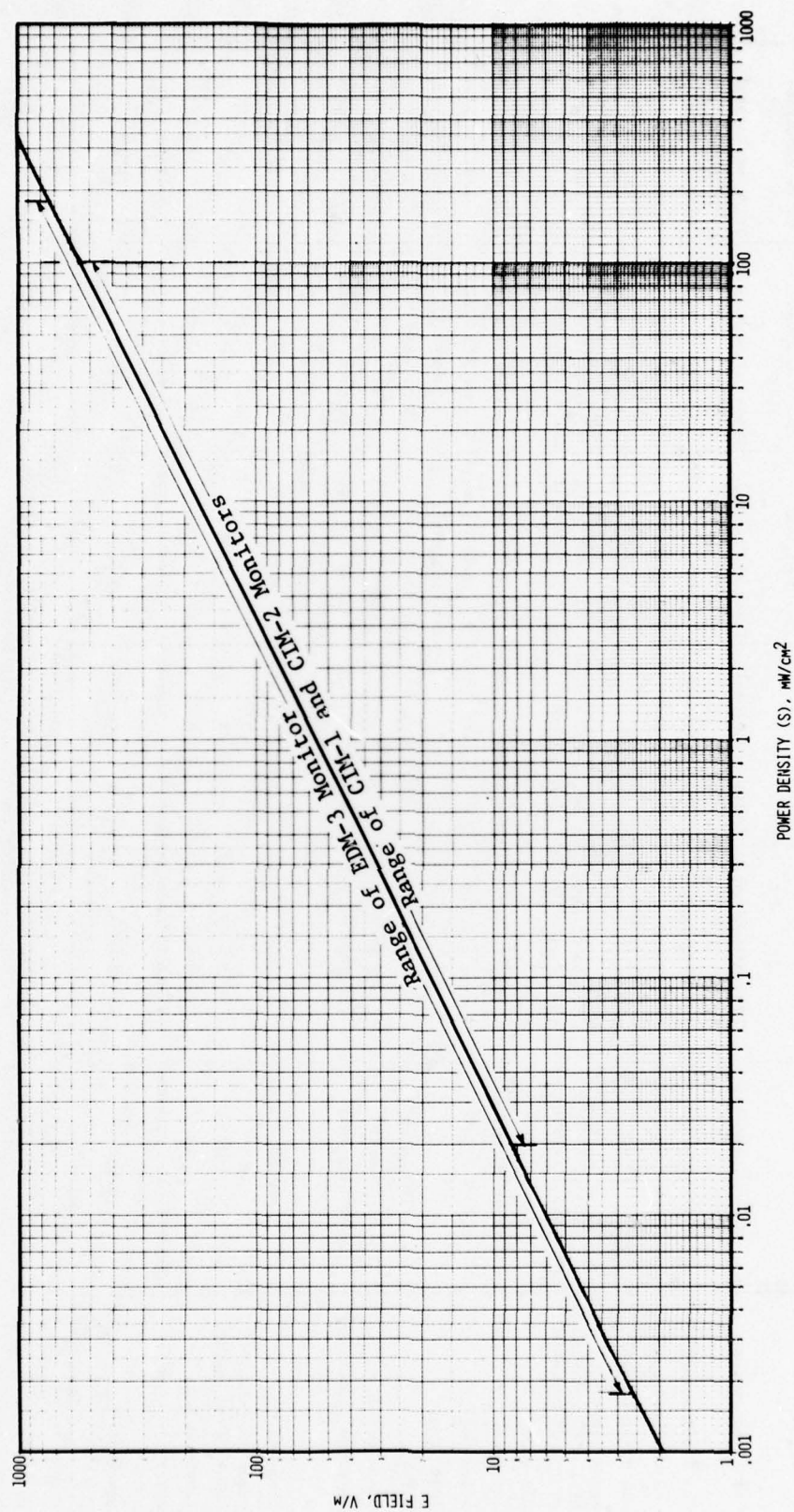


Figure 2-2. Graph of amplitude ranges of the radiation monitors, comparing units of V/m and mW/cm².

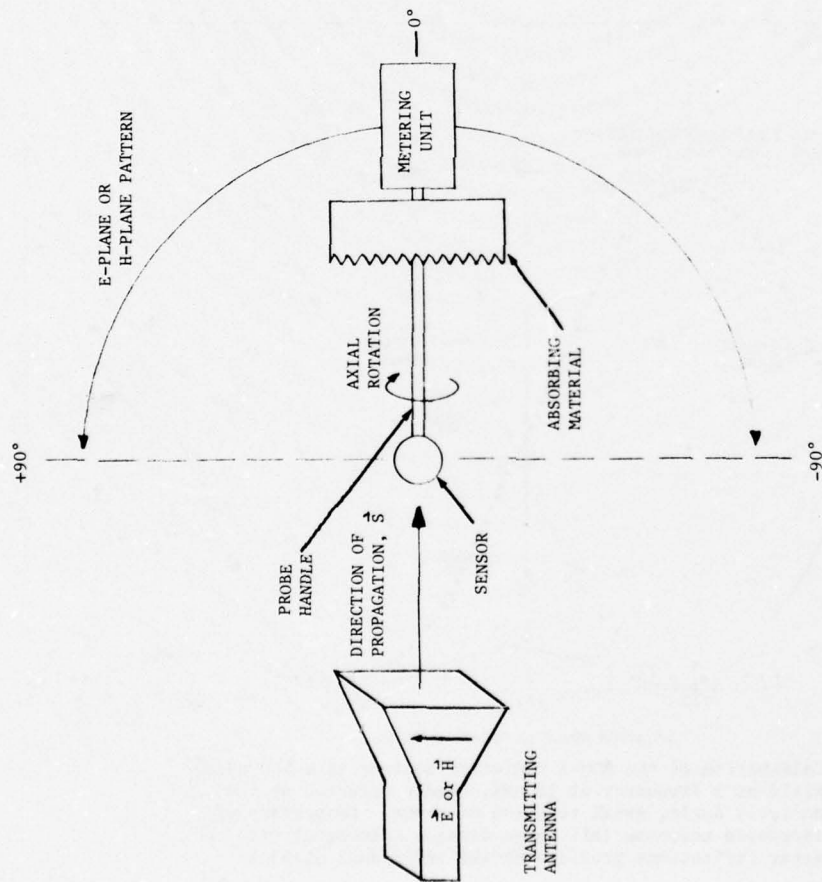


Figure 2-3. Sketch of the standard field setup used to calibrate the radiation monitors and record probe pattern responses.

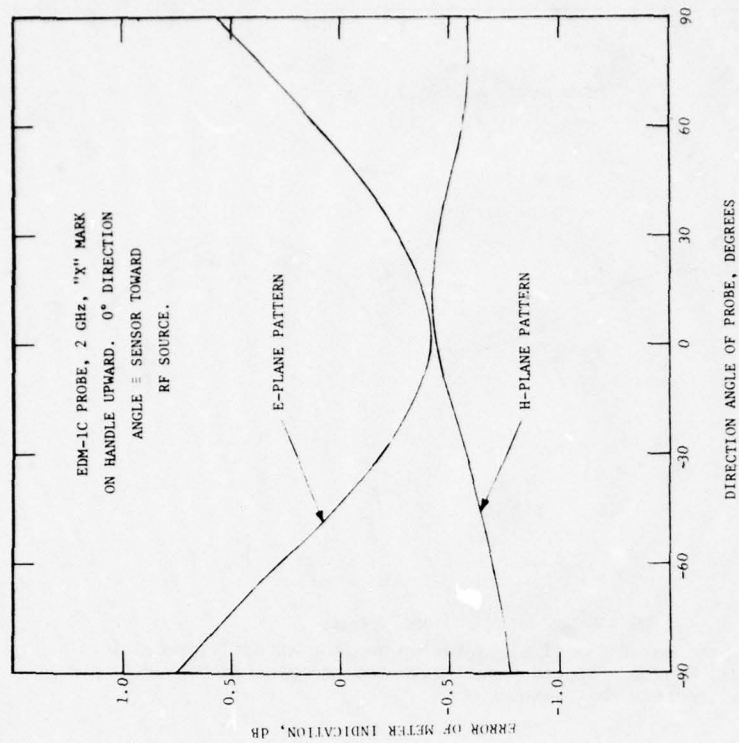


Figure 2-4. Calibration of the EDM-1C radiation monitor in a standard field at a frequency of 2 GHz, E-plane and H-plane patterns.

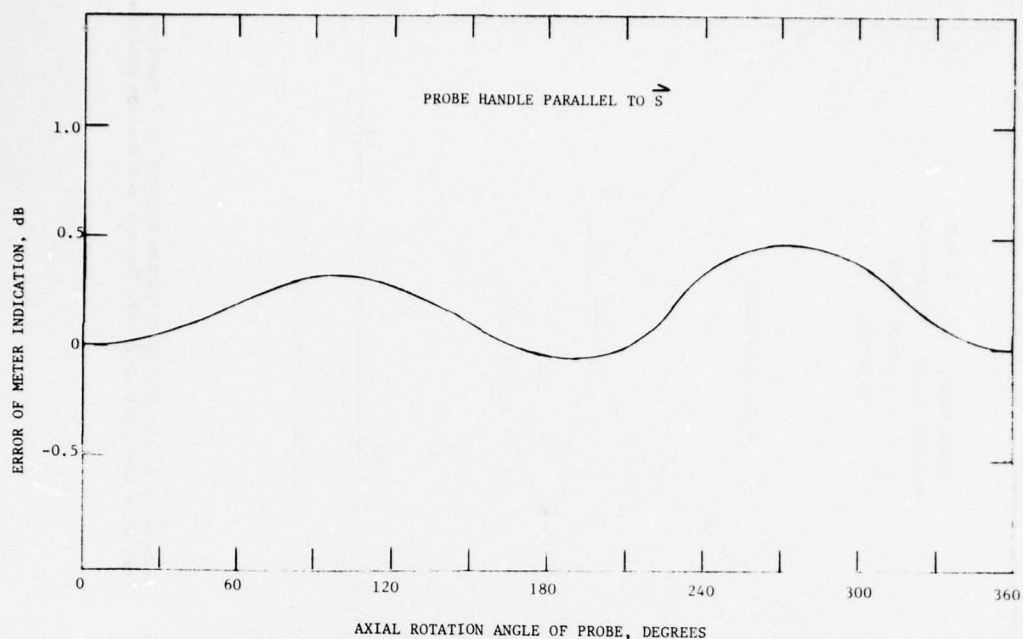


Figure 2-5. Calibration of the CIM-1 radiation monitor at a frequency of 3 GHz, handle oriented parallel to the propagation vector, axial rotation of probe.

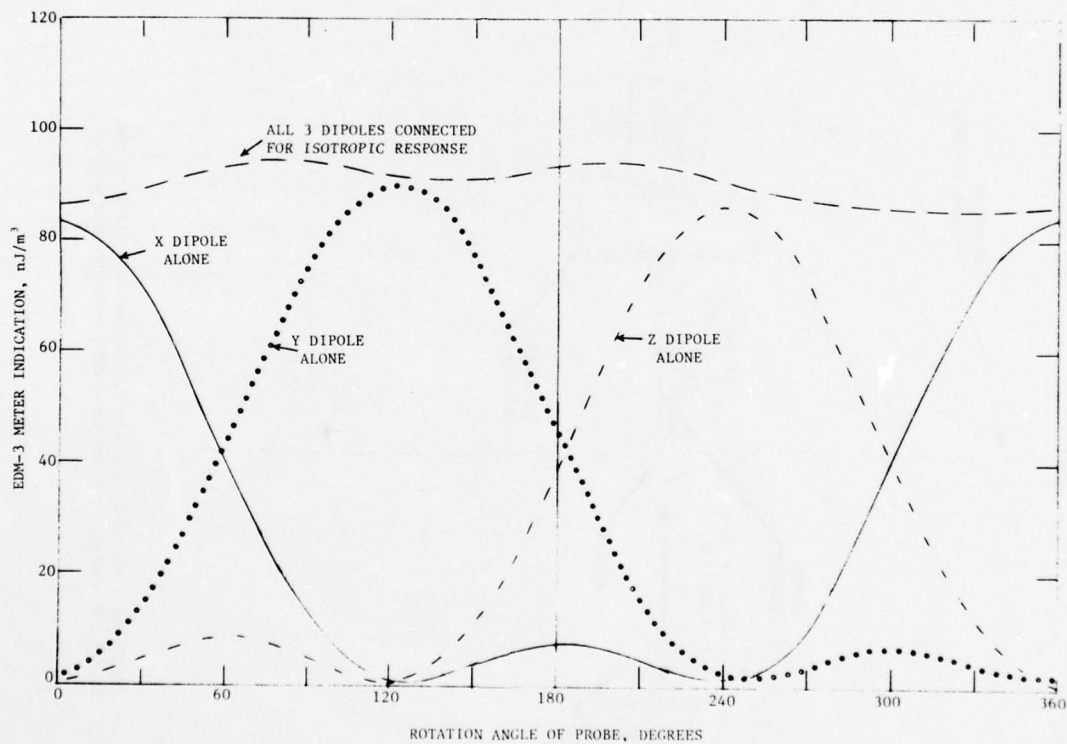


Figure 2-6. Calibration of the EDM-3 radiation monitor in a 100 nJ/m^3 field at a frequency of 10 MHz, handle oriented at the analytic angle, axial rotation of probe. Comparison of isotropic response (all three dipoles connected) with the meter indications produced by the individual dipoles.

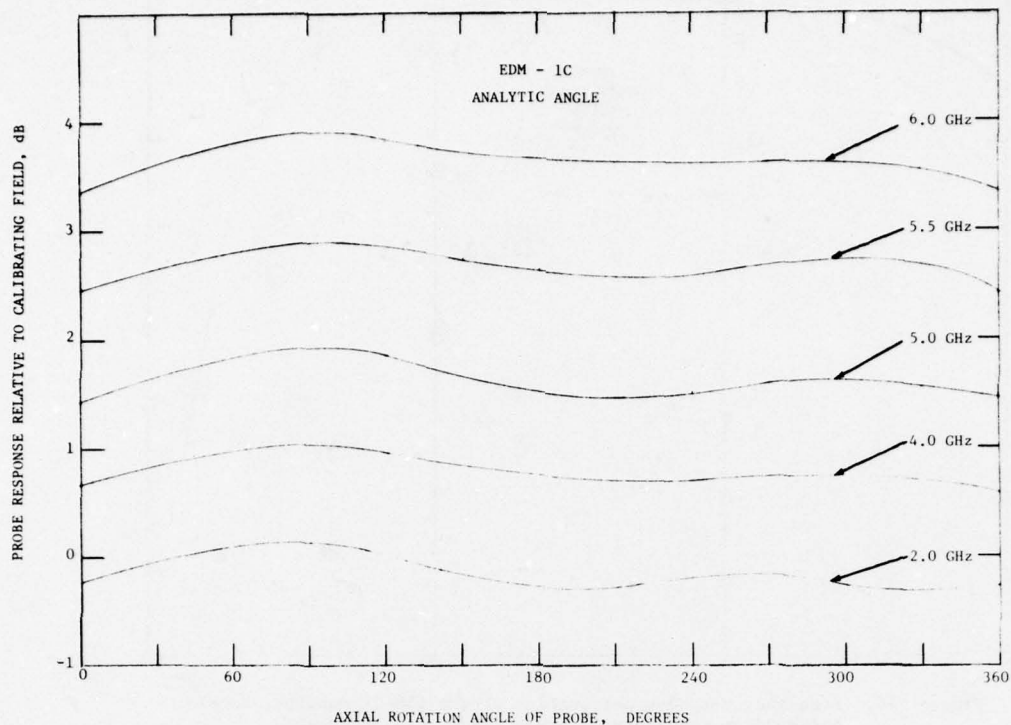


Figure 2-7. Calibration curves of the EDM-1C monitor at five different frequencies, handle oriented at the analytic angle, axial rotation of probe.

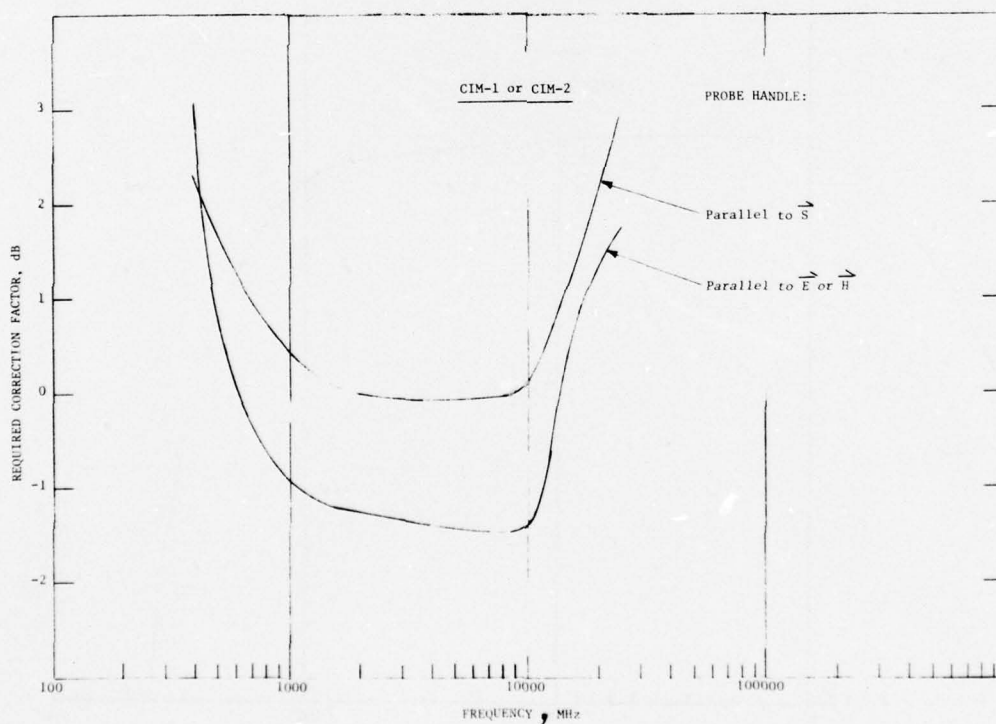


Figure 2-8. Frequency response calibrations of the CIM-1 and CIM-2 monitors. Comparison of two orientations of the probe handle, parallel to or perpendicular to the propagation vector.

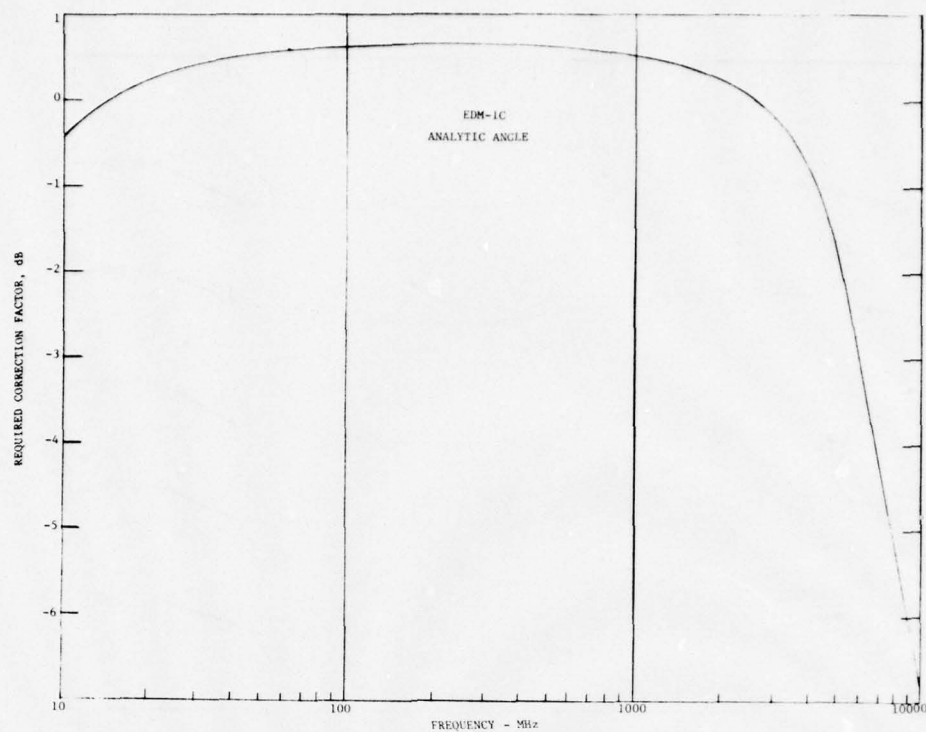


Figure 2-9. Frequency response calibration of the EDM-1C monitor, handle oriented at the analytic angle, mean axial response.



Figure 2-10. Frequency response calibration of the EDM-3 monitor, handle oriented at the analytic angle, mean axial response.



Figure 3-1. Photograph of airplane mechanics and a radar technician raising the radome of an RDR-1B radar antenna mounted in the nose of a DC-3 aircraft.

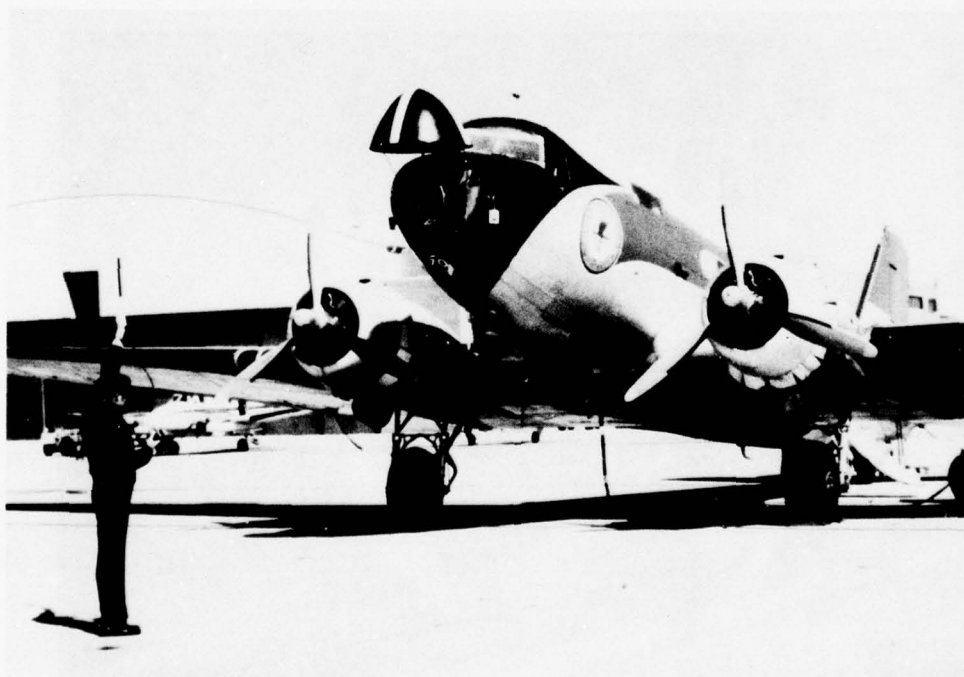


Figure 3-2. Photograph of an operator making preliminary checks of the field intensity in front of a DC-3 aircraft.



Figure 3-3. Photograph of an operator measuring stray fields with a CIM-1 radiation monitor in the cockpit of a DC-3 airplane.



Figure 3-4. Photograph of an operator measuring leakage fields with an EDM-1C monitor in the fuselage of a DC-3 airplane, Flight Inspector's position.

Measuring instrument used: CIM-1, fast time constant.

Type of measurement: Power density of "pencil" beam, radome tied up, antenna pointing forward.

Frequency = 9.375 GHz; Transmitter nominal power = 40 kW pk \approx 24 W av.

Notes: (1) Parked DC-3 plane tilts upward 11° above horizontal.

(2) Maximum reachable probe height was 4 m.

(3) Height of airplane antenna = 3.87 m.

Reflector elevation angle	Horizontal distance to antenna		Probe height for max indication meters	Measured Power Density		
	feet	meters		S av mW/cm ²	Equiv E av V/m	Calc E pk V/m
11° down	70	21.3	0.15	0.5	43	1770
"	50	15.2	0.91	0.6	48	1940
"	30	9.14	1.83	1.2	67	2740
"	20	6.10	2.87	3.2	110	4480
"	15	4.57	3.20	5.6	145	5930
"	12	3.66	3.11	7.4	167	6810
"	9.5	2.90	3.11	12.7	219	8930
"	8.5	2.59	3.11	13.5	225	9200
"	7.5	2.29	3.11	15.0	238	9700
5.5° down	70	21.3	2.29	0.3	34	1370
"	50	15.2	2.68	0.8	55	2240
"	30	9.14	3.08	1.9	85	3450
"	20	6.10	3.32	4.3	127	5190
"	15	4.57	3.44	7.2	165	6720
"	12	3.66	3.60	12.5	217	8860
0° (Airplane center line)	70	21.3	4.11	0.3	34	1370
"	50	15.2	4.11	0.7	51	2100
"	30	9.14	4.11	2.0	87	3540
"	20	6.10	4.11	5.5	144	5870
"	15	4.57	4.11	8.5	179	7300
"	12	3.66	3.96	13.0	221	9030

Figure 3-5. Field intensity in the center of the beam of an RDR-1B aircraft radar, measured in front of a DC-3 airplane.

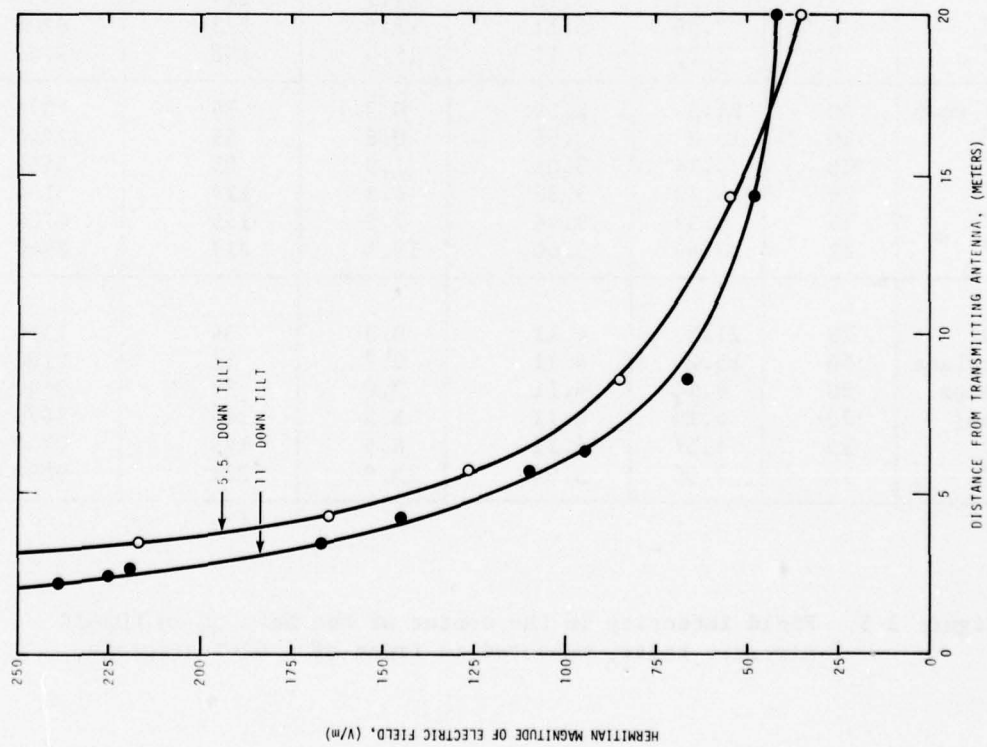


Figure 3-6. Graphs of field intensity in the "pencil" beam of an RDR-1B aircraft radar as a function of distance from the antenna.

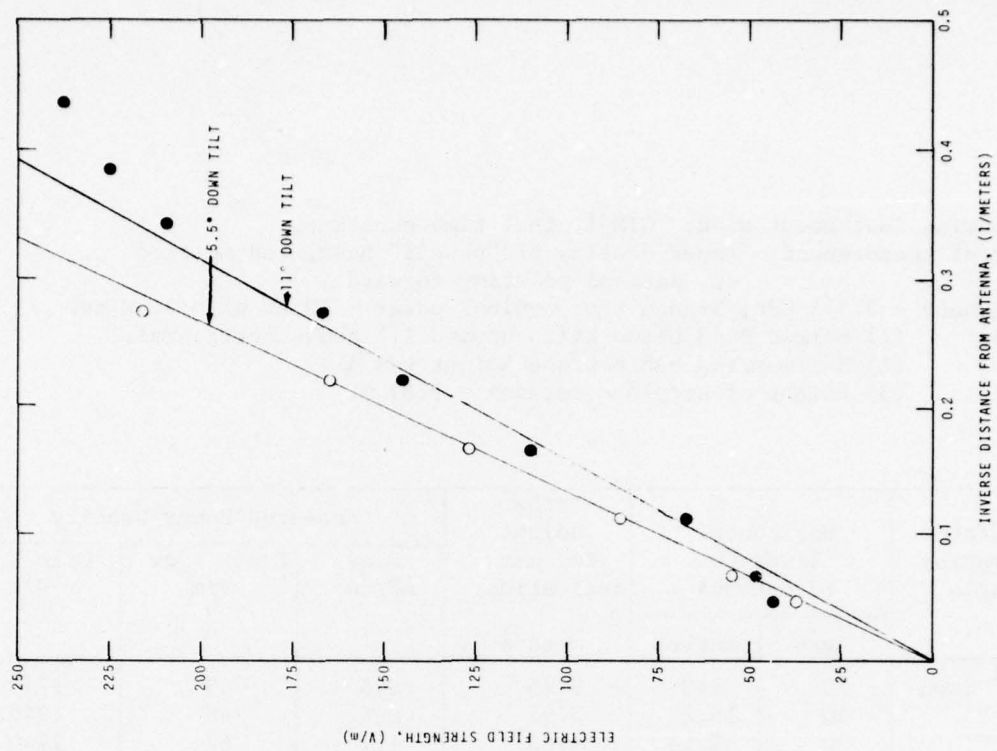


Figure 3-7. Graphs of field intensity versus inverse distance from the antenna, RDR-1B aircraft radar, "pencil" beam.

Measuring instrument: EDM-1C, Pk mode, 10 s time constant
Type of measurement: Pulse-peak field of "pencil" beam, antenna
elevation = 0° with respect to plane center line.
Frequency = 9.375 GHz; Transmitter nominal power = 40 kW pk \approx 24 W av.

Location of measurement point	Measured Field Intensity		
	E pk V/m	Calc E av V/m	Calc S av mW/cm ²
I. Antenna stationary, pointing back toward cockpit, radome tied up.			
1. Pilot's side of cockpit:			
Position of head	168	4.1	0.005
Position of chest	187	4.6	0.006
Directly above throttle	297	7.3	0.014
Between stick (wheel) and cowl above stick	222	5.4	0.008
Near floor, back of rudder controls	349	8.6	0.019
Five cm from right rudder control	605	15	0.058
*Between right rudder control and floor	702	17	0.078
2. Copilot's side of cockpit:			
Position of head	147	3.6	0.003
Position of chest	187	4.6	0.006
Near stick (wheel)	297	7.3	0.014
Near floor, back of rudder controls	605	15	0.058
*Between left rudder control and floor	795	19	0.101
3. Remainder of airplane interior:			
Near air filter of radar transmitter	62	1.5	0.001
*Near jump-seat behind Flight Inspector's area	97	2.4	0.002
* Indicates maximum hot spot in each of the three areas examined.			
II. Antenna rotating 360° at 15.4 RPM, radome down in place.			
Pilot's side of cockpit:			
15 cm in front of head position	297	7.3	0.014
15 cm behind head position	252	6.2	0.010
Maximum hot spot near head position	322	7.9	0.017
Maximum hot spot between seat and stick	352	8.6	0.020
Maximum hot spot between floor and rudder controls	795	19	0.101
Maximum hot spot near stick (wheel)	645	16	0.066
Maximum hot spot between stick and windshield	349	8.6	0.019
Maximum hot spot between throttle and ceiling	297	7.3	0.014

Figure 3-8. Leakage fields of an RDR-1B aircraft radar measured inside a DC-3 airplane.

Measuring instrument: CIM-1, fast time constant.

Type of measurement: Power density at antenna height (1.98 m), radome in place,
antenna pointing forward at elevation angle = 0.5° upward.

Frequency = 9.375 GHz; Transmitter nominal power = 50 kW pk \approx 30 W ave.

Horizontal distance to antenna,		Measured Power Density, mW/cm ²			
		30-Mile Range		180-Mile Range	
		Pencil beam	Map beam	Pencil beam	Map beam
feet	meters				
170	51.8	0.14	0.10	0.12	0.09
150	45.7	0.11	0.10	0.12	0.10
130	39.6	0.18	0.07	0.19	0.08
110	33.5	0.20	0.11	0.18	0.10
90	27.4	0.37	0.22	0.35	0.22
70	21.3	0.54	0.38	0.55	0.35
50	15.2	1.11	0.75	1.08	0.73
40	12.2	1.53	0.98	1.50	0.97
33	10.1	2.7	1.63	2.5	1.65
28	8.53	3.2	2.0	3.2	2.0
23	7.01	4.7	2.9	4.7	2.8
18	5.49	6.2	4.0	6.3	3.9
13	3.96	8.6	5.0	8.8	4.9
11	3.35	8.9	5.1	9.0	5.1
6	1.83	10.0	6.1	10.0	6.0

Figure 3-9. Field intensity versus distance from the antenna of an RDR-1E aircraft radar, measured in front of a DC-9 aircraft.

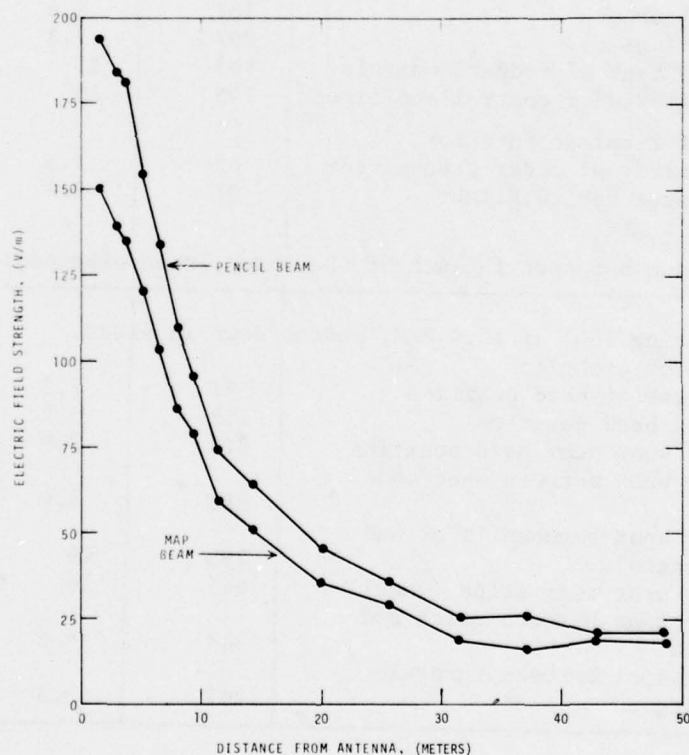


Figure 3-10. Graphs of field intensity versus distance from the antenna of an RDR-1E aircraft radar, 180 mile range.

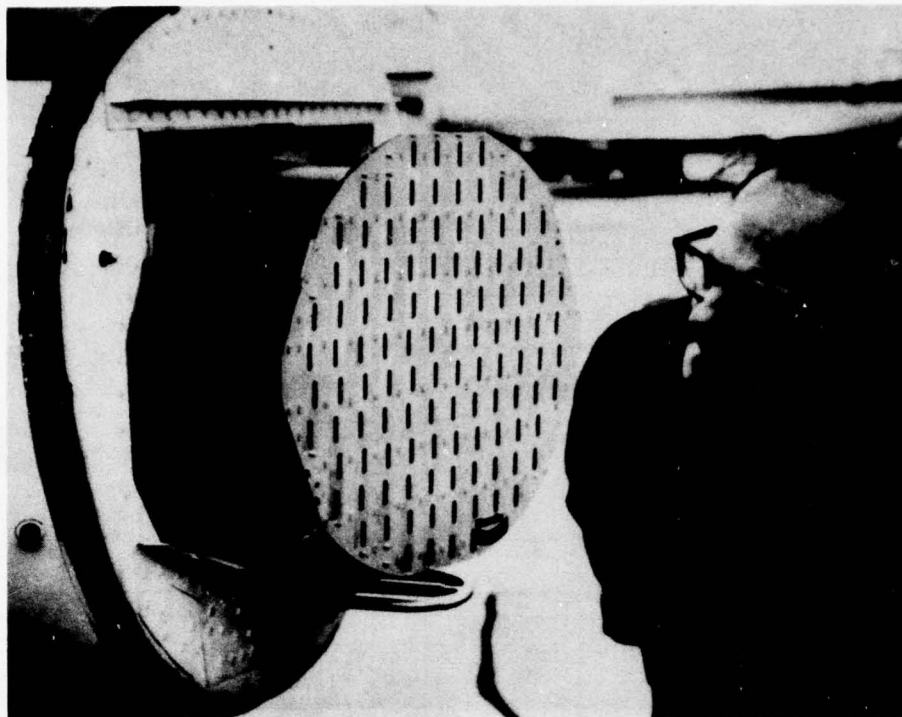


Figure 3-11. Photograph of the slotted array antenna for the RDR-1200 aircraft radar on a Sabre Liner airplane.

Measuring instrument: CIM-1, fast time constant.

Type of measurement: Power density of "pencil" beam, antenna pointing forward, 25-mile range.

Frequency = 9.345 GHz; transmitter nominal power = 12 kW pk \approx 4.2 W av.

* Sensor ball touching front tip of radar nose cone.

Horizontal distance to antenna		Probe Height for maximum indication	Measured field intensity	
feet	meters		S mW/cm ²	Equiv. E V/m
50	15.24	1.66 m	.055	14.4
45	13.72	1.60 m	.07	16.2
40	12.19	1.61 m	.08	17.4
35	10.67	1.59 m	.10	19.4
30	9.14	1.55 m	.13	22.1
25	7.62	1.56 m	.25	30.7
20	6.10	1.60 m	.35	36.3
15	4.57	1.57 m	.60	47.5
10	3.05	1.56 m	1.2	67.2
9	2.74	1.55 m	1.7	80.0
8	2.44	1.55 m	2.1	88.9
7	2.13	1.55 m	2.4	95.1
6	1.829	1.55 m	3.0	106
5	1.524	1.55 m	3.8	120
4	1.219	1.55 m	5.5	144
3	.914	1.55 m	7.7	170
2	.610	1.55 m	8.5	179
1*	.305	1.55 m	10.0	194

Figure 3-12. Field intensity in the beam of an RDR-1200 aircraft radar, measured in front of a Sabre Liner.

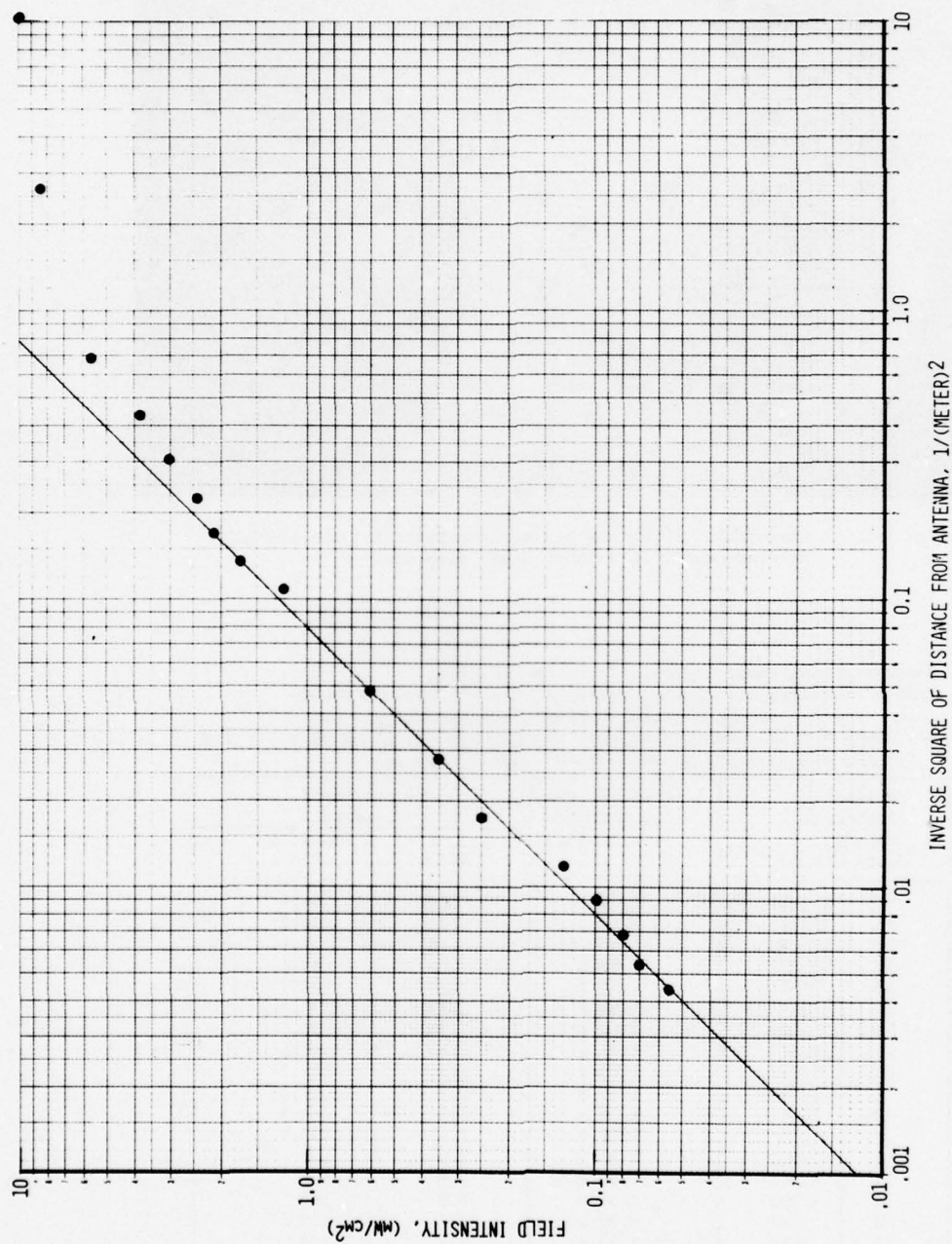


Figure 3-13. Graph of field intensity versus the inverse square of distance from the antenna, RDR-1200 aircraft radar.

Measuring instrument: CIM-1, fast time constant.
 Type of measurement: Power density at antenna height (3.2 m), radome in place,
 antenna pointing forward at elevation angle = 1.5° upward.
 Frequency = 5.4 GHz; Transmitter nominal power = 75 kW pk \approx 60 W av.

Horizontal distance to antenna	feet	meters	Measured Power Density, mW/cm ²			
			20-mile Range		150-Mile Range	
			Pencil beam	Contour beam	Pencil beam	Contour beam
160	48.8		0.24	0.18	0.19	0.23
140	42.7		0.16	0.26	0.31	0.22
120	36.6		0.31	0.25	0.29	0.31
100	30.5		0.52	0.45	0.50	0.48
80	24.4		0.65	0.68	0.63	0.64
60	18.3		1.20	1.07	1.14	1.15
40	12.2		2.6	2.7	2.6	2.6
30	9.1		4.8	4.8	4.8	4.8
25	7.6		7.0	6.9	6.8	6.9
20	6.1		10.5	10.5	10.4	10.4

Horizontal distance	feet	meters	Equivalent Electric Field Strength, E, V/m			
			20-mile Range		150-Mile Range	
			Pencil	Contour	Pencil	Contour
160	48.8		30	26	27	29
140	42.7		25	31	34	29
120	36.6		34	31	33	34
100	30.5		44	41	43	43
80	24.4		49	51	49	49
60	18.3		67	63	66	66
40	12.2		99	101	99	99
30	9.1		130	134	134	134
25	7.6		162	161	160	161
20	6.1		199	199	198	198

Figure 3-14. Field intensity in the beam of an AVQ-10 aircraft radar, measured in front of a 720 E airplane.

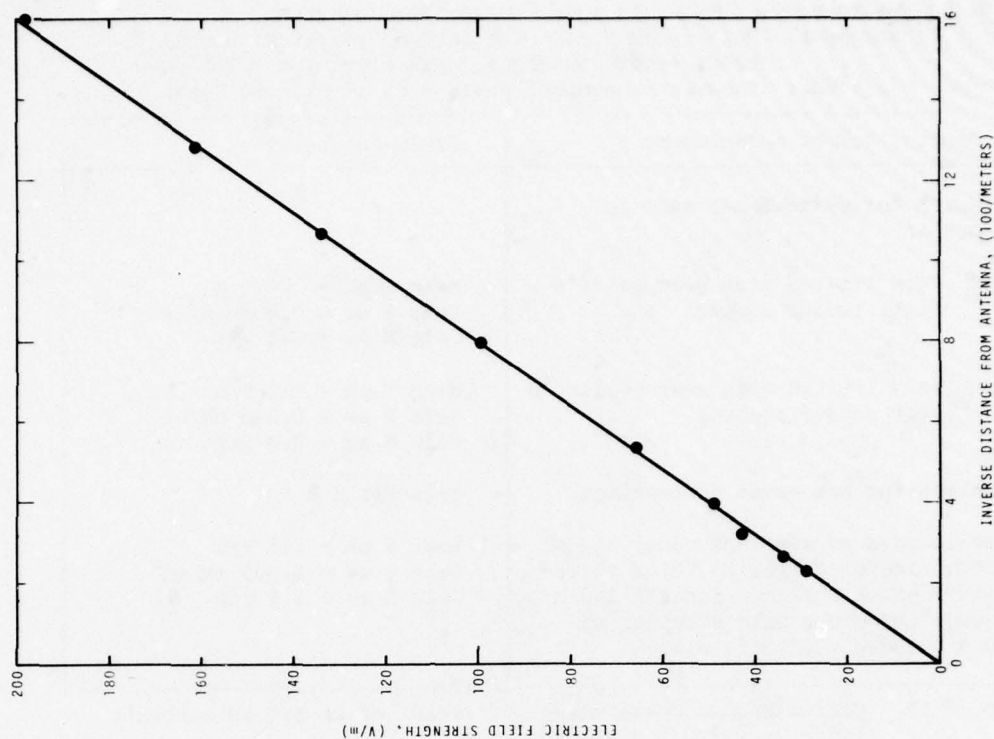


Figure 3-15. Graph of field intensity versus inverse distance from the antenna, AVQ-10 aircraft radar, pencil beam, 150 mile range.

Measuring instrument: EDM-1C, Pk mode, 10 sec time constant
 Type of measurement: Pulse-peak field with antenna rotating, pencil beam, radome in place, dish elevation = 1.5° down.
 Frequency = 5.4 GHz; Transmitter nominal power = 75 kW pk \approx 60 W av.

Description of measurement	Field intensity
I. Search for maximum hot spot in cockpit	
1. Very limited area near pilot's right rudder control	Meas E pk = 106 V/m Calc S av = 0.002 mW/cm ² Calc E av = 3.0 V/m
2. Very limited area near copilot's left rudder control	Meas E pk = 113 V/m Calc S av = 0.003 mW/cm ² Calc E av = 3.2 V/m
II. Search for hot spots in fuselage	Meas field \approx 0
III. Reflection of airplane radar signal from side of Hangar No. 9, a three-story brick building located 100 m away; EDM probe held straight up 0.9 m above copilot's window.	Meas E pk = 146 V/m Calc S av = 0.005 mW/cm ² Calc E av = 4.1 V/m

Figure 3-16. Miscellaneous measurements of field of an AVQ-10 aircraft radar in a 720 E airplane.

Measuring instrument: CIM-1, fast time constant.
 Type of measurement: Power density at two heights above ground, pencil beam, radome in place, antenna pointing forward, dish elevation = 0.5° up.
 Frequency = 5.4 GHz; Transmitter nominal power = 75 kW pk \approx 60 W av.
 Note: Values indicated by * were measured three feet directly below the antenna.

Horizontal distance to antenna		Measured Power Density mW/cm ²		Equivalent Electric Field V/m	
		Ant Height (2.6 m)	Head Height (1.7 m)	Ant Height (2.6 M)	Head Height (1.7 m)
feet	meters				
160	48.8	0.11	0.06	20	15
140	42.7	0.13	0.17	22	25
120	36.6	0.19	0.16	27	25
100	30.5	0.24	0.22	30	29
80	24.4	0.42	0.21	40	28
60	18.3	0.77	0.24	54	30
40	12.2	2.0	0.20	87	27
30	9.1	3.1	0.12	108	21
20	6.1	7.7	0.12	170	21
15	4.6	10.1	0.04	195	12
10	3.1		0.08		17
5	1.5		0.27		32
0	0.0		0.40*		39*

Figure 3-17. Field intensity of an AVQ-10 aircraft radar measured near a turboprop airplane.

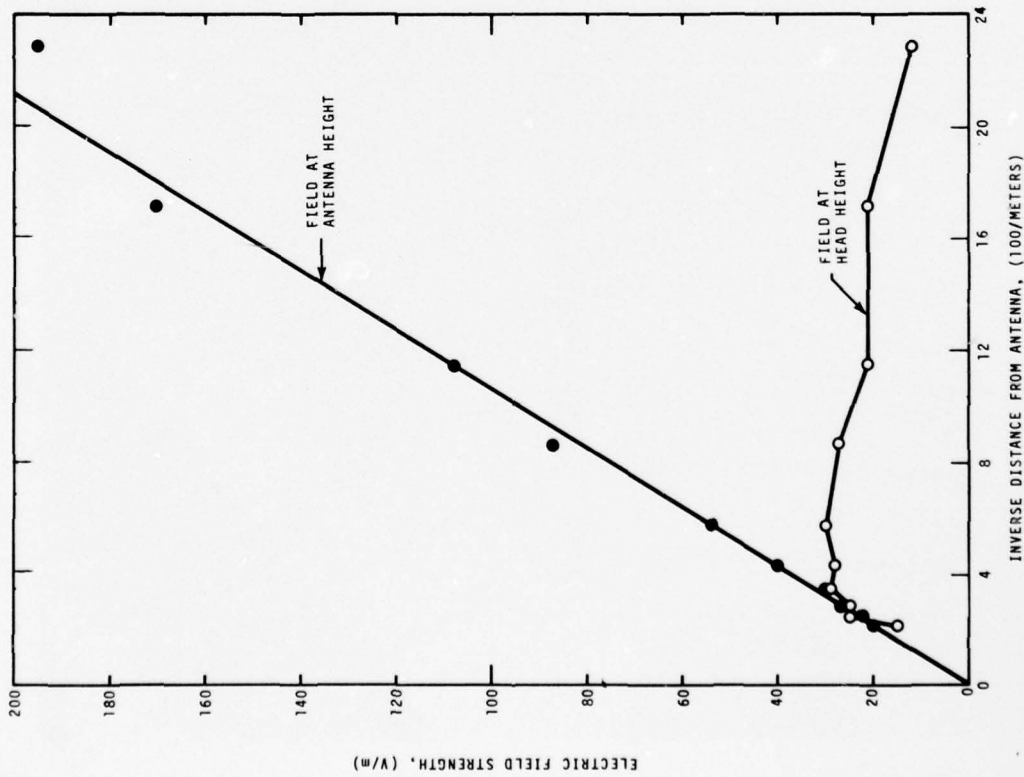


Figure 3-18. Graphs of field intensity versus inverse distance from the antenna, AVQ-10 aircraft radar, "pencil" beam.

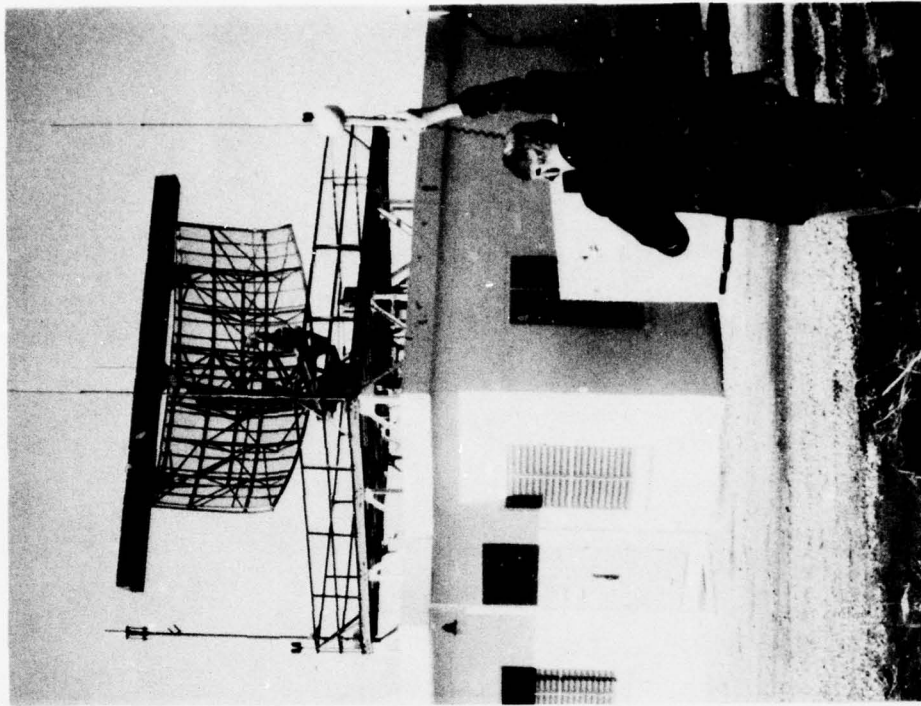


Figure 4-1. Photograph of an operator making preliminary checks of the field intensity near an airport surveillance radar (ASR).



Figure 4-2. Photograph of measurements being taken in the field of an ASR antenna, closeup view of the feed and reflector screen.

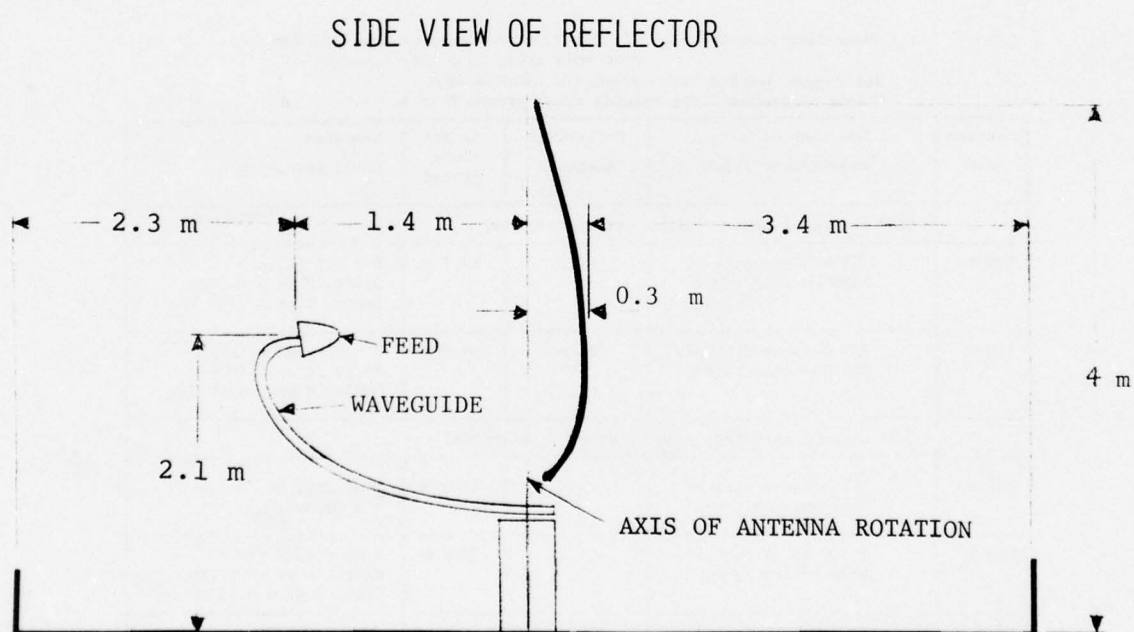
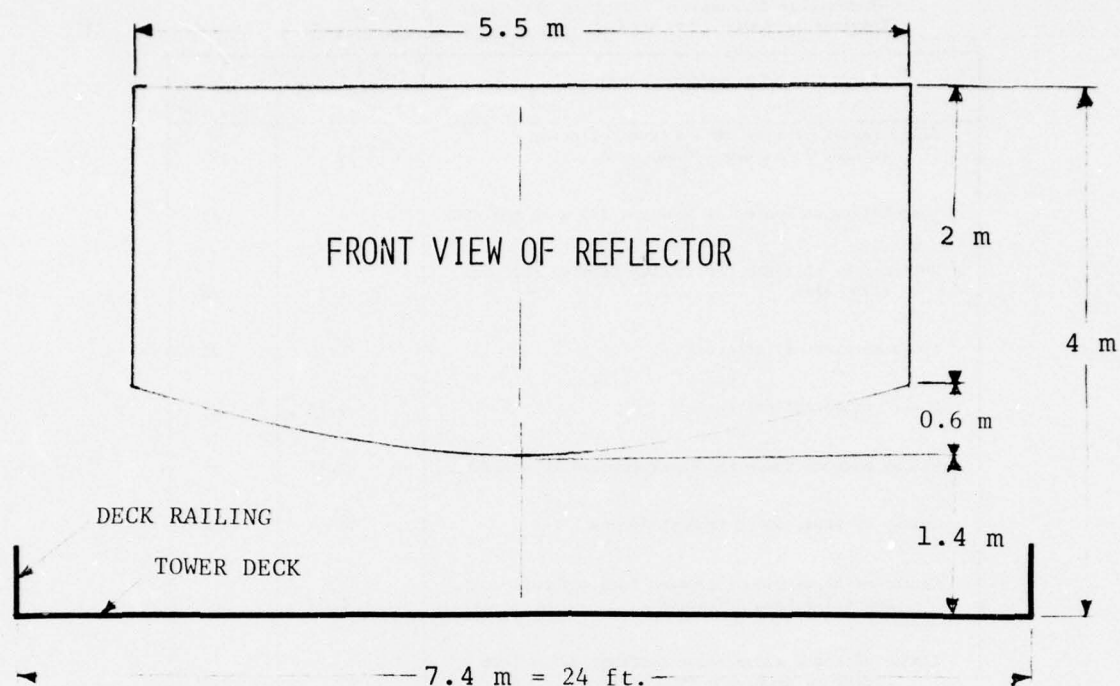


Figure 4-3. Sketch of an ASR-7 antenna including approximate dimensions.

Measuring instrument used: CIM-2, fast time constant.
 Transmitter frequency = 2.72 GHz; PRR = 1140 per second.
 Transmitter power = 425 kW peak (pk) \approx 400 W average (av).

Location of measurement point	Field intensity	
	S, mW/cm ²	E , V/m
Below center of beam, 60 cm from reflector screen, 1.8 m above tower deck.	10	194
Same height as center of beam but 1.5 m to the side	1	61
Bottom edge of reflector, midway between left and right side	1.3	70
Upper corners of reflector	0.16	25
Lower corners of reflector	0.17	25
Midway between upper and lower corners of reflector	0.33	35
Center of beam, 40 cm from reflector	70	514
Center of beam, midway between feed and reflector, about 1 m from reflector.	90	582
Center of beam, above tower railing, 3.7 m from center of deck, 4 m from reflector.	45	412

Figure 4-4. Field intensity of an ASR-4B airport surveillance radar measured on the antenna tower, Oklahoma City.

Measuring instruments: (1) CIM-1, fast time constant, (2) EDM-1C, peak mode (pk), 10 s time constant.

See figure 4-4 for transmitter characteristics.

Height of transmitting antenna above ground \approx 20 m

Monitor used	Location of measurement point	Horizontal distance	Height above ground	Measured field intensity
(ASR antenna fixed, pointing toward observer)				
CIM-1	2.5 m above deck of ARSR antenna tower	84 m	17.7 m	S = 0.5 mW/cm ² Equiv. E av = 43 V/m Equiv. E pk = 1410 V/m
CIM-1	3.7 m above deck of ARSR antenna tower	84 m	18.9 m	S = 0.6 mW/cm ² Equiv. E av = 48 V/m Equiv. E pk = 1540 V/m
(ASR antenna rotating, mean value of 3 rotations)				
CIM-1	3.7 m above deck of ARSR antenna tower	84 m	18.9 m	Indicated S \approx 0 mW/cm ²
EDM-1C	4.0 m above deck of ARSR antenna tower	84 m	19.2 m	E pk = 1700 V/m Equiv. E av = 52 V/m Equiv S av = 0.73 mW/cm ²
EDM-1C	VORTAC building, 2 m above roof	404 m	5.5 m	E pk = 195 V/m Equiv. E av = 6.0 V/m Equiv. S av = 0.01 mW/cm ²
EDM-1C	Office building, third floor window, maximum hot spot.	475 m	7.6 m	E pk = 130 V/m Equiv. E av = 4.0 V/m Equiv. S av = 0.004 mW/cm ²

Figure 4-5. Field intensity of an ASR-4B radar measured at several distant locations, Oklahoma City.

Measuring instruments: CIM-1 and CIM-2.

Transmitter frequency = 2.75 GHz; PRR = 810 /s.

Transmitter power = 430 kW pk \approx 290 W av. *Denotes center of beam.

Distance from antenna (tower center) to middle measurement point = 3.66 m (12 ft.).

Vertical cut through center of beam, above tower railing			Horizontal cut through center of beam, above tower railing		
Height above deck, meters	Field intensity		Lateral distance from beam center, meters	Field intensity	
	mW/cm ²	V/m		mW/cm ²	V/m
2.0	0	0	4.1 left	.13	22
2.1	.05	14	2.9 left	.20	27
2.2	.15	24	2.0 left	5	137
2.3	.17	25	1.2 left	15	238
2.4	.60	48	.54 left	35	363
2.5	2	87	.22 left	38	378
2.6	5	137	.16 left	40	388
2.7	10	194	.09 left	45	412
2.8	25	307	.03 left	47	421
2.9	40	388	0	*49	*430
2.97	*45	*412	.03 right	47	421
3.0	40	388	.09 right	45	412
3.1	12	213	0.7 right	35	363
3.2	1.5	75	1.4 right	17	253
3.3	22	288	2.2 right	3	106
3.4	16	246	3.2 right	.19	27
3.5	6	150	4.5 right	.12	21

Figure 4-6. Field intensity 3.7 m from an ASR-4B radar antenna; horizontal and vertical cuts through the center of the beam, above the tower railing, Los Angeles.

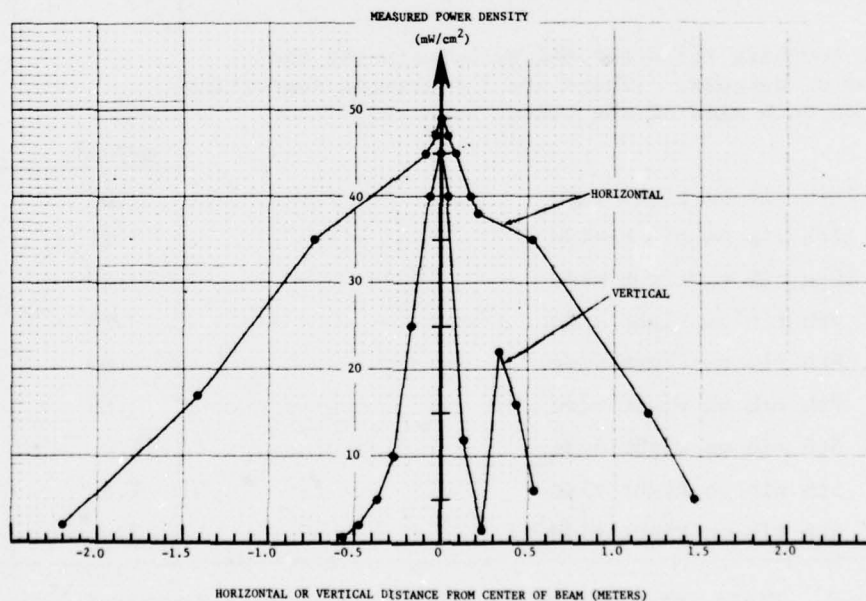


Figure 4-7. Graphs of the field 3.7 m from an ASR-4B radar antenna; horizontal and vertical cuts through the center of the beam.

Measuring instrument: CIM-1, fast time constant.

Transmitter frequency = 2.85 GHz; PRR = 852 /s.

Transmitter power = 425 kW pk \approx 300 W av.

Measurement distance, probe sensor to antenna reflector screen = 5 cm.

Measurement location	Field intensity	
	mW/cm ²	V/m
I. Probe touching antenna reflector at given points:		
Lower right corner of reflector	.12	21
Upper right corner	.12	21
Right edge, upper horizontal rib	.18	26
Right edge, lower horizontal rib	.16	25
Right edge, midway between top and bottom	.20	27
Lower left corner	.14	23
Upper left corner	.13	22
Left edge, upper horizontal rib	.19	27
Left edge, lower horizontal rib	.12	21
Left edge, midway between top and bottom	.30	34
Bottom of reflector, midway between left & right side	1.0	61
II. Probe touching reflector midway between top and bottom of antenna. (There are 12 vertical supporting ribs on each side of the center support.)		
	mW/cm ²	V/m
12th rib on right side	.08	17
11th rib on right side	.11	20
10th rib on right side	.20	27
9th rib on right side	.25	31
8th rib on right side	.60	48
7th rib on right side	.85	57
6th rib on right side	1.6	78
5th rib on right side	1.8	82
4th rib on right side	2.5	97

Figure 4-8. Field intensity of an ASR-7 radar measured near the antenna reflector screen, Los Angeles.

Measuring instruments: CIM-1 and CIM-2.

See figure 4-8 for transmitter characteristics.

Measurement distance = 3.66 m (12 ft.). *Denotes beam center.

Height above deck, meters	Field intensity	
	mW/cm ²	V/m
1.0	< 0.02	< 9
1.2	< 0.02	< 9
1.4	.05	14
1.6	.05	14
1.8	.05	14
2.0	.05	14
2.1	.10	19
2.2	.15	24
2.3	.30	34
2.4	.90	58
2.5	2.5	97
2.6	8.0	174
2.7	17	253
2.8	30	336
2.85	*35	*363
2.9	33	353
3.0	30	336
3.1	2.0	87
3.2	12	213
3.3	4.0	123

Figure 4-9. Field intensity 3.7 m from an ASR-7 radar antenna; vertical cut through the center of the beam, Los Angeles.

Measuring instruments: CIM-1 and CIM-2.

Transmitter frequency = 2.735 GHz; PRR = 930 /s.

Transmitter power = 400 kW pk \approx 310 W av.

Measurement location	Field Intensity	
	mW/cm ²	V/m
I. Center of main beam, between the antenna feed and reflector screen:		
Touching center (focusing dot) of reflector.	6.5	156
30 cm from reflector (above center of tower).	30	336
60 cm from reflector.	40	388
85 cm from reflector.	50	434
1 m from reflector (midway between the rf feed and reflector dot).	60	475
II. Miscellaneous measurements not in center of beam:		
30 cm from reflector, midway between top and bottom vertically, left edge of reflector.	0.2	27
30 cm out from bottom edge of reflector, below center of beam, near waveguide elbow.	2.0	87

Figure 4-10. Field intensity of an ASR-7 radar measured on the antenna tower, Atlantic City.

Measuring instruments: CIM-1 and CIM-2.
 See figure 4-10 for transmitter characteristics.
 Measurement distance = 3.66 m (12 ft.). *Denotes beam center.

Vertical cut through center of beam (antenna azimuth angle = 128°)			Horizontal cut through center of beam (probe height = 2.96 m above deck)		
Height above deck, meters	Field intensity		Antenna azimuth, degrees	Field intensity	
	mW/cm ²	V/m		mW/cm ²	V/m
1.0	< 0.02	< 9	0	.10	19
1.2	0.05	14	10	.05	14
1.4	0.05	14	20	.05	14
1.6	0.05	14	30	.10	19
1.8	0.05	14	40	.10	19
2.0	0.05	14	50	.15	24
2.2	0.10	19	60	.10	19
2.4	0.20	27	70	.20	27
2.5	0.75	53	80	.30	34
2.6	3.0	106	90	2.5	97
2.7	8.0	174	95	4.5	130
2.8	20	274	100	10	194
2.9	35	363	105	12	213
2.96	*42	*398	110	17	253
3.0	40	388	115	25	307
3.1	15	238	120	27	319
3.2	3.0	106	121	29	331
3.3	20	274	122	31	342
3.4	15	238	123	33	353
3.5	1.0	61	124	34	358
			125	33	353
			126	35	363
			127	38	378
			128	*42	*398
			130	38	378
			140	25	307
			150	10	194
			160	.15	24
			170	.35	36
			180	.15	24
			190	.15	24
			200	.15	24
			210	.20	27
			220	.15	24
			230	.15	24
			240	.15	24
			250	.15	24
			260	.15	24
			270	.15	24
			280	.15	24
			290	.10	19
			300	.05	14
			310	.05	14
			320	.05	14
			330	.05	14
			340	.10	19
			350	.15	24
			360	.10	19

Figure 4-11. Field intensity 3.7 m from an ASR-7 radar antenna; horizontal and vertical cuts through the center of the beam, Atlantic City.

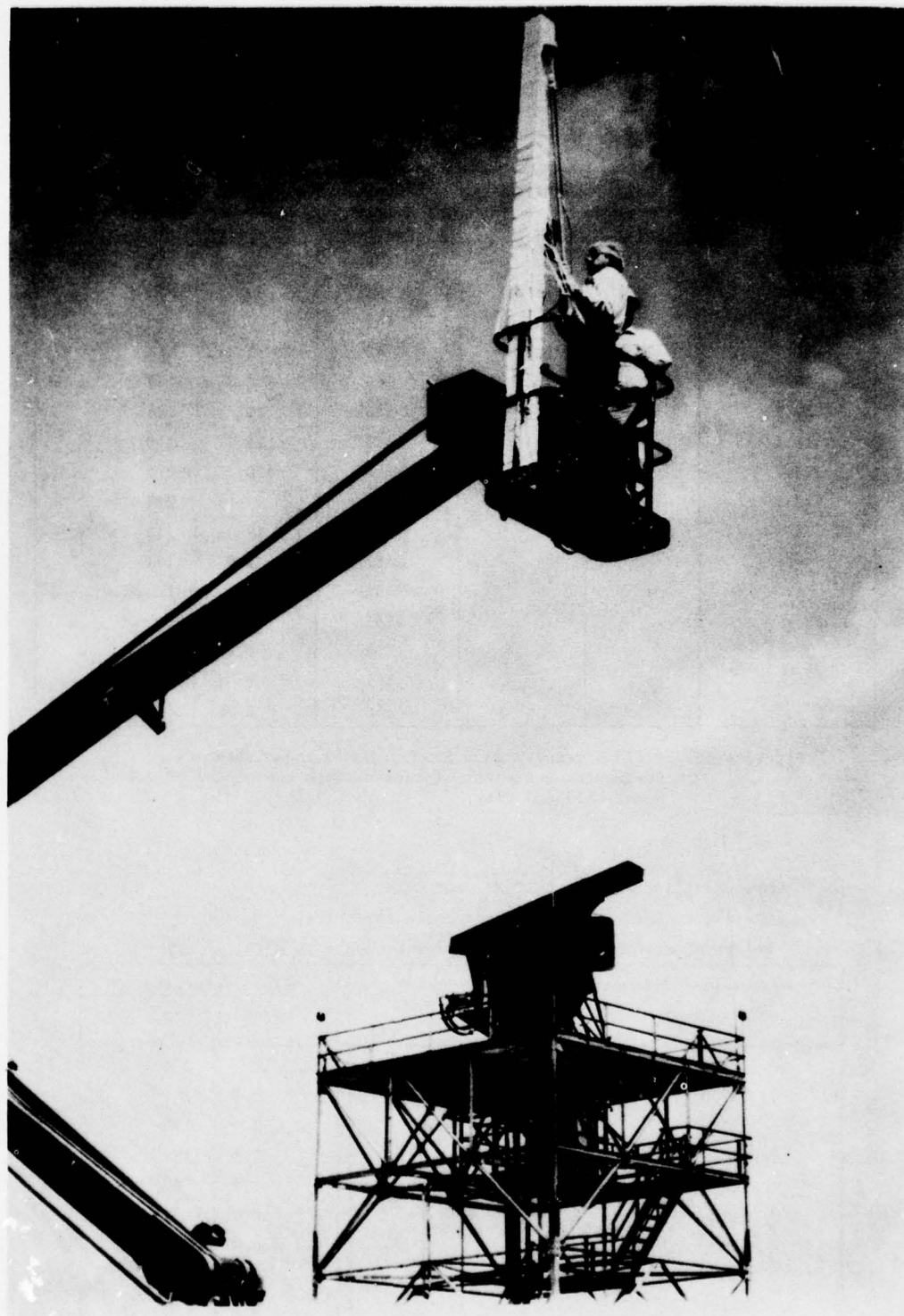


Figure 4-12. Photograph of an ASR-8 antenna (background) and the "cherry picker" used when measuring the field intensity, Oklahoma City.

Measuring instruments: CIM-1 and CIM-2.

Transmitter power, channel A = 1.16 MW pk = 725 W av.

Transmitter power, channel B = 1.30 MW pk = 812 W av.

Measurement distance = 23.1 m . *Denotes center of beam.

Vertical cut through center of beam, (antenna azimuth angle = 148°)			Horizontal cut through center of beam, (probe height = 14.6 m above ground)		
Height above ground, meters	Field intensity		Antenna azimuth, degrees	Field intensity	
	mW/cm ²	V/m		mW/cm ²	V/m
15.5	14	230	136	0.06	15
15.2	12	213	140	0.17	25
15.0	*20	*274	141	0.17	25
14.7	15	238	143	1.1	64
14.4	8.5	179	145	5.0	137
14.2	5.0	137	146	10	194
14.1	4.0	123	147	15	238
13.7	0.4	39	148	*20	*274
13.5	0.1	19	149	17	253
			150	12	213
			151	5.0	137
			152	3.4	113
			153	1.0	61
			154	0.4	39
			157	< 0.02	< 9
			160	< 0.02	< 9

Figure 4-13. Field intensity 23 m from an ASR-8 radar antenna; horizontal and vertical cuts through the center of the beam, Oklahoma City.

Measuring instruments : CIM-1 and CIM-2.

See figure 4-13 for transmitter characteristics.

Height of transmitting antenna above ground = 15 m (49.2 ft.).

Measurement distance, meters	Field intensity	
	mW/cm ²	V/m
23.1	20	274
37.0	9.8	192
53.6	3.7	118
70.2	2.1	89
102	1.2	67
148	0.71	52
193	0.31	34
293	0.18	26
397	0.10	19

Figure 4-14. Field intensity in the beam of an ASR-8 radar as a function of distance from the transmitter antenna, Oklahoma City.

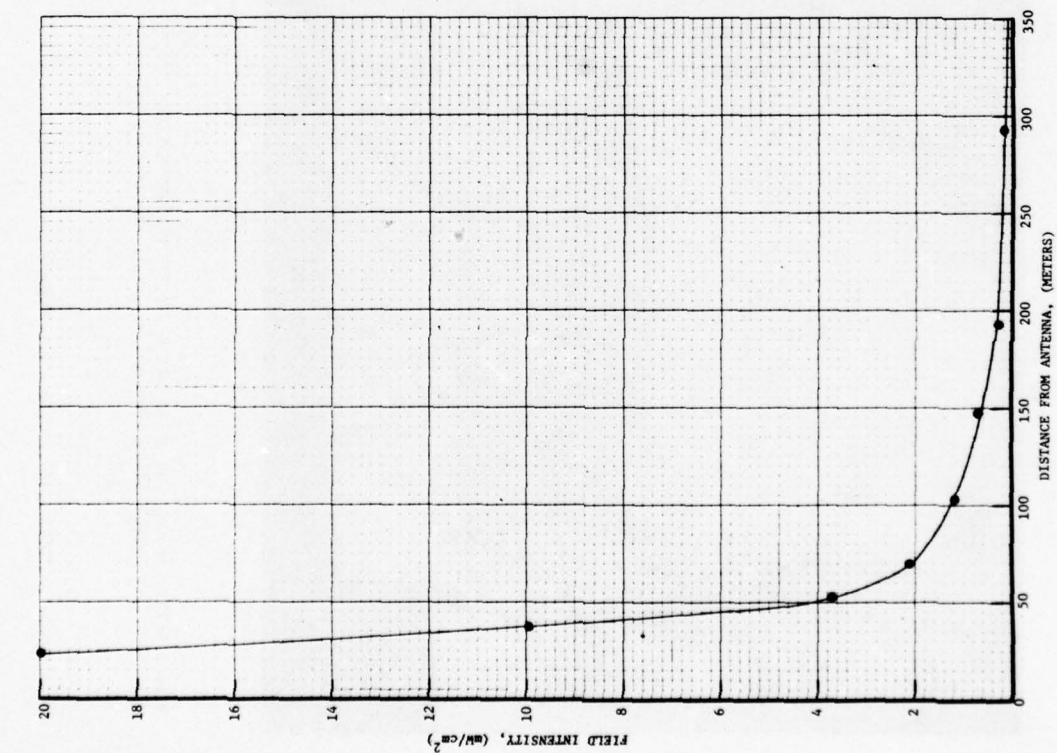


Figure 4-15. Graph of field intensity in the beam of an ASR-8 radar versus distance from the transmitting antenna.

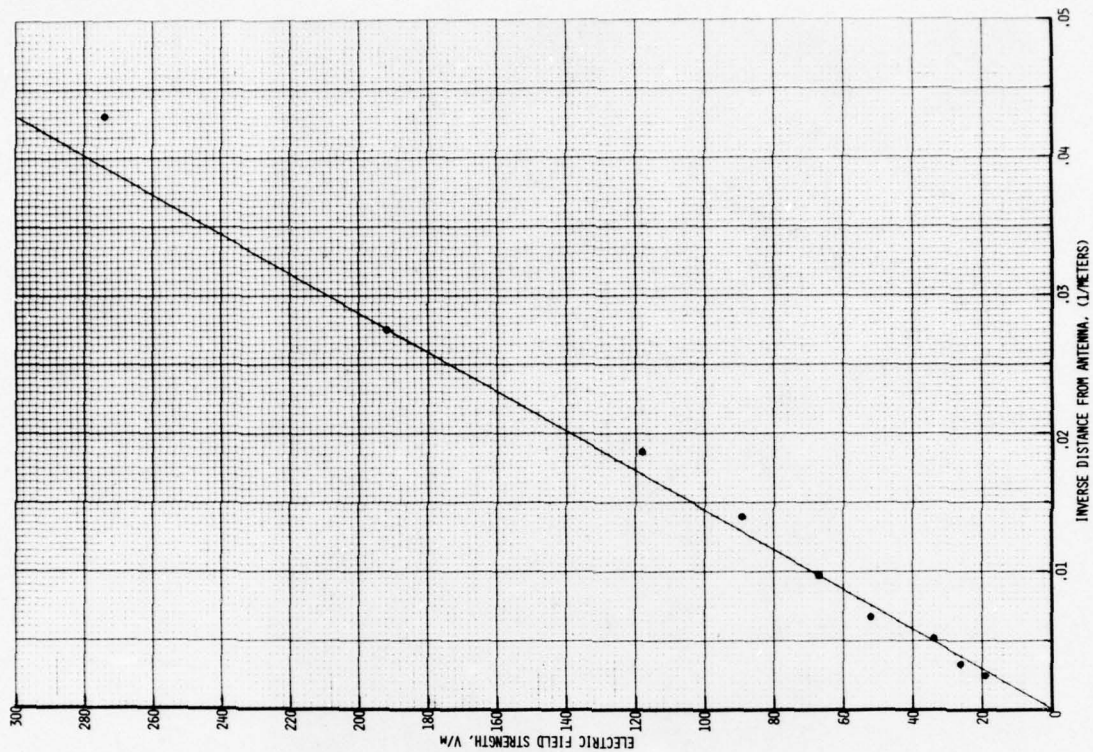


Figure 4-16. Graph of electric field strength in the beam of an ASR-8 radar versus inverse distance from the antenna.

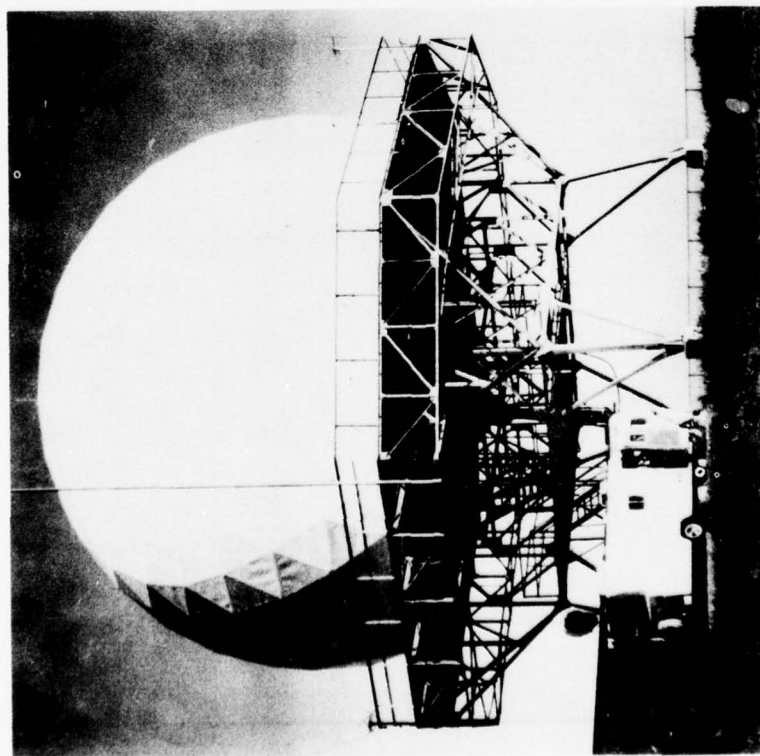


Figure 4-17. Photograph of an Air Route Surveillance Radar (ARSR) installation, Denver.

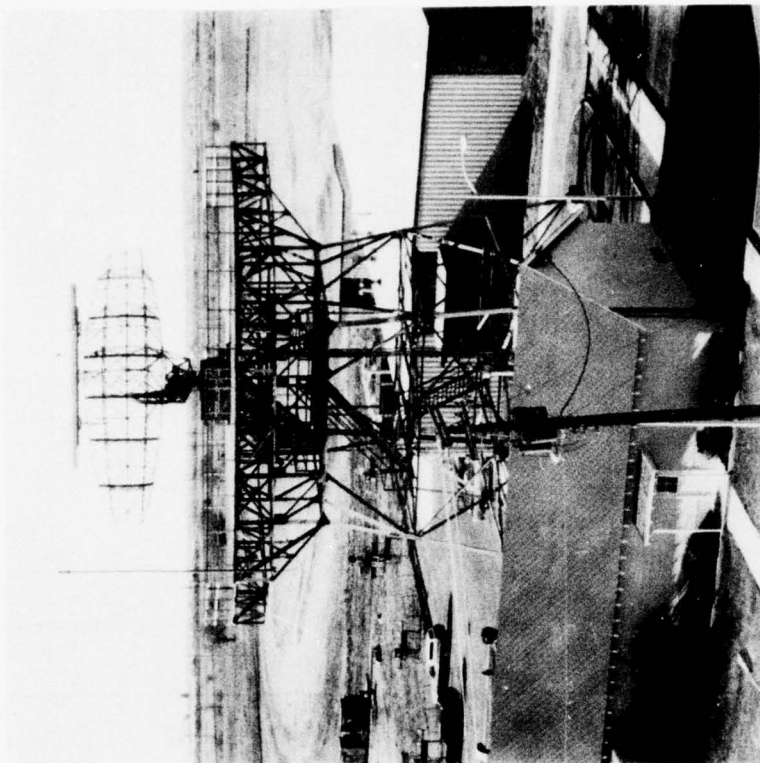


Figure 4-18. Photograph of an ARSR transmitter building and antenna mounted on a tower, Oklahoma City.

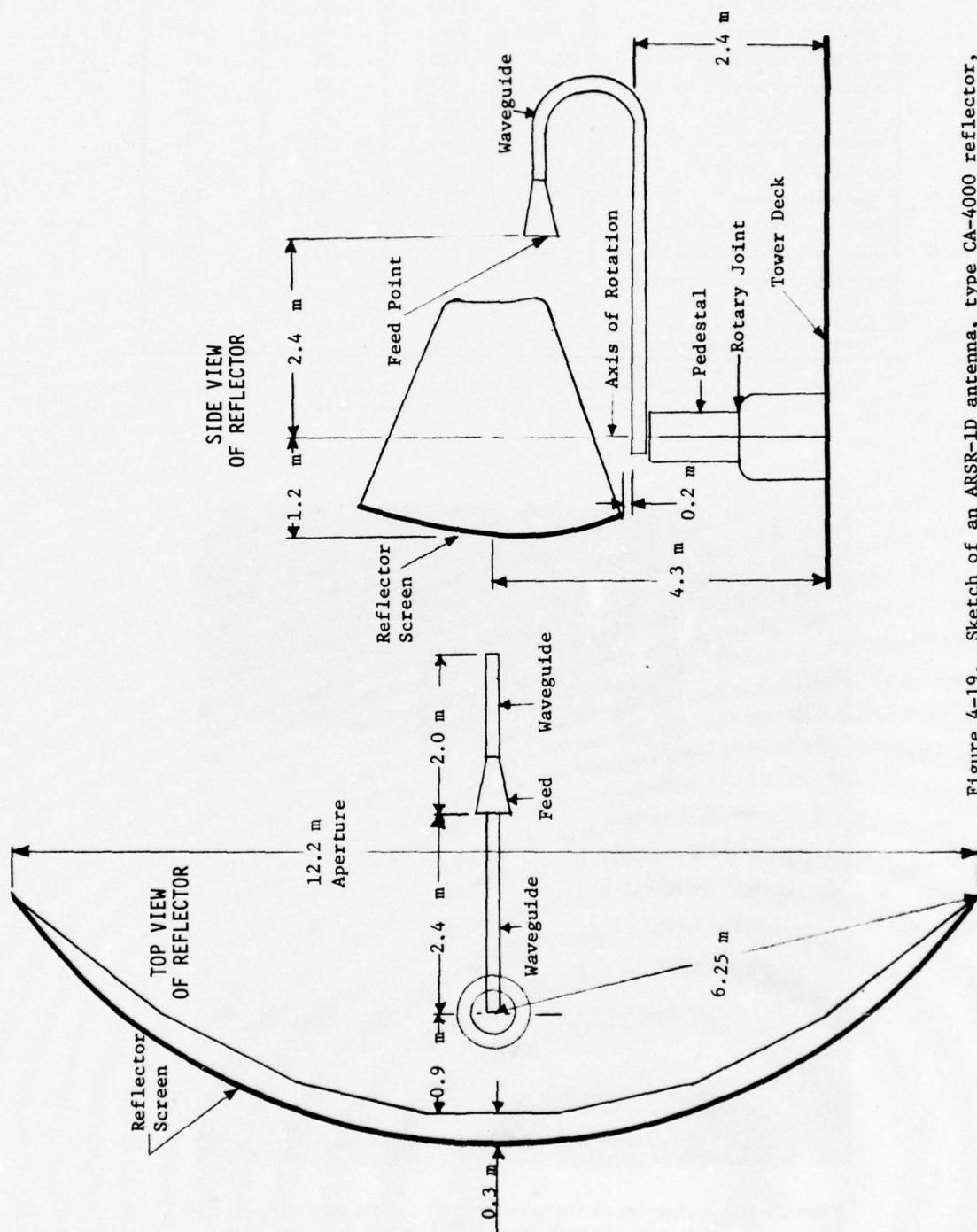


Figure 4-19. Sketch of an ARSR-1D antenna, type CA-4000 reflector, giving approximate dimensions.

Measuring instrument: EDM-1, peak mode, 10 s time constant.
 Type of measurement: Pulse-peak E field of a rotating ARSR antenna.
 Transmitter frequency = 1.33 GHz; PRR = 360/s.
 Transmitter power = 4 MW pk \approx 2.6 kW av.

Measurement position on mezzanine deck	Height above deck, meters	Measured E pk, V/m	Equivalent E av, V/m	Equivalent S av, mW/cm ²
Center of mezzanine deck	2.5	850	23	.14
Middle of west side	2.5	1330	36	.34
Northwest corner	2.5	1200	32	.28
Middle of north side	2.5	1140	31	.25
Northeast corner	2.5	930	25	.17
Middle of east side	2.5	820	22	.13
Southeast corner	2.5	1140	31	.25
Middle of south side	2.5	930	25	.17
Southwest corner	2.5	1100	30	.23
Near gate to top deck	2.5	970	26	.18
Near gate to top, head height	1.7	650	17	.08
Maximum hot spot on stairway to top	-	970	26	.18
Maximum hot spot at head height, near southeast corner	1.7	1220	33	.29

Figure 4-20. Leakage fields of an ARSR-1D radar measured in the area below the top deck of the antenna tower, Oklahoma City.

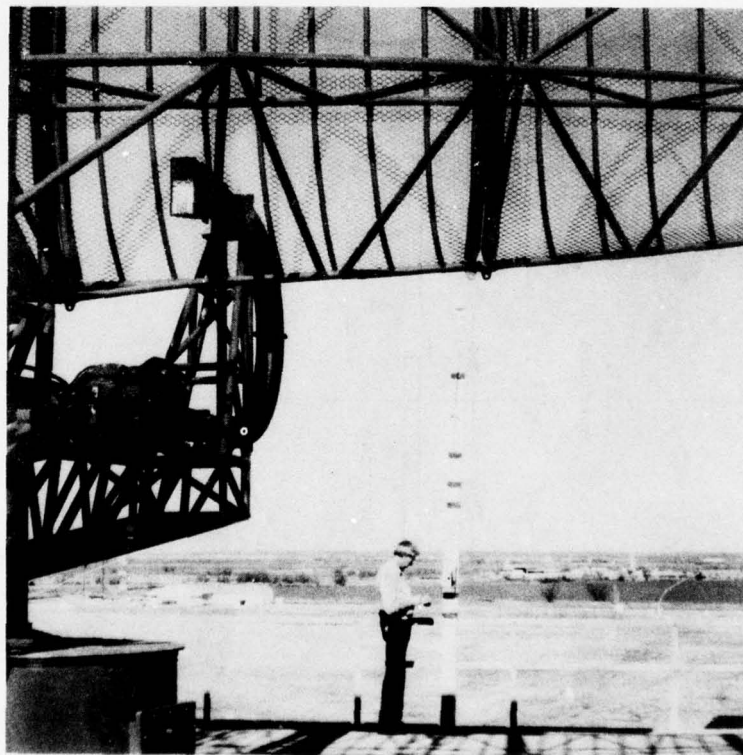


Figure 4-21. Photograph of the setup used to measure field intensity in the near-zone beam of an ARSR radar.

Measuring instruments: CIM-1 and CIM-2.

Transmitter power ≈ 3.9 MW pk ≈ 2.5 kW av.

Note: See text for explanation of the field intensity measurements exceeding 60 mW/cm^2 .

Measurement location on ARSR antenna tower.	Field intensity	
	mW/cm ²	V/m
Search of tower area, head height above the metal deck:		
Top of stairway, 4 m from center of tower	0.5	43
Average field on tower at head height	0.3	34
Hot spot near the antenna pedestal, in view of feed point	0.5	43
Maximum hot spot found, beneath the antenna feed	1.0	61
Search of tower area, 1 m above the deck:		
Average field around outside periphery of tower, near radome	0.1	19
Maximum hot spot found at this height	0.2	27
Field 30 cm in front of bottom edge of antenna reflector:		
Left end of reflector	0.05	14
Midway between left end of reflector & center of tower	0.6	48
Field 1 m in front of reflector:		
Left end of reflector	0.4	39
1 m from left end of reflector, midway vertically	0.8	55
Below center of beam, midway vertically between bottom edge and center of reflector	6.5	156
Behind the bend in the waveguide, 4.4 m from center of tower	1.3	70
Above antenna pedestal, on axis of antenna rotation:		
0.3 m above pedestal	1	61
0.9 above pedestal	10	194
1.2 m above pedestal	20	274
1.5 m above pedestal	30	336
1.8 m above pedestal, center height of reflector	40	388
Maximum hot spot above pedestal, in center of beam	48	425
Center of beam, above tower railing, 9.5 m from antenna	15	238
Center of beam on a line between feed point and reflector:		
Between reflector and axis of antenna rotation, standing wave pattern	15 to 60	238 to 475
Midway between feed point and center of reflector	65	495
Maximum hot spot between above point and axis of rotation	100	614
1 m from feed point	300	1060
60 cm from feed point	600	1500
Measurement location on distant ASR antenna tower:		
Maximum intensity found in center of beam at a distance 83 m from the center of the ARSR antenna tower	1.2	67

Figure 4-22. Average field intensity of three ARSR radars tested at Oklahoma City, Denver, and Atlantic City.

Measuring instrument: EDM-1C, peak mode, 10 s time constant.

Type of measurement: Pulse-peak field of a rotating ARSR antenna,
mean value of three antenna rotations.

See figure 4-20 for transmitter characteristics.

Note: Height of ARSR antenna \approx 20 m above ground.

	Location of measurement point	Horizontal distance, meters	Height above ground, meters	Field intensity
I.	Above roof of VORTAC building, maximum hot spot at head height.	310	4.9	Meas. E pk = 766 V/m Equiv. E av = 21 V/m Equiv. S av = 0.11 mW/cm ²
	Above roof of VORTAC building, maximum at heights up to 6 m above ground.	310	5.5	Meas. E pk = 1270 V/m Equiv. E av = 34 V/m Equiv. S av = 0.31 mW/cm ²
II.	Third floor of CAMI building, north wall of northeast corner office.	560	8.5	Meas. E pk \approx 0
	Third floor of CAMI building, northeast corner office, maximum field in center of upper windows.	560	8.5	Meas. E pk = 294 V/m Equiv. E av = 8.0 V/m Equiv. S av = 0.017 mW/cm ²
	Third floor of CAMI building, northeast corner office, maximum hot spot found in a window.	560	8.5	Meas. E. pk = 322 V/m Equiv. E av = 8.7 V/m Equiv. S av = 0.020 mW/cm ²
III.	Parked airplane near Hanger No. 9, in line of sight of ARSR antenna, interior of fuselage.	625	4.5	Meas. E pk \approx 0
	Parked airplane near Hanger No. 9, center of fuselage window.	625	4.5	Meas. E pk = 136 V/m Equiv. E av = 3.7 V/m Equiv. S av = 0.004 mW/cm ²
	Parked airplane near Hanger No. 9, EDM probe held outside copilot's window, above fuselage.	625	6	Meas. E pk = 260 V/m Equiv. E av = 7.0 V/m Equiv. S av = 0.01 mW/cm ²

Figure 4-23. Field intensity of an ARSR-1D radar measured at several distant locations, below the direct beam, Oklahoma City.

Measuring instrument: CIM-1, fast time constant.
 Transmitter frequency = 14.2 GHz; PRR = 15.6 kHz.
 Transmitter power = 24.1 kW pk \approx 11.3 W av.

Measurement location	Field intensity	
	mW/cm ²	V/m
Touching the radiating edge (5 cm distance) of the antenna:		
Midpoint of blade antenna	.34	36
Ends of antenna, average of left and right end	< .02	< 9
Midway between center and ends of antenna, average	.16	25
Search for hot spots along radiating edge of antenna:		
Near midpoint of antenna	.59	47
0.85 m from midpoint, average of left and right	.50	43
1.7 m from midpoint, average of left and right	.18	26
2.6 m from midpoint, average of left and right	.08	17
3.4 m from midpoint, average of left and right	.03	11
Miscellaneous measurements:		
Back of blade antenna, opposite the radiating edge	< .02	< 9
Outside tips at ends of blade	< .02	< 9

Figure 4-24. Measurements of field intensity near the antenna of an ASDE-1 radar, Los Angeles.

Measuring instrument: CIM-1 and CIM-2.
 Transmitter frequency = 23.9 GHz; PRR = 14.4 kHz.
 Transmitter power = 48.6 kW pk \approx 14 W av.

Measurement location	Field intensity	
	mW/cm ²	V/m
Touching side of rectangular reflector:		
Top corner, average value of left and right sides	.03	11
Bottom corner, average of left and right sides	.03	11
Midway between top & bottom, average of left & right	.06	15
Touching top of reflector, at midpoint horizontally	.11	20
Touching bottom of reflector, at midpoint horizontally	.17	25
30 cm directly above the feed point	.79	55
60 cm directly above the feed point	.48	43
90 cm directly above the feed point	1.6	78
Center of main beam, between feed and reflector:		
Touching center of reflector, above center of antenna rotation.	1.3	70
30 cm from center of reflector	1.2	67
50 cm from center of reflector	1.6	78
Midway between feed and reflector, or 75 cm	2.4	95
50 cm from feed point	7.9	173
30 cm from feed point	16	246
5 cm from aperture of feed horn	80	549

Figure 4-25. Measurements of field intensity near the antenna of an ASDE-2 radar, Atlantic City.

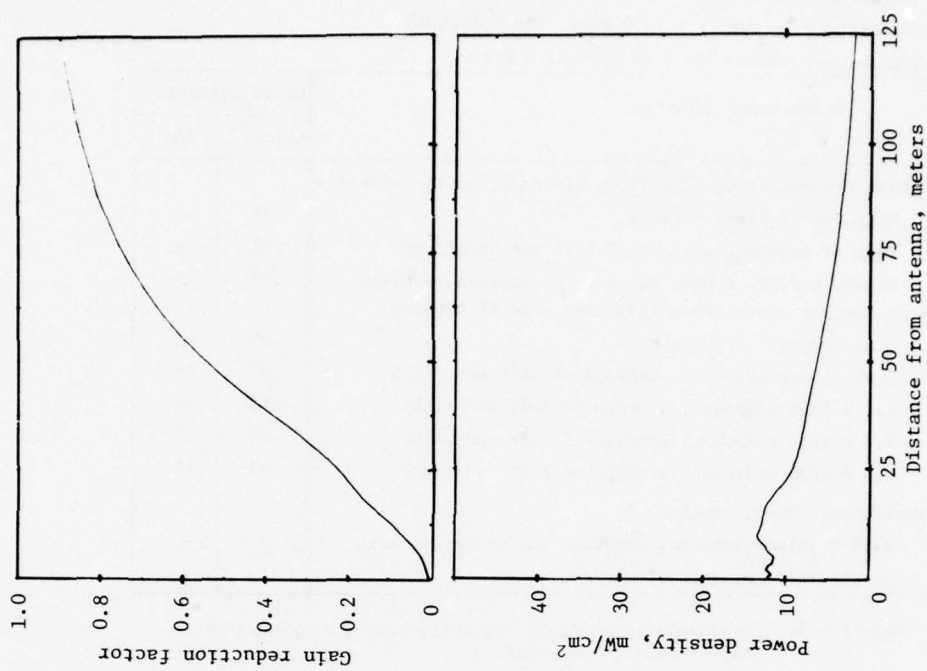


Figure 4-26. Computed field intensity in the near-zone beam of an ASR radar antenna, assuming uniform phase and amplitude in the aperture illumination.

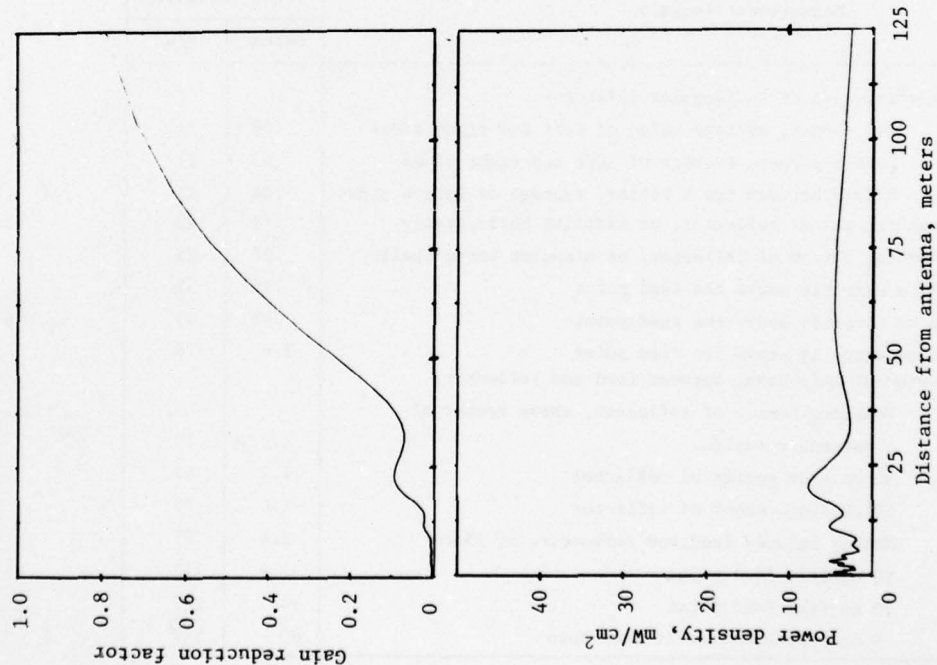


Figure 4-27. Computed field intensity in the near-zone beam of an ASR antenna, cosine taper of aperture illumination.

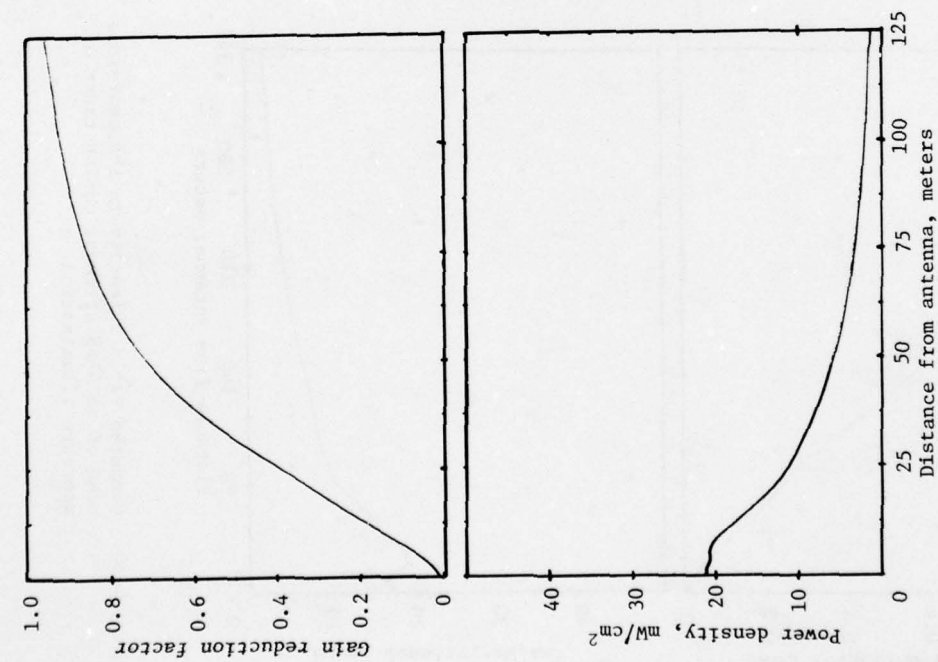


Figure 4-28. Computed field intensity in the near-zone beam of an ASR antenna, cosine-squared taper of aperture illumination.

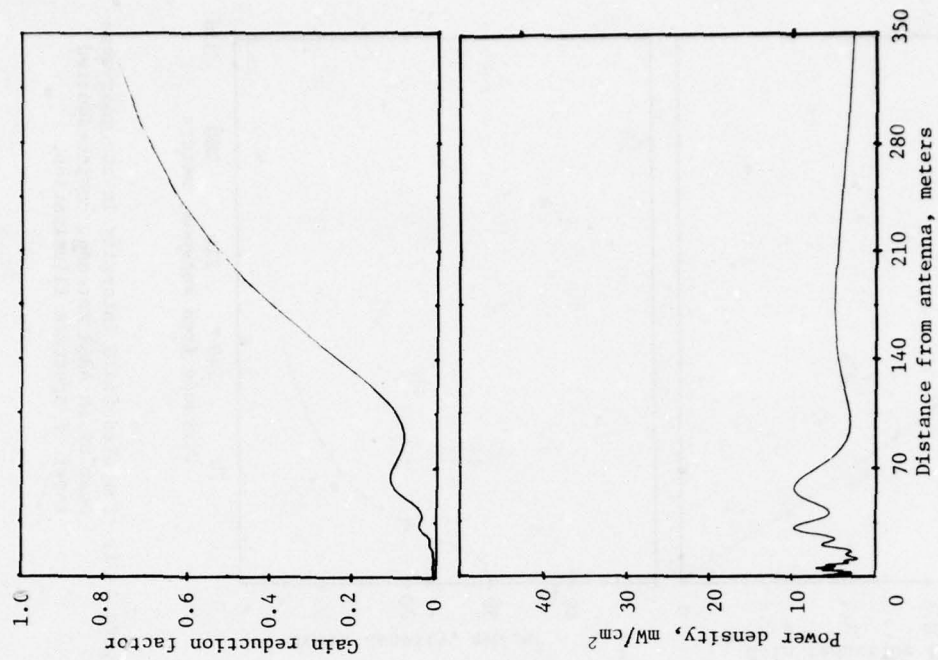


Figure 4-29. Computed field intensity in the near-zone beam of an ARSR antenna, uniform aperture illumination.

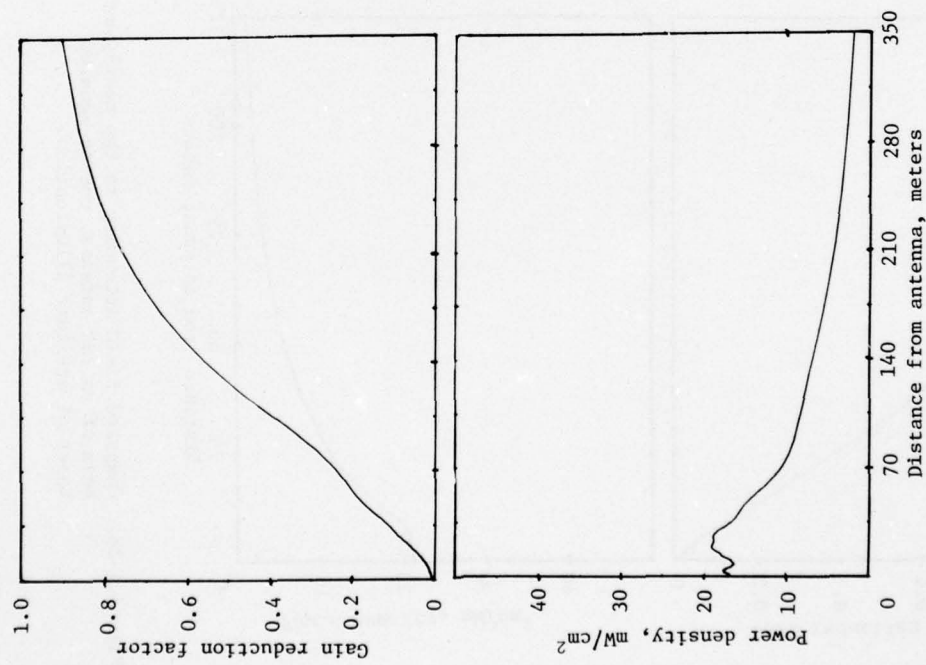


Figure 4-30. Computed field intensity in the near-zone beam of an ARSR antenna, cosine taper of aperture illumination.

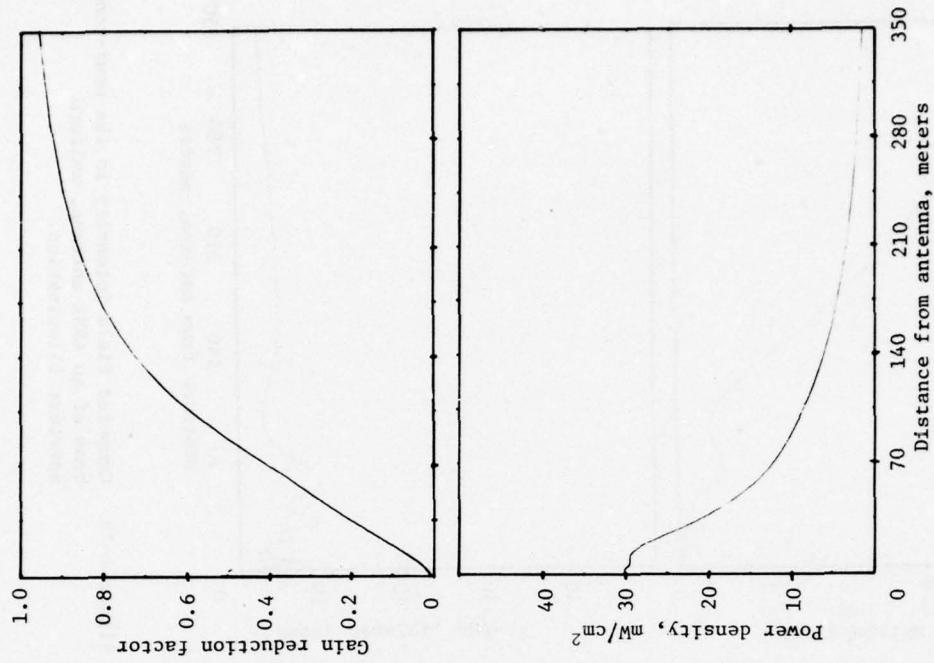


Figure 4-31. Computed field intensity in the near-zone beam of an ARSR antenna, cosine-squared taper of aperture illumination.

VHF LOCALIZER

FUNCTION: Provides Horizontal Guidance.
ANTENNA: Optimum (A) 1000 FT from end of RWY & on Centerline. Horizontal polarization.
BUILDING: Transmitter building (B) is located 100 FT minimum from the center of the approach end.
FREQUENCY: 108 to 111 MHz, odd numbers only.
MODULATION: No-identification modulation depth on Course 20% for 90Hz and for 150Hz.
CODE IDENTIFICATION: 1020Hz at 5%.
VOICE COMMUNICATION: (available at some facilities) 50%.

COURSE WIDTH: Course Width (C) varies, tailored to provide 700 FT at Threshold (Full scale limits).

ILS

FAA Instrument Landing System STANDARD CHARACTERISTICS AND TERMINOLOGY

Revised by FEDERAL AVIATION ADMINISTRATION, 1972

MIDDLE MARKER

FUNCTION: Indicates Decision Height Point.
LOCATION: At Decision Height Point, (G)
 ± 500 FT Longitudinal +
 ± 300 FT Lateral
FREQUENCY: 75 MHz
MODULATION: 1300Hz at 95%
KEYING: Alternate dot and dash

OUTER MARKER

FUNCTION: Indicates Glide Slope Intercept Point.
LOCATION: Directly below point (H) where Glide Slope intersects the minimum holding altitude, ± 800 FT Longitudinal & Lateral.

FREQUENCY: 75 MHz
MODULATION: 400Hz at 95%
KEYING: Two dashes second

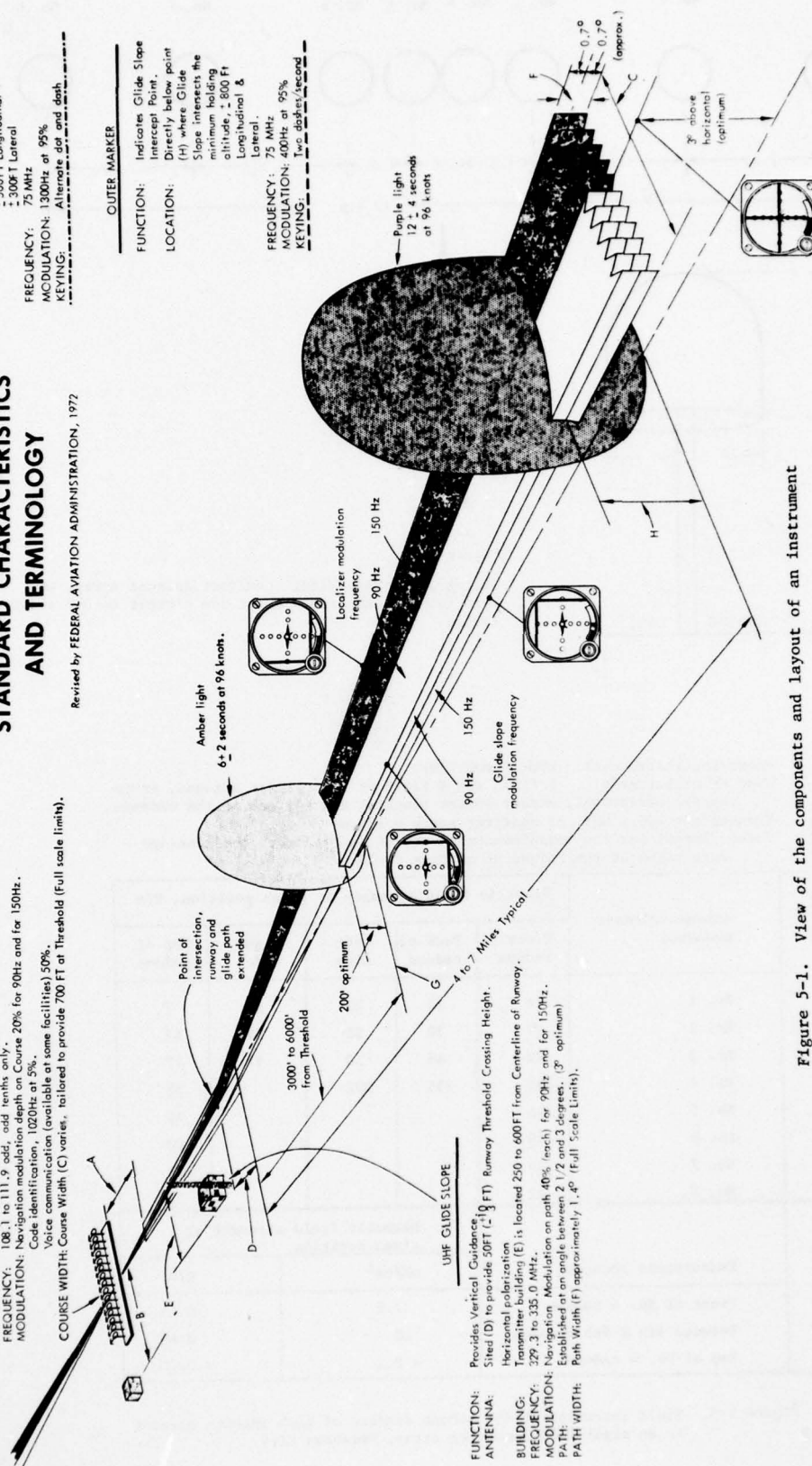


Figure 5-1. View of the components and layout of an instrument landing system.

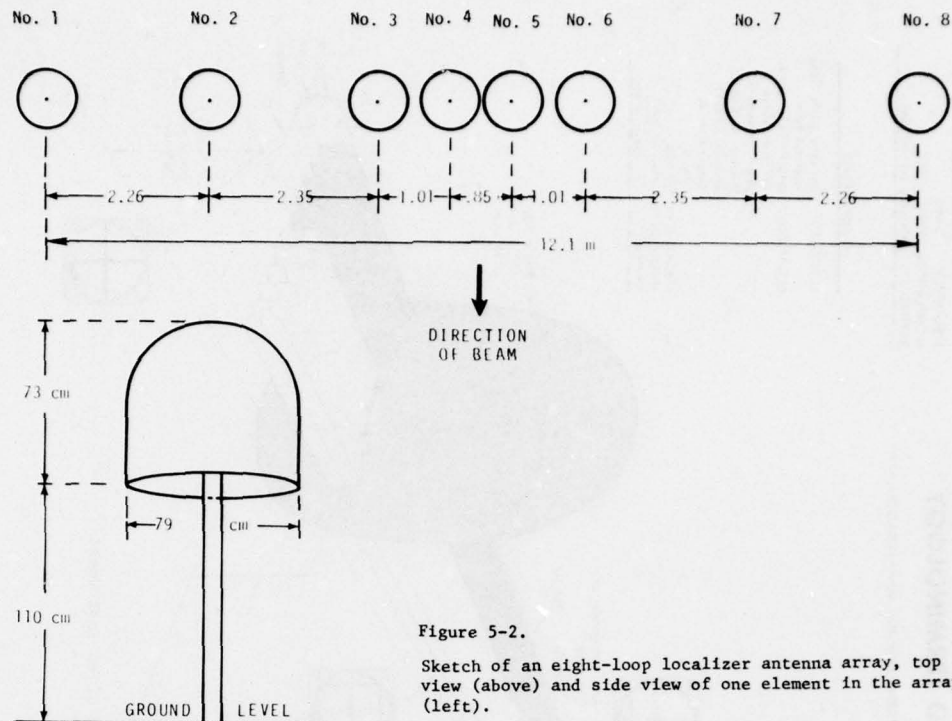


Figure 5-2.

Sketch of an eight-loop localizer antenna array, top view (above) and side view of one element in the array (left).

Measuring instruments: EDM-1C and CIM-3.

Type of measurement: E field and H field of a localizer antenna, probe handle horizontal, sensor sphere touching the surface of the radomes. Frequency = 108.5 MHz; transmitter power = 135 W.

Note: Except for the measurements on top of the radomes, the readings were taken at the height of maximum field.

I.	Antenna element measured	Electric field strength at given position, V/m				
		Front of radome	Back of radome	Left side	Right side	Top of radome
	No. 1	14	12	11	14	7
	No. 2	27	25	25	28	12
	No. 3	49	46	50	97	27
	No. 4	255	255	232		31
	No. 5	245				19
	No. 6	49				20
	No. 7	29				11
	No. 8	12				7
II.	Measurement location	Magnetic field strength at given position				
		mW/cm ²		A/m		
	Front of No. 4 radome	7.5		0.45		
	Between 4th & 5th radomes	18		0.69		
	Top of No. 4 radome	< 0.1		< 0.05		

Figure 5-3. Field intensity at the radome surface of each antenna element in an eight-loop localizer array, Oklahoma City.



Figure 5-4. Photograph of a V-ring localizer antenna array, ILS, Denver.



Figure 5-5. Photograph of an operator using the EDM-1C field strength meter, on the metal counterpoise of a V-ring localizer antenna, Denver.

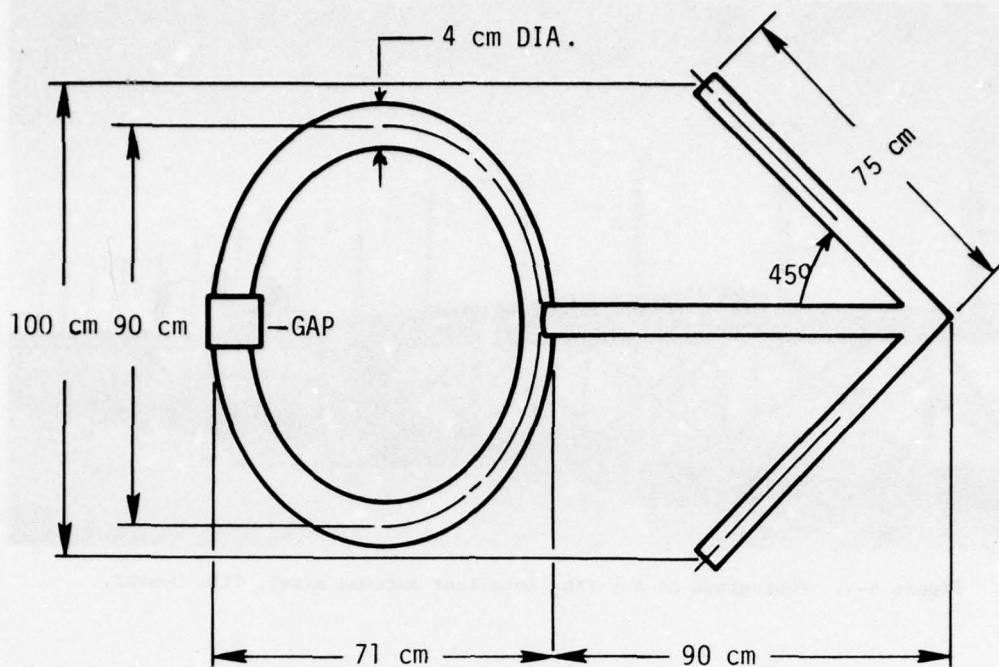


Figure 5-6. Sketch of one element in a V-ring localizer antenna array giving approximate dimensions.

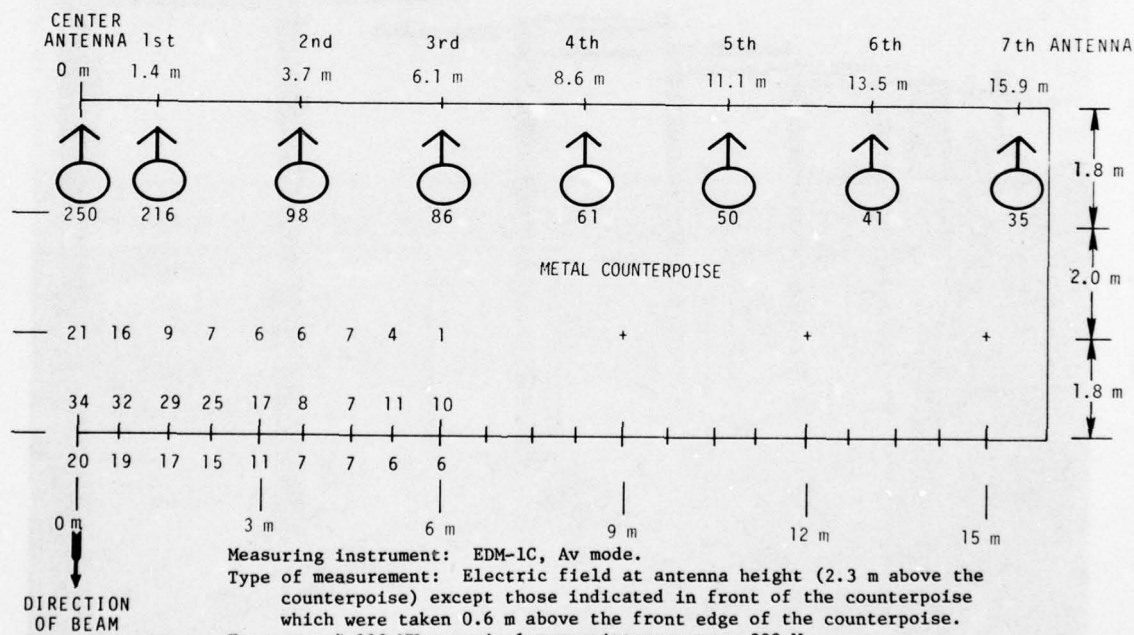


Figure 5-7. Top view of a V-ring localizer antenna, including mean values of the measured field intensity at several positions, Denver.

Measuring instrument: EDM-1C, Av mode.
 Type of measurement: E field energy density near the antenna,
 probe handle horizontal, sensor at gap in ring.
 Frequency \approx 110 MHz; transmitter power \approx 50 W.

Measurement location (sensor touching gap in ring)	Field intensity 5 cm in front of antenna gap		Field intensity 33 cm in front of antenna gap	
	nJ/m ³	V/m	nJ/m ³	V/m
7th element left of center	0.43	10	0.01	1.5
6th element left of center	0.54	11	0.01	1.5
5th element left of center	0.82	14	0.02	2.1
4th element left of center	1.20	16	0.03	2.6
3rd element left of center	2.40	23	0.05	3.4
2nd element left of center	2.88	26	0.06	3.7
1st element left of center	14.4	57	0.46	10
Center element of array	49.4	106	1.36	18
1st element right of center	14.4	57	0.48	10
2nd element right of center	2.88	26	0.06	3.7
3rd element right of center	2.82	25	0.07	4.0
4th element right of center	1.32	17	0.04	3.0
5th element right of center	0.80	13	0.03	2.6
6th element right of center	0.60	12	0.02	2.1
7th element right of center	0.48	10	0.01	1.5

Figure 5-8. Field intensity at antenna height in front of a V-ring
 localizer array, Oklahoma City.

Measuring instrument: EDM-1C.

Type of measurement: E field above the ground screen of a localizer
 antenna, probe mounted on plastic pole, handle horizontal, sensor
 toward the antenna.

Frequency \approx 110 MHz; Transmitter power \approx 50 W.

Note: Height of V-ring antenna = 2.3 m above the ground screen.

Vertical height	Electric field strength V/m, at the given position									
	2.3 m	2.0 m	1.7 m	1.4 m	1.1 m	0.8 m	0.5 m	0.2 m		
Horizontal distance										
5 cm	129	21	13.8	10.6	10.8	11.6	8.9	3.7		
0.3 m	18.8	14.9	11.4	10.2	11.1	12.0	9.6	4.0		
0.6 m	11.6	9.0	8.1	8.9	11.0	12.2	9.6	4.1		
0.9 m	7.7	6.2	6.2	8.1	10.9	11.6	9.0	4.0		
1.2 m	4.8	4.3	5.6	7.7	10.6	10.9	8.2	3.4		
1.5 m	3.4	4.0	5.6	8.0	10.2	10.0	7.5	3.0		
1.8 m	2.1	4.3	5.6	8.1	9.9	9.0	6.7	2.8		
2.1 m	3.4	5.0	6.2	8.0	9.0	8.2	6.0	2.6		
2.4 m	4.0	5.6	6.6	7.7	8.4	7.5	5.4	2.1		
2.7 m	5.0	6.2	6.7	7.4	7.7	7.0	5.0	2.1		
3.0 m	5.6	6.2	7.0	7.2	7.2	6.4	4.3	1.8		
3.3 m	5.8	5.5	7.2	6.7	6.6	5.4	4.0	1.5		
3.6 m	6.0	5.2	6.6	6.2	5.6	4.8	3.7	1.5		

Figure 5-9. Profile of field intensity in front of the center element
 of a V-ring localizer antenna, Oklahoma City.

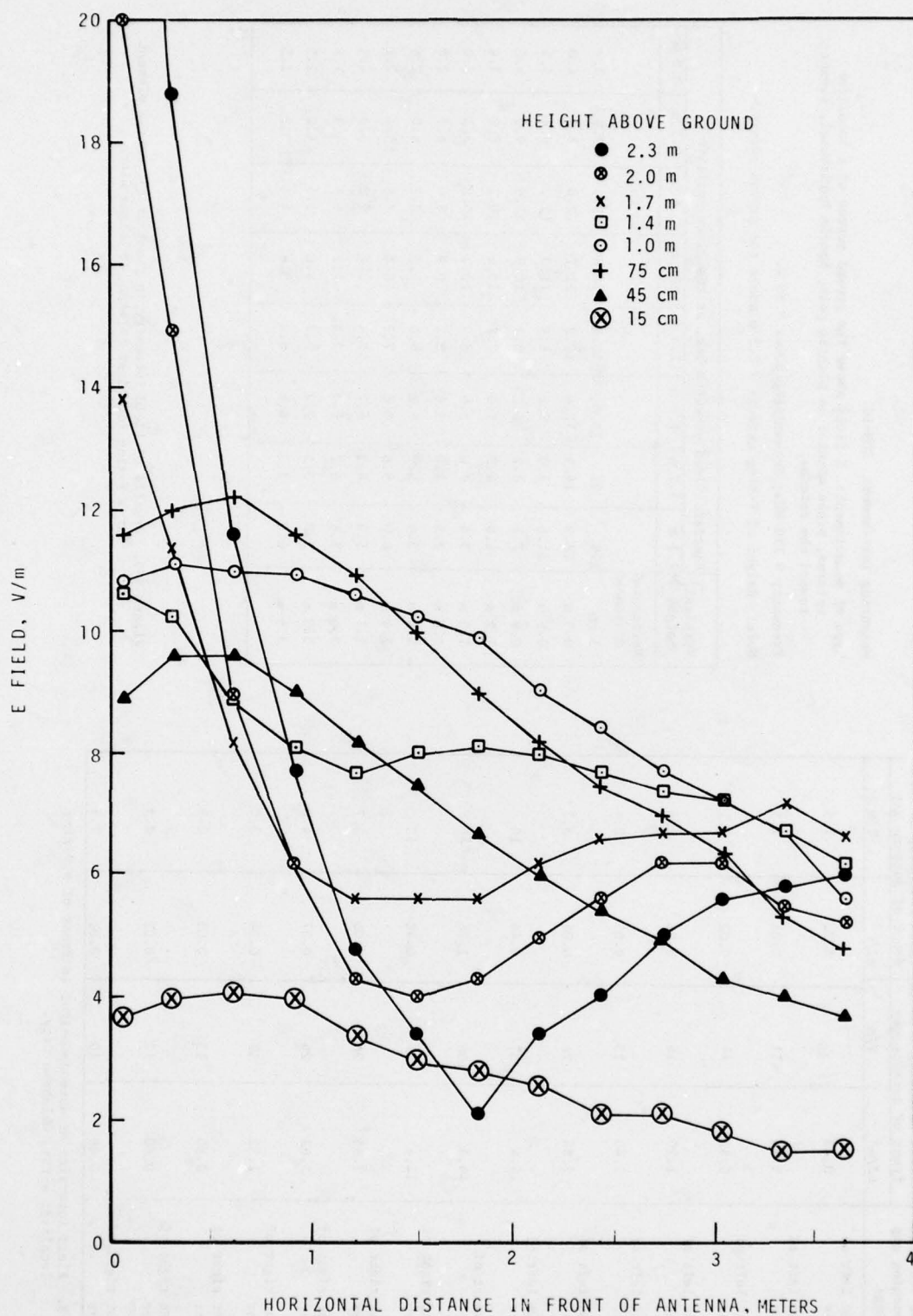


Figure 5-10. Graph showing profile of the electric field strength in front of a V-ring localizer antenna, data given in figure 5-9.

Measuring instrument: EDM-3, Av mode.

Type of measurement: E field energy density near the antenna.

Frequency = 111.7 MHz; Transmitter power = 55 W.

Measurement location	Field intensity	
	nJ/m ³	V/m
I. Sensor touching front of gap in ring.		
7th element left of center	0.60	12
6th element left of center	0.78	13
5th element left of center	1.15	16
4th element left of center	1.75	18
3rd element left of center	3.9	30
2nd element left of center	8.3	43
1st element left of center	30	82
Center element of array	82	136
1st element right of center	25	75
2nd element right of center	6.0	37
3rd element right of center	2.5	24
4th element right of center	1.10	16
5th element right of center	0.82	14
6th element right of center	0.53	11
7th element right of center	0.49	11
II. Near the center element of the antenna.		
Sensor touching front of gap in ring	82	136
Sensor touching bottom of gap in ring	80	134
Sensor touching back (inside) of gap in ring	75	130
III. Inside each ring of the array.	Field intensity	
	15 cm inside of gap, V/m	25 cm inside of gap, V/m
5th element left of center	5.6	-
4th element left of center	7.4	4.5
3rd element left of center	9.9	7.5
2nd element left of center	16	9.5
1st element left of center	30	18
Center element of array	52	34
1st element right of center	27	18
2nd element right of center	14	9.5
3rd element right of center	9.4	6.7
4th element right of center	6.4	4.5
5th element right of center	5.6	-

Figure 5-11. Field intensity near the antenna of a V-ring localizer, south site, Oklahoma City.

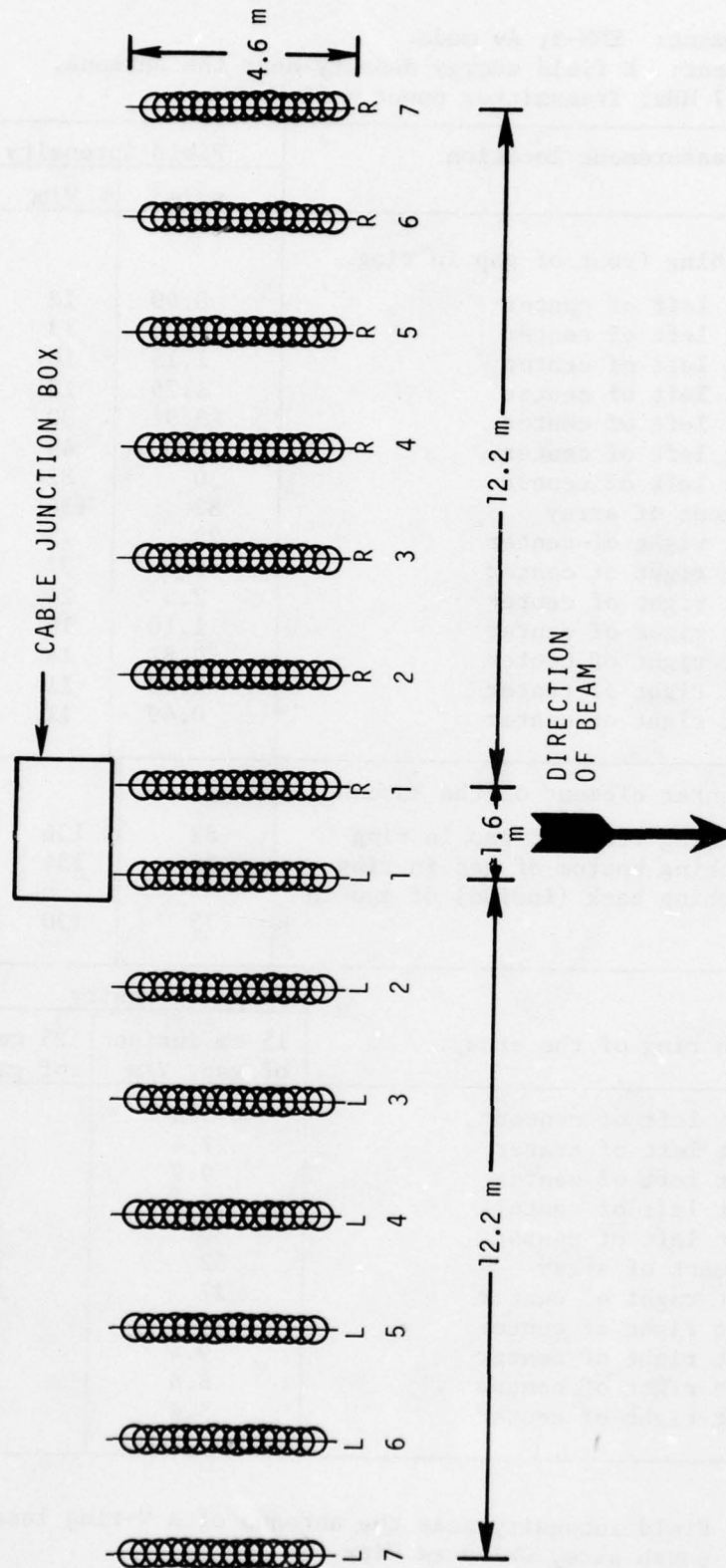


Figure 5-12. Top view of a traveling-wave localizer antenna array, with approximate dimensions.

Measuring instrument: EDM-1C.
 Type of measurement: E field at antenna height (2.2 m above ground),
 probe handle vertical, sensor on top.
 Frequency \approx 109 MHz; Transmitter power \approx 90 W.

Measurement location (30 cm in front of antenna)	Field intensity	
	nJ/m ³	V/m
7th element left of center	0.01	1.5
6th element left of center	0.02	2.1
5th element left of center	0.03	2.6
4th element left of center	0.08	4.3
3rd element left of center	0.15	5.8
2nd element left of center	0.24	7.4
1st element left of center	0.22	7.0
1st element left of center	0.20	6.7
2nd element left of center	0.24	7.4
3rd element left of center	0.12	5.2
4th element left of center	0.07	4.0
5th element left of center	0.03	2.6
6th element left of center	0.02	2.1
7th element left of center	0.01	1.5

Figure 5-13. Field intensity 30 cm in front of each antenna element of a traveling-wave localizer, Oklahoma City.



Figure 5-14. Photograph of a waveguide localizer showing one of the slot antennas.

AD-A051 717

NATIONAL BUREAU OF STANDARDS BOULDER COLO ELECTROMA--ETC F/G 9/1
SURVEYS OF ELECTROMAGNETIC FIELD INTENSITIES NEAR REPRESENTATIV--ETC(U)
DEC 77 E B LARSEN, J F SHAFER DOT-FA73WAI-388

UNCLASSIFIED

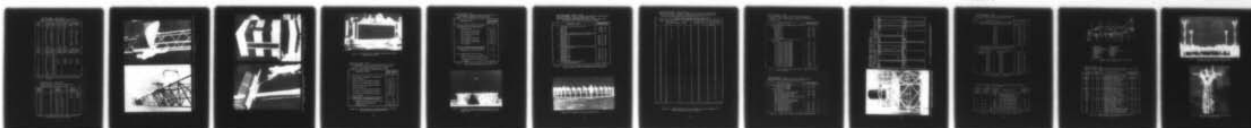
NBSIR-76-849

FAA-RD-77-179

NL

2 OF 2

AD
A051 717

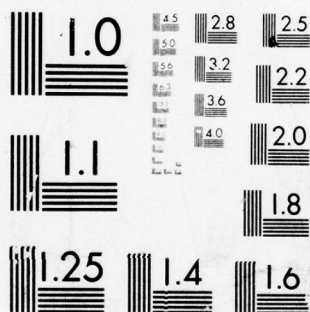


END

DATE
FILMED

4-78

DDC



MICROCOPY RESOLUTION TEST CHART
NATIONAL BUREAU OF STANDARDS-1963-A

Measuring instruments: EDM-3 and CIM-3.
 Type of measurement: E and H fields near the slot radiators.
 Frequency \approx 110 MHz; Transmitter power \approx 150 W.

Antenna slot number	E field 5 cm in front of radome		E field 15 cm in front of radome		E field 100 cm in front of radome	
	nJ/m ³	V/m	nJ/m ³	V/m	nJ/m ³	V/m
1	0.40	9.5	0.15	5.8		
2	2.1	22	0.70	12.6		
3	4.6	32	1.7	19.6	0.20	6.7
4	18	64	6.0	37	0.30	8.2
5	24	74	8.8	45	0.60	11.6
6	54	110	18	64	1.2	16.5
7	62	118	23	72	1.8	20
8	83	137	29	81	2.0	21
9	89	142	32	85	2.8	25
10	94	146	32	85	2.4	23
11	81	135	29	81	2.3	23
12	59	115	20	67	1.4	17.8
13	49	105	18	64	1.3	17.1
14	33	86	11	50	0.82	13.6
15	20	67	7.0	40	0.40	9.5
16	6.8	39	2.3	23	0.23	7.2
17	2.7	25	0.90	14.3		
18	0.36	9.0	0.13	5.4		
Antenna slot number	H field 5 cm in front of radome		H field 10 cm in front of radome		H field 15 cm in front of radome	
	mW/cm ²	A/m	mW/cm ²	A/m	mW/cm ²	A/m
1	0.14	0.06				
2	0.65	0.13				
3	2.0	0.23				
4	8.0	0.46				
5	12	0.56	6.0	0.40	3.0	0.28
6	23	0.78	11	0.54	5.0	0.36
7	28	0.86	13	0.59	6.5	0.42
8	38	1.00	16	0.65	8.0	0.46
9	45	1.09	20	0.73	10	0.52
10	45	1.09				
11	35	0.96				
12	30	0.89				
13	28	0.86				
14	17	0.67				
15	8.5	0.47				
16	6.0	0.40				
17	1.8	0.22				
18	0.60	0.13				

Figure 5-15. Field intensity near the antenna of a waveguide localizer Los Angeles.

Measuring instruments: EDM-3 and CIM-3.
 Type of measurement: E and H fields at antenna height.
 Frequency \approx 110 MHz; Transmitter power \approx 150 W.

Distance in front of localizer	E field intensity		H field intensity	
	nJ/M ³	V/m	mW/cm ²	A/m
1 m	2.5	24	0.2	0.073
2 m	2.0	21	0.1	0.052
3 m	1.8	20	0.05	0.036
4 m	0.90	14.3		
5 m	0.85	13.9		
6 m	0.72	12.8		
7 m	0.54	11.0		
8 m	0.44	10.0		
9 m	0.25	7.5		
10 m	0.14	5.6		
11 m	0.10	4.8		
12 m	0.09	4.5		

Figure 5-16. Field intensity as a function of distance in front of a waveguide localizer antenna, Los Angeles.

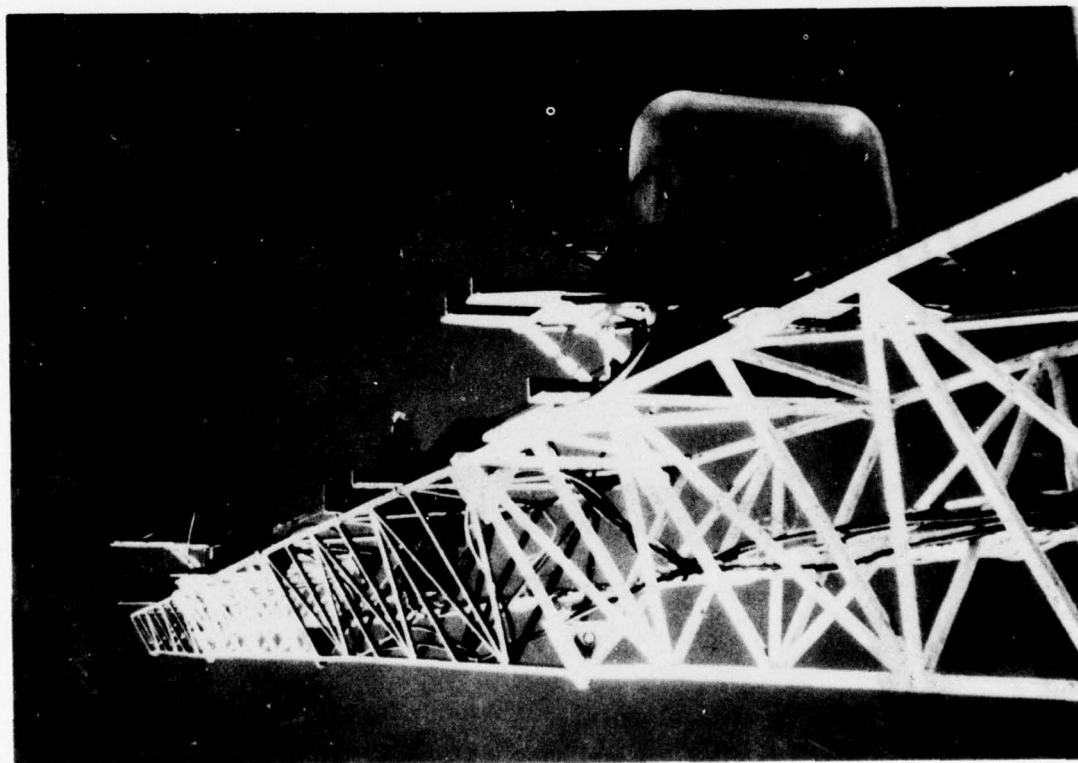


Figure 5-17. Photograph of a UHF localizer antenna installation.

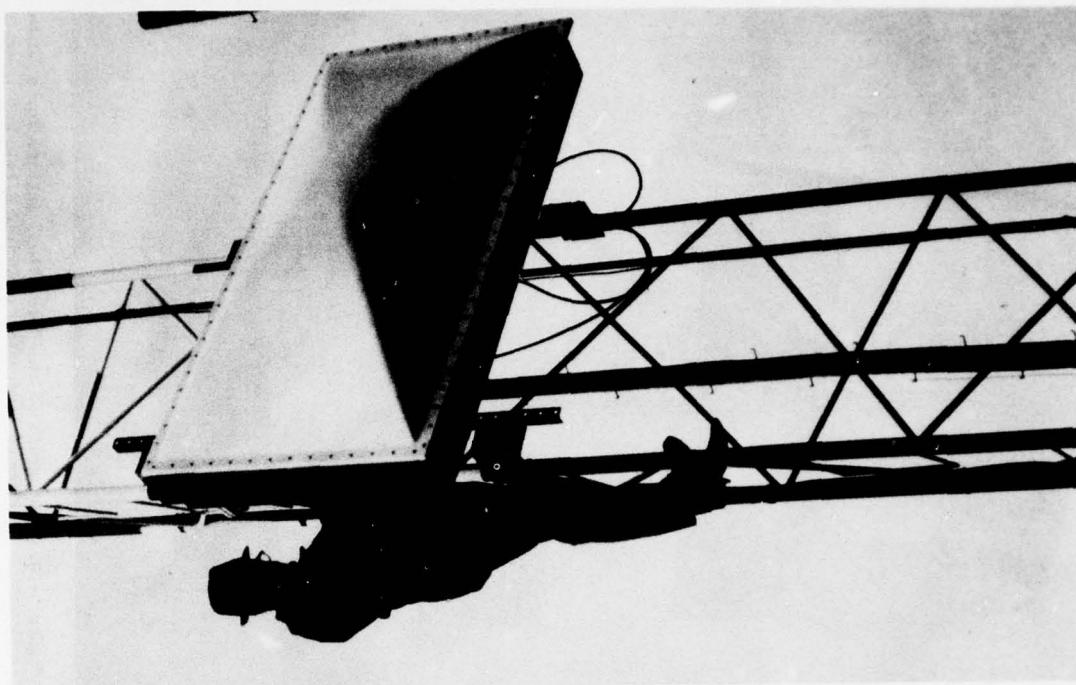


Figure 5-18. Photograph of the lower antenna element in one glide-slope array surveyed.

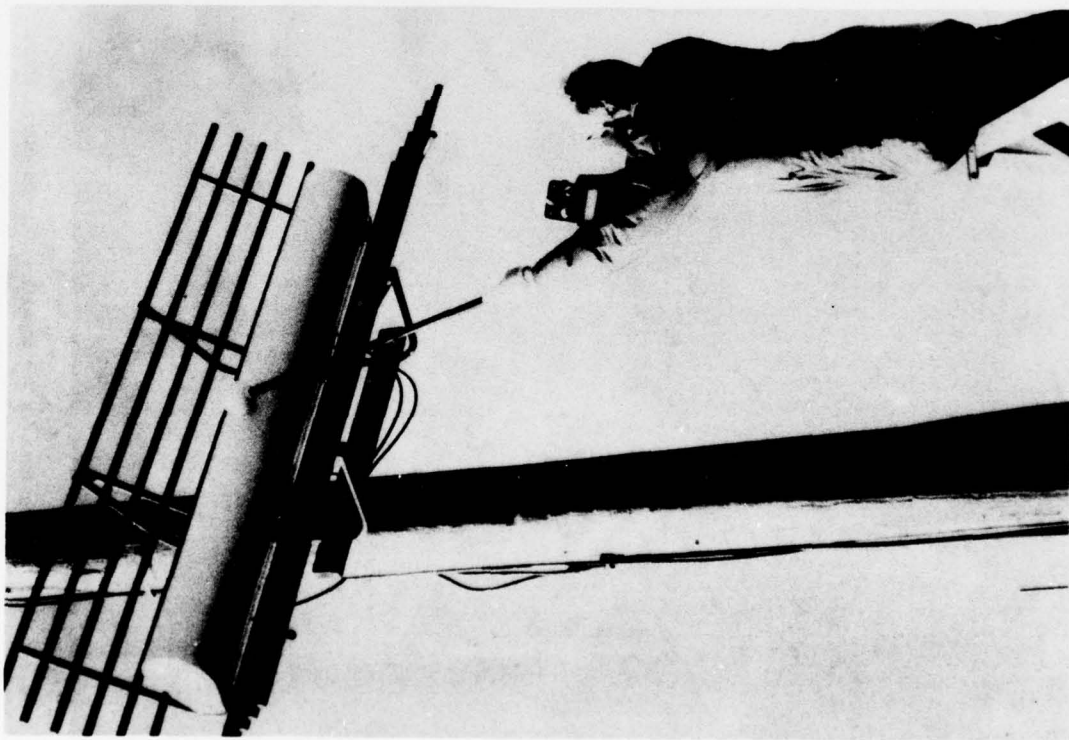


Figure 5-19. Photograph of another type of glide-slope antenna, being surveyed with an EDM-3 radiation monitor.

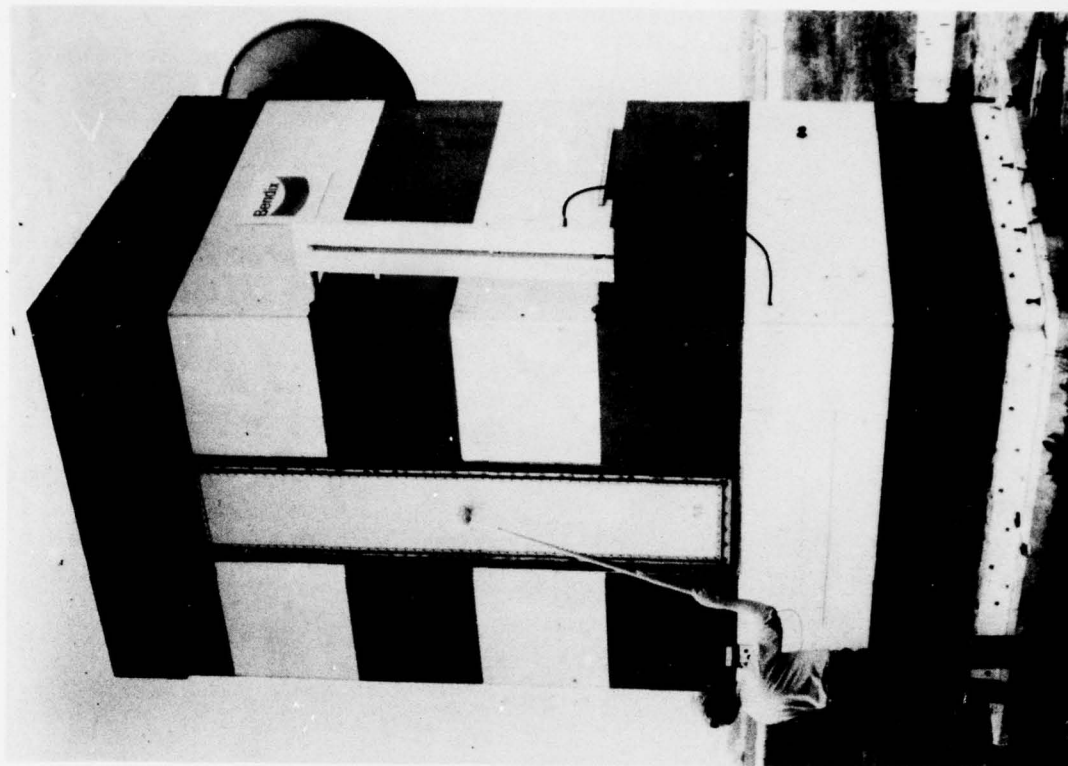


Figure 5-20. Photograph of the "elevation" antenna for a Ku band microwave landing system, El-2 site.

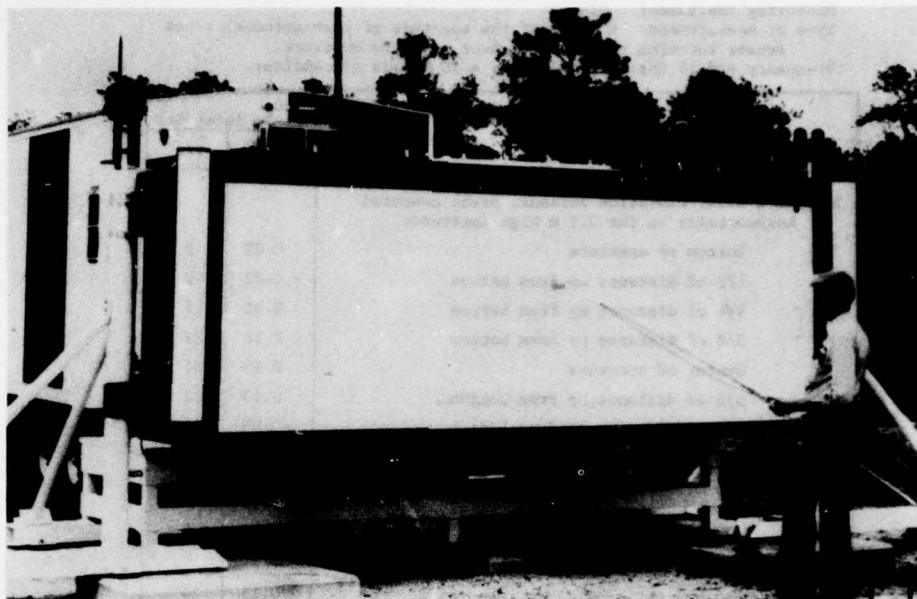


Figure 5-21. Photograph of the "azimuth" antenna for an S band microwave landing system.

Measuring instrument: CIM-1.

Type of measurement: E field at the aperture of the EL-2 elevation antenna, probe sensor touching the plastic sheet over the 0.46 m x 2.44 m aperture (18 in. wide x 8 ft. high).

Frequency = 15.47 GHz; nominal transmitter power = 20 W.

Measurement location	Field intensity	
	mW/cm ²	V/m
I. Probe centered horizontally in the aperture:		
Bottom of aperture	< 0.02	< 9
30 cm (1 ft.) up from bottom of aperture	< 0.02	< 9
60 cm (2 ft.) up from bottom of aperture	0.011	6
90 cm (3 ft.) up from bottom of aperture	0.038	12
Center of aperture	0.05	14
1.5 m (5 ft.) up from bottom of aperture	0.033	11
1.8 m (6 ft.) up from bottom of aperture	0.011	6
2.1 m (7 ft.) up from bottom of aperture	< 0.02	< 9
Top of aperture	< 0.02	< 9
II. Leakage from 1.5 m high slot source mounted on the side of the transmitter building:		
Maximum hot spot 15 cm from top of slot	0.2	27
Midpoint of the vertical slot	0.1	19
Bottom of slot	< 0.02	< 9

Figure 5-22. Field intensity at the antenna aperture of a Ku band microwave landing system, Atlantic City.

Measuring instrument: CIM-1.

Type of measurement: E field at the aperture of each antenna, probe sensor touching the plastic sheet over the aperture.

Frequency = 5.19 GHz; nominal power = 20 W each transmitter.

Measurement location	Field intensity	
	mW/cm ²	V/m
I. EL-1 site, elevation antenna, probe centered horizontally in the 3.7 m high aperture:		
Bottom of aperture	< 0.02	< 9
1/8 of distance up from bottom	< 0.02	< 9
1/4 of distance up from bottom	0.03	11
3/8 of distance up from bottom	0.14	23
Center of aperture	0.15	24
5/8 of distance up from bottom	0.13	22
3/4 of distance up from bottom	0.03	11
7/8 of distance up from bottom	< 0.02	< 9
Top of aperture	< 0.02	< 9
II. EL-1 site, leakage from slot source mounted vertically on side of transmitter building:		
Maximum hot spot 15 cm from top of slot	0.15	24
III. Front azimuth site, probe for hot spots:		
Maximum hot spot near center of aperture	0.12	21
Another hot spot 60 cm from upper left corner		
Corresponding point 60 cm from upper right corner	0.02	9

Figure 5-23. Field intensity at the aperture of two S band antennas for a microwave landing system, Atlantic City.

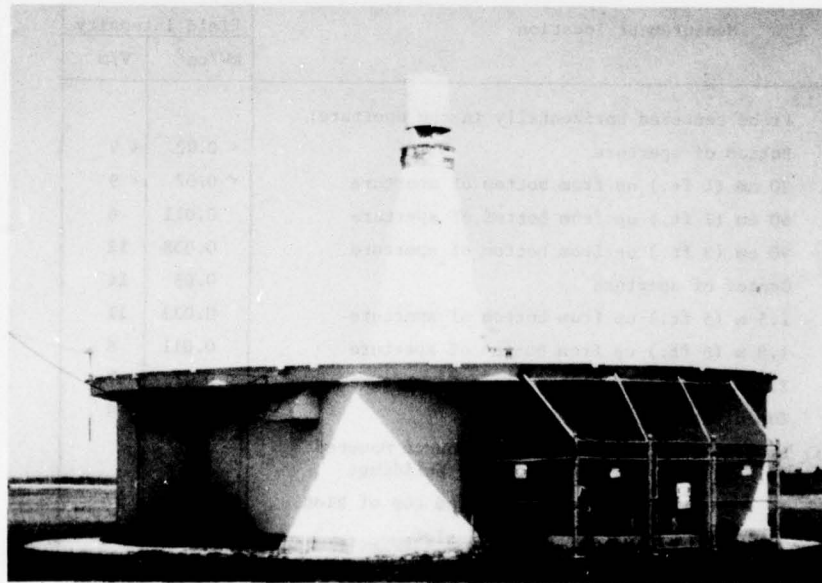


Figure 6-1. Photograph of a VORTAC transmitter building with circular roof, showing the conical tower with enclosed VOR antenna and TACAN radome on top.

Measuring instrument: EDM-IC. Av mode.
 Type of measurement: E field of an Alford Loop VOR antenna, TACAN turned off.
 Frequency = 110.2 MHz; transmitter nominal power = 200 W.
 Note: VOR antenna is located inside the base of the conical tower, about 1.2 m above the roof. Probe held at height of maximum E.

Measurement Location	Field Intensity	
	nJ/m ³	V/m
I. 6 m from the side of the conical tower:		
North side	1.38	18
East side	1.18	16
South side	1.44	18
West side	1.44	18
II. Probe sensor touching the side of the conical tower, electrical rotation of beam turned on (normal):		
North side	20.9	69
Northeast side	20.2	68
East side	20.2	68
Southeast side	20.2	68
South side	18.9	65
Southwest side	19.5	66
West side	20.9	69
Northwest side	20.9	69
III. Probe sensor touching the tower, electrical rotation of beam turned off:		
North side	13.1	54
Northeast side	9.4	46
East side	9.7	47
Southeast side	12.2	52
South side	18.9	65
Southwest side	26.6	78
(Maximum value)	27.9	79
West side	25.3	76
Northwest side	21.6	70
IV. Probing inside of the conical tower: 23 cm from the antenna gap	167	194

Figure 6-2. Field intensity of the VOR signal measured at the antenna height, about 1.2 m above the roof of the VORTAC building, Oklahoma City.



Figure 6-3. Photograph of a Doppler VOR antenna array.

Measuring instrument: EDM-3, Av mode.
 Type of measurement: E field of a Doppler VOR array near the antenna height.
 Frequency = 113.6 MHz; transmitter nominal power = 200 W. power delivered
 to the 50 antenna elements on the outer perimeter \approx 10 W.

Radome number	Electric field strength at given location, V/m			
	20 cm from side of radome, 15 cm above base (max E)	5 cm above top of radome	5 cm from side of radome, 13 cm above base (max E)	5 cm from two adjacent radomes, 8 cm above base (max E)
1	7	6	11	16
2	7	6	12	16
3	8	6	12	16
4	7	6	12	16
5	8	6	12	16
6	7	7	12	17
7	7		12	17
8	8		12	17
9	8	6	12	16
10			12	16
11			12	17
12		6	12	16
13			12	17
14			12	17
15		6	12	16
16			12	16
17			12	16
18		6	12	16
19			12	16
20			12	16
21		6	12	16
22			12	15
23			11	15
24		6	11	15
25			11	15
26			12	15
27		7	11	15
28			11	15
29			11	15
30		6	12	16
31			11	15
32			11	15
33		7	12	15
34			11	16
35			11	16
36		7	11	16
37			11	16
38			11	
39		7	12	16
40			11	
41			11	16
42		7	12	
43			12	16
44			11	
45		7	12	16
46			11	
47			12	16
48		7	11	
49			12	16
50			12	

Figure 6-4. Field intensity near the 50 radomes on the outer perimeter of a Doppler VOR antenna array, Los Angeles.

Measuring instrument: EDM-3.

Type of measurement: Average E field at antenna height within the perimeter of the 50 radomes, about 12 cm above the radome base.

Frequency = 113.6 MHz; transmitter power delivered to the center antenna element = 55 W.

Measurement Location	Field Intensity	
	nJ/m ³	V/m
I. 5 cm from side of center radome, about 12 cm above base for maximum E:		
North side	245	235
Northeast side	45	101
East side	150	184
Southeast side	18	64
South side	230	228
Southwest side	35	89
West side	160	190
Northwest side	18	64
(Top of radome)	.36	9
II. On a north-south line across the center of the antenna array:		
5.7 m north of center radome	0.6	12
5.1 m north of center radome	0.6	12
4.5 m north of center radome	0.7	13
3.9 m north of center radome	0.9	14
3.3 m north of center radome	1.0	15
2.7 m north of center radome	1.7	20
2.1 m north of center radome	2.4	23
1.5 m north of center radome	3.5	28
0.9 m north of center radome	7.5	41
30 cm north of radome surface	14	56
20 cm north of radome surface	30	82
0.9 m south of center radome	8.0	43
1.5 m south of center radome	5.0	34
2.1 m south of center radome	2.5	24
2.7 m south of center radome	1.5	18
3.3 m south of center radome	1.0	15
3.9 m south of center radome	1.0	15
4.5 m south of center radome	0.80	13
5.1 m south of center radome	0.65	12
5.7 m south of center radome	0.60	12

Figure 6-5. Field intensity near the center radome of a Doppler VOR antenna array, Los Angeles.

Measuring instrument: CIM-3.

Type of measurement: Average H field near the VOR antenna radomes.

Frequency = 113.6 MHz; transmitter nominal power = 200 W.

Measurement Location	Field Intensity	
	mG/cm ²	A/cm ²
I. The 50 radomes on outer perimeter:		
5 cm from side of radomes	< 0.1	< .05
5 cm above top of radomes	< 0.1	< .05
II. Near the single center radome:		
Top of radome	0.72	0.14
50 cm above base, north or south side	1.0	0.16
50 cm above base, east or west side	1.0	0.16
Base of radome, all four sides	5.0	0.36
Max value around base of radome	6.0	0.40
5 cm from radome support pole, midway between radome base and ground	1.5	0.20
Beneath radome, 5 cm below surface, maximum value about 25 cm from center:		
(a) North side of support pole	40	1.0
(b) Northeast side of pole	60	1.3
(c) East side of pole	40	1.0
(d) Southeast side of pole	60	1.3
(e) South side of pole	40	1.0
(f) Southwest side of pole	60	1.3
(g) West side of pole	40	1.0
(h) Northwest side of pole	60	1.3

Figure 6-6. Magnetic field intensity near a Doppler VOR antenna array.

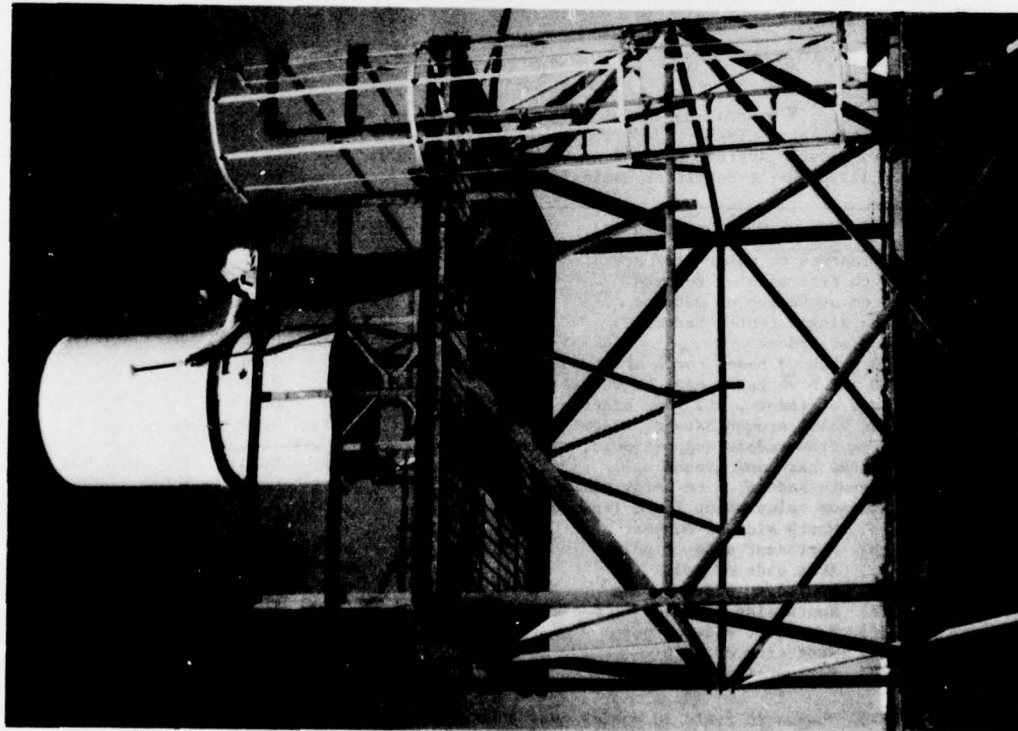


Figure 6-7. Photograph of a TACAN antenna mounted on a tower, showing an operator making preliminary checks at the side of the radome.

Measuring instrument: CIM-1, fast time constant.
Type of measurement: Average E field, modulation turned on.
Frequency = 983 MHz; transmitter power = 130 W Av = 6.5 kW pk.

I. Measurements near corner of tower, 1.9 m from side of radome:				II. Measurements near center of west side of tower, 1.1 m from side of radome:			
Height above deck of tower, cm	Field intensity mW/cm ²	Field intensity V/m	Height above deck of tower, cm	Field intensity mW/cm ²	Field intensity V/m	Height above deck of tower, cm	Field intensity mW/cm ²
20	< .01	< 6	20	.01	6	20	.01
40	< .01	< 6	40	.01	6	40	.01
60	.01	6	60	< .01	< 6	60	< .01
80	.01	6	80	< .01	< 6	80	< .01
100	.01	6	100	.015	8	100	.015
120	.015	8	120	.01	6	120	.01
140	.015	8	140	.015	8	140	.015
160	.01	6	160	.03	11	160	.03
180	.01	6	180	.02	9	180	.02
200	.02	9	200	.015	8	200	.015
220	.03	11	220	.05	14	220	.05
240	.07	16	240	.14	23	240	.14
260	.25	31	260	.40	39	260	.40
280	.45	41	280	.65	49	280	.65
285 (max)	.475	42	285 (max)	.67	50	285 (max)	.67
300	.40	39	300	.42	40	300	.42
320	.25	31	320	.30	34	320	.30
340	.20	27	340	.30	34	340	.30
III. On a horizontal line between side of radome and edge of tower:				Field intensity measured on a tower by the TACAN Academy building, Oklahoma City.			
Distance from side of radome, cm	Field intensity mW/cm ²	Field intensity V/m	Height above tower deck for max field, cm	Field intensity mW/cm ²	Field intensity V/m	Height above tower deck for max field, cm	Field intensity mW/cm ²
5			285	3.7	118	285	3.7
10			284	3.4	113	284	3.4
20			291	3.1	108	291	3.1
30			295	2.4	95	295	2.4
40			291	1.9	85	291	1.9
50			296	1.5	75	296	1.5
60			292	1.3	70	292	1.3
70			277	.93	59	277	.93
80			277	.73	52	277	.73
90			277	.70	51	277	.70
100			276	.70	51	276	.70
110			276	.67	50	276	.67
120			280	.67	50	280	.67
130			280	.63	49	280	.63
140			280	.60	48	280	.60

Figure 6-8. Field intensity of the ground TACAN signal measured on a tower by the TACAN Academy building, Oklahoma City.

Measuring instrument: CIM-1.
 Type of measurement: Average E field, modulation turned on.
 Frequency = 1 GHz; transmitter nominal power = 200 W.

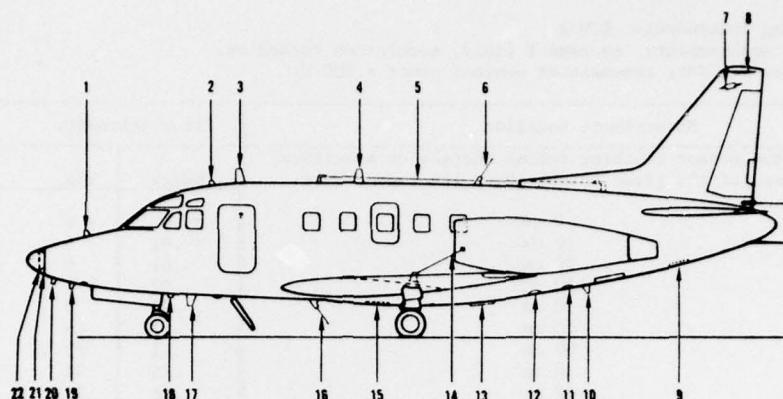
Measurement Location		Field Intensity	
I. Probe sensor touching radome surface on a vertical line, at the given height above the radome base:		mW/cm ²	V/m
0 cm		< .01	< 6
10 cm		< .01	< 6
20 cm		.01	6
30 cm		.02	9
40 cm		.02	9
50 cm		.025	10
60 cm		.11	20
70 cm		.15	24
80 cm		.16	25
90 cm		.18	26
100 cm		.13	22
110 cm		.03	11
120 cm		< .01	< 6
130 cm		< .01	< 6
II. Field intensity as a function of horizontal distance from the radome side, probe height adjusted for maximum indication:			
Horizontal distance from radome surface	Vertical height above radome base	mW/cm ²	V/m
5 cm	90 cm	.16	25
10 cm	90 cm	.13	22
20 cm	90 cm	.11	20
30 cm	95 cm	.09	18
40 cm	95 cm	.07	16
50 cm	75 cm	.06	15
60 cm	80 cm	.05	14
70 cm	80 cm	.045	13
80 cm	80 cm	.04	12
90 cm	80 cm	.04	12
100 cm	80 cm	.03	11
110 cm	80 cm	.025	10
120 cm	80 cm	.025	10
130 cm	80 cm	.02	9

Figure 6-9. Field intensity of a ground TACAN signal measured near the antenna, Los Angeles.

Measuring instrument: Commercial x-ray monitor with a nominal measurement range of 0.3 to 300 mR/hr.

TACAN unit number	Transmitter cabinet doors:	Front or back of cabinet:	Measurement location	Radiation intensity, mR/hr
1	Closed	Front	Vent screen near Klystron tube	< 0.2
		Back	Vent screen behind the rectifier tubes, hot spot 30 cm from bottom and 30 cm from left side of screen.	0.2
1	Open	Front	Vent screen near Klystron	0.5
		Back	Vent screen behind rectifiers	18
2	Open	Front	Vent screen near Klystron	0.1
		Back	Vent screen behind rectifiers	1.0
3	Open	Front	Vent screen near Klystron	0.3
		Back	Vent screen behind rectifiers	5.0

Figure 6-10. Intensity of X-rays near a TACAN transmitter rack.



1. TACAN 1 (L-band)
2. TACAN 2 (L-band)
3. VHF/UHF communication (system No. 1)
4. VHF/UHF communication (system No. 3)
5. ADF sensing (LFI)
6. Emergency locator transmitter
7. VOR/LOC (No. 3 and 4)
8. VOR/LOC (No. 1 and 2)
9. UHF/ADF
10. ATC (L-band)
11. Radio altimeter transmit
12. Radio altimeter receive
13. Marker beacon (DMN 273)
14. HF communication
15. ADF loop (LFI)
16. Emergency locator receiver
17. VHF/UHF communications (system No. 2)
18. DME (L-band)
19. TACAN 2 (L-band)
20. TACAN 1 (L-band)
21. Glide/slope
22. Weather radar

Figure 6-11. Locations of the navigation, communication and radar antennas on a Sabre 75A aircraft.

Measuring instrument: CIM-1.

Type of measurement: Average E field of the pulsed transmissions of airborne TACANS.
Frequency ≈ 1.1 GHz; transmitter nominal pulse-peak power = 500 W.

Transmitter in use	Antenna (See fig. 6-12)	Measurement location	Field intensity	
			mW/cm ²	V/m
TACAN 1	No. 1	Probe sensor touching (5 cm distance) the top edge of the blade antenna	0.04	12
TACAN 1	No. 1	Touching side of antenna	0.10	19
TACAN 1	No. 20	Touching bottom edge of antenna	0.05	14
TACAN 1	No. 20	Touching side of antenna and bottom of fuselage simultaneously	0.15	24
TACAN 1	No. 20	Touching back edge of antenna	0.16	25
TACAN 1	No. 20	Upper surface of sensor 5 cm below the bottom edge of the antenna	0.03	11
TACAN 1	No. 20	Sensor surface 5 cm in front of the edge of the antenna	0.06	15
TACAN 2	No. 19	Touching bottom edge of antenna	0.45	41
TACAN 2	No. 19	Touching side of antenna and bottom of fuselage simultaneously	1.3	70
TACAN 2	No. 19	Touching back edge of antenna	0.30	34
TACAN 2	No. 19	Upper surface of sensor 5 cm below the bottom edge of the antenna	0.08	17
TACAN 2	No. 19	Sensor surface 20 cm in front of the edge of the antenna	0.10	19
DME	No. 18	Touching bottom edge of antenna	0.30	34
DME	No. 18	Touching side of antenna and bottom of fuselage simultaneously	1.3	70
DME	No. 18	Touching back edge of antenna and bottom of fuselage	0.80	55
DME	No. 18	Touching front edge of antenna and bottom of fuselage	1.0	61
DME	No. 18	Touching bottom of fuselage but sensor surface 5 cm behind edge of antenna	0.50	43
DME	No. 18	Touching bottom of fuselage but sensor surface 5 cm in front of antenna	0.12	21

Figure 6-12. Field intensities near the airborne TACAN antennas on a Sabre Jet aircraft, Oklahoma City.

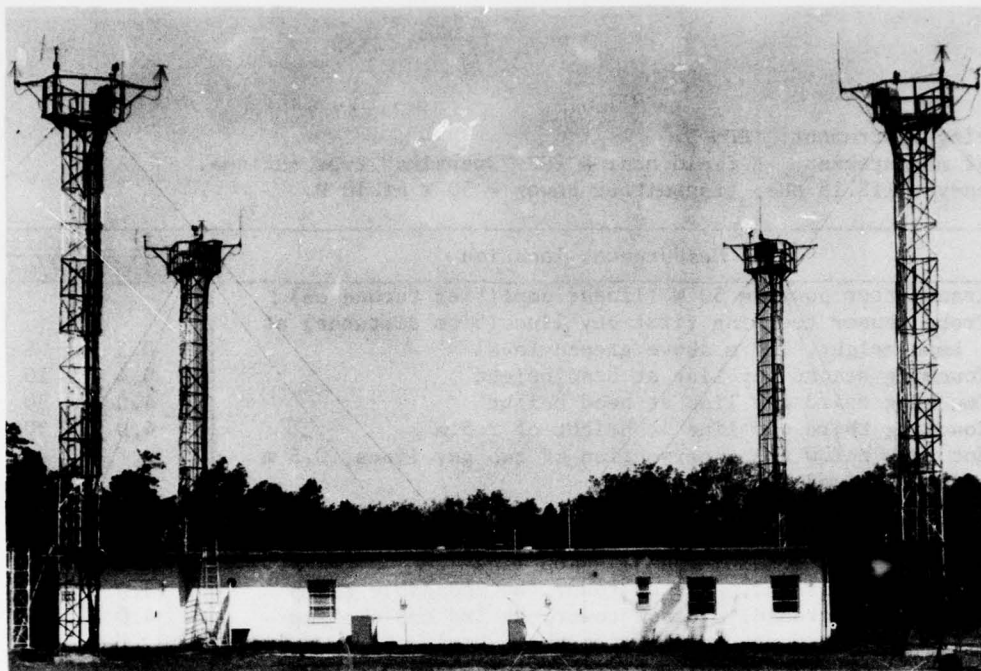


Figure 7-1. Photograph of VHF antenna towers and transmitter building at a communication antenna site, NAFEC, near Atlantic City.

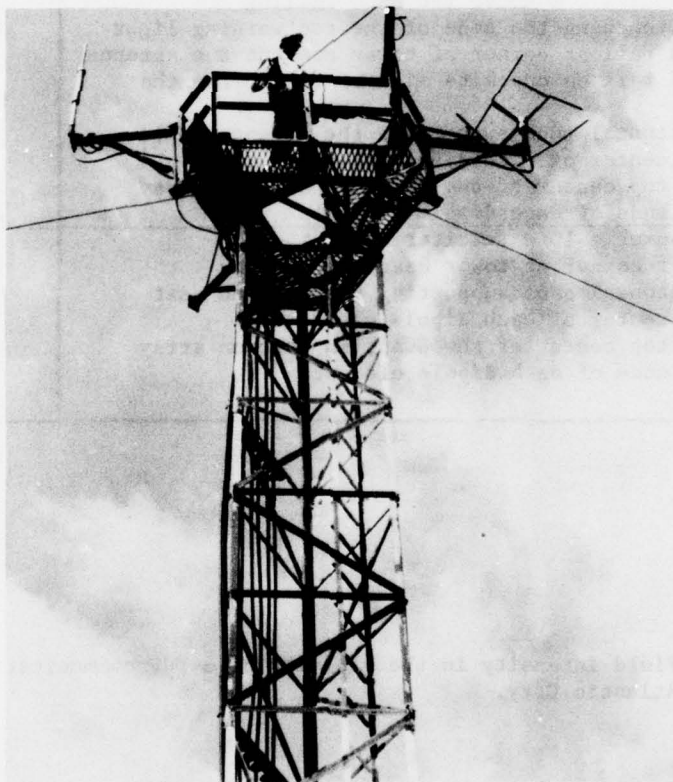


Figure 7-2. Closer view of a VHF communication antenna showing the "Swastika" type of antenna surveyed.

Measuring instrument: EDM-3.

Type of measurement; E field near a VHF "Swastika" type antenna.

Frequency = 118.15 MHz; transmitter power = 50 W or 10 W.

Measurement location	Field intensity	
	nJ/m ³	V/m
I. Transmitter power = 50 W (linear amplifier turned on) :		
Probe sensor touching first guy line (5 cm distance) at head height, 1.7 m above ground level	0.3	8
Touching second guy line at head height	0.4	10
Touching third guy line at head height	4.0	30
Touching third guy line at height of 2.5 m	4.0	30
Hot spot below the intersection of two guy lines, 0.5 m above ground level	6.0	37
3.3 m above ground level, center of tower area	0.3	8
3.3 m above ground, side of tower, touching the 1st clamp holding the coaxial transmission lines	5.0	34
6.3 m above ground, side of tower, by 2nd cable clamp	3.0	26
9.4 m above ground, side of tower, by 3rd cable clamp	4.0	30
9.4 m above ground, holding the probe horizontally outward from the tower, beneath the Swastika antenna	0.1	5
12.4 m above ground, side of tower, by 4th cable clamp	2.0	21
Head height (1.7 m) above center of tower platform, 17.2 m above ground level	4.0	30
Head height at corner of tower nearest to the transmitting antenna, about 0.6 m above the hand railing	5.5	35
Probe sensor touching the side of the red warning light	2.0	21
Touching hand rail at corner of tower nearest the antenna	25	75
Touching hand rail on opposite side of tower from the antenna	20	67
Touching horizontal boom supporting the antenna mast	30	82
Touching the center of each dipole element	50	106
Touching the top center of the Swastika antenna array	20	67
Touching the ends of each dipole element	190	207
II. Transmitter power = 10 W (exciter only) :		
Head height at corner of tower near the antenna	1.5	18
Touching horizontal boom supporting the antenna mast	6.0	37
Touching the center of each dipole element	12	52
Touching the top center of the Swastika antenna array	5.0	34
Touching the ends of each dipole element	60	116

Figure 7-3. Field intensity in the vicinity of a VHF communication antenna, Atlantic City.

Measuring instrument: CIM-3.

Type of measurement: H field near a VHF "Swastika" type antenna.

Frequency = 118.15 MHz; transmitter power = 50 W.

Measurement location	Field intensity	
	mW/cm ²	A/m
3.3 m above ground level, center of tower area	< 0.1	< 0.05
Head height (1.7 m) above center of tower platform, 17.2 m above ground level	0.2	0.07
Probe sensor touching the side of the red warning light	0.2	0.07
Touching horizontal boom supporting the antenna mast	4.0	0.33
Touching the center of each dipole element	15	0.63
Touching the top center of the Swastika antenna array	3	0.28
Touching the ends of each dipole element	10	0.52

Figure 7-4. Magnetic field intensity near a VHF communication antenna, Atlantic City.

Measuring instrument: EDM-3.

Type of measurement: E field of VHF and UHF transmissions from airborne transceivers.

Frequency = 123 MHz or 278 MHz; transmitter power = 25W (VHF) or 5 W (UHF).

Transmitter in use	Antenna (See fig. 6-12)	Measurement Location	Field intensity	
			nJ/m ³	V/m
VHF	No. 3	Probe sensor touching (5 cm distance) the top edge of the blade antenna	2000	672
VHF	No. 3	Maximum hot spot along top edge of antenna, located near front of blade	2600	766
"	"	Touching front edge of antenna and fuselage	600	368
"	"	Touching rear edge of antenna and fuselage	300	260
"	"	30 cm above top edge at center of antenna	100	150
"	"	90 cm above top edge at center of antenna	5	34
"	"	30 cm behind rear edge of antenna, at same height as center of antenna	40	95
"	"	30 cm in front of front edge of antenna, at same height as center of antenna	90	143
"	"	Head height (1.7 m) above upper step at entry door of fuselage	6	37
"	"	2.1 m above upper step at entry, which is 1 m horizontally from the side of the antenna	6	37
UHF	No. 3	Touching top edge (center) of antenna	150	184
"	"	30 cm above top edge of antenna	10	48
"	"	15 cm behind rear edge of antenna, at same height as center of antenna	20	67
"	"	15 cm in front of front edge of antenna, at same height as center of antenna	20	67
VHF	No. 17	Touching rear edge of antenna and fuselage simultaneously	300	260
"	"	Touching front edge of antenna and fuselage simultaneously	400	301
"	"	Surface of sensor 7.5 cm from side and middle of the antenna	3000	823

Figure 7-5. Field intensity near the VHF/UHF antennas on a Sabre 75A aircraft, Oklahoma City.

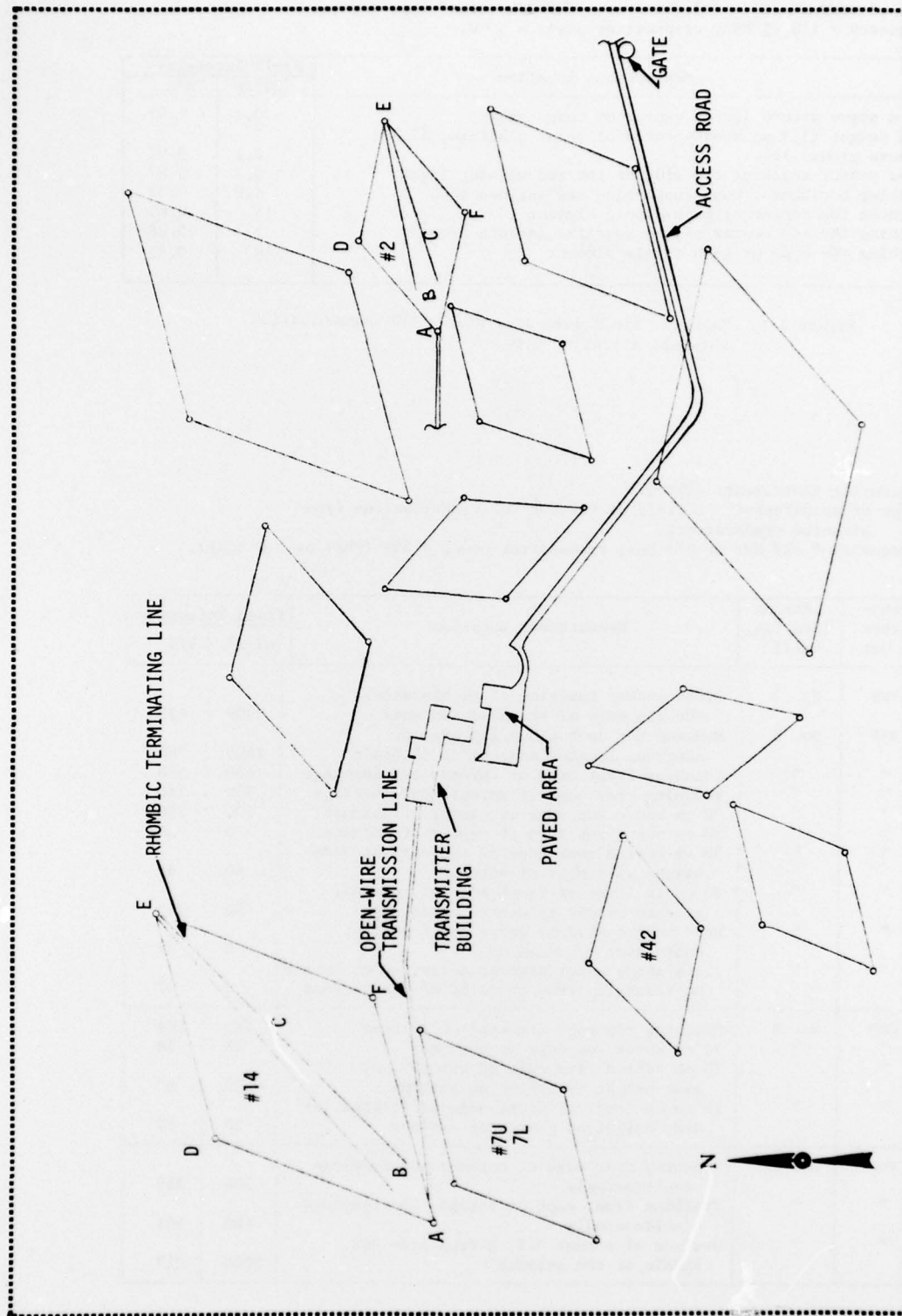


Figure 7-6. Sketch of a portion of the transmitting site and rhombic antenna layout on Long Island, used for HF transoceanic transmissions.

Measuring instrument: EDM-3 and EDM-4.

Type of measurement: Unintended leakage E fields.

Measurement Location	Field Intensity	
	nJ/m ³	V/m
I. Near the transmitter cabinet for rhombic antenna No. 42, 16.28 MHz:		
Probe sensor 60 cm below center of horizontal open-wire transmission line, near the transmitter cabinet	150	184
25 cm below the open-wire line	3000	823
Leakage from transmitter cabinet, crack along front vertical edge, about 1.8 m above floor	175	199
Touching (5 cm spacing) the upper right rear corner of transmitter cabinet, hot spot 45 cm below the open-wire line	200	213
Touching center of viewing window by the transmitter tuner	150	184
Front surface of sensor sphere 5 cm from center of viewing window	16.7	61
Front surface of sensor 15 cm from center of viewing window	1.67	19
Head height in transmitter room, 3 m in front of trans- mitter cabinet, directly beneath the open-wire line	3	26
II. Near the transmitter cabinet for rhombic antenna No. 7U, 13.27 MHz:		
Touching the RG-17A/U coaxial cable behind transmitter cabinet, hot spot of the standing-wave pattern	1000	475
Sensor surface 2.5 cm from the neutralizing capacitor above the transmitter cabinet	1000	475
III. Desk area near the transmitter cabinets:		
Touching top to telephone on technician's desk	5.0	34
Touching bottom end of wire antenna near broadcast-band receiver. (Far end of wire at a tower near the transmitter building)	40	95
Position of desk chair, 1 m above floor level	-	2

Figure 7-7. Intensity of stray fields inside the HF transmitter building, Long Island.

Measuring instrument: EDM-3.

Type of measurement: E fields outside of transmitter building.

Frequency = 8.11 MHz; transmitter power = 15 kW.

Measurement Location	Field Intensity	
	nJ/m ³	V/m
I. Beneath the open-wire transmission line, just outside of transmitter building:		
(a) 3.7 m above ground level	20	67
(b) head height (1.7 m) above ground	11	50
(c) Sensor trouching metal cover over building vent, at head height	18	64
II. 100 m from transmitter building, toward antenna #14, where the transmission line is about 8 m high:		
(a) Beneath center of open-wire line, 3.7 m above ground	5	34
(b) Beneath center of open-wire line, head height	2	21
(c) Touching guy wire for transmission line pole, 3.7 m above ground	2000	672
(d) Touching guy wire for transmission line pole, head height	1600	601
III. 150 m from transmitter building where the transmission line is about 5 m high:		
(a) 30 cm beneath center of open-wire line, 3.7 m above ground	3000	823
(b) Beneath the line at head height	10	48
IV. Near point A of antenna number 14 in figure 7-6, by last transmission line pole before the line ascends vertically to the rhombic antenna:		
(a) Touching a guy wire of open-wire line pole, 3.7 m above ground	300	260
(b) Touching guy wire near gound level	10	48
(c) Touching guy wire midway between the above two points	7	40
V. Point B of antenna 14, near gounded end of terminating line for the antenna:		
(a) 10 cm from grounded end of one wire, 10 cm above ground	167	194
(b) 10 m from grounded end of terminating line, 25 cm to one side where the wire is about 25 cm above ground	167	194
(c) 30 m from grounded end of terminating line, 30 cm to one side of line	167	194
VI. Midway between points A and D of antenna 14:		
(a) 3.7 m above ground	3	26
(b) Head height	2	21
VII. Near point D of antenna 14:		
(a) Touching bottom end of counter weight wire, about 1.5 m above gound	1400	562
(b) Toucing guy wire bolt for rhombic pole, about 2.4 m above ground	250	238

Figure 7-8. Field intensity near the rhombic antenna and transmission line for antenna number 14, Long Island.

Measuring instrument: EDM-3.

Type of measurement: E fields outside of transmitter building.

Frequency = 12.20 MHz; transmitter power \approx 15 kW.

Measurement Location	Field Intensity	
	nJ/m ³	V/m
I. Near point A of antenna number 2 in figure 7-6:		
(a) Beneath the open-wire line near the rhombic input, head height	2	21
(b) Search for a hot spot 3.7 m above ground	175	199
(c) Sensor touching a guy wire for the last transmission line pole, head height	20	67
II. Near point B of antenna 2, grounded end of terminating line:		
(a) Bottom of sensor 17 cm above a terminating wire	167	194
(b) Bottom of sensor 45 cm above a terminating wire	16.7	61
(c) Bottom of sensor 95 cm above a terminating wire	1.67	19
(d) Sensor touching ground, 20 cm from end of a terminating wire	167	194
III. Midway between points A and B of antenna 2:		
(a) 3.7 m above ground	0.2	7
(b) Head height	0.1	5
IV. Point C of antenna 2, beneath center of rhombic antenna. (The terminating wires are about 40 cm apart and 15 cm above ground at this point):		
(a) 3.7 m above ground	0.2	7
(b) Head height	0.6	12
V. Midway between points C and D of antenna 2:		
(a) 3.7 m above ground	0.27	8
(b) Head height	0.30	8
(c) Sensor touching ground	0.40	10
VI. Point D of antenna 2:		
(a) Touching bottom end of counterweight cable, which is 1.8 m above ground	100	150
(b) Maximum hot spot near bottom end of counterweight cable	125	168
(c) Touching guy line for antenna post near D, at head height	40	95
VII. Point E of antenna 2, near bottom end of vertical line at terminating end of rhombic antenna, which is about 1 m above ground:		
(a) 45 cm horizontally from bottom end of vertical line	167	194
(b) 1 m horizontally from bottom end of vertical line	16.7	61
(c) 2.5 m horizontally from bottom end of vertical line	1.67	19

Figure 7-9. Field intensity near the rhombic antenna and transmission line for antenna number 2, Long Island.

Measuring instrument: CIM-3.

Type of measurement: H field at an HF transmitting site.

Frequency = 12.20 MHz; transmitter power \approx 15 kW.

Measurement Location	Field Intensity	
	mW/cm ²	A/m
I. Inside the transmitter building, ground floor:		
(a) Surface of probe sensor 2.5 cm from neutralizing capacitor above the transmitter cabinet	50	1.15
(b) Behind transmitter cabinet, near hot spot of standing wave on RG-17A/U coaxial cable:		
(1) Sensor touching side of coaxial cable	100	1.63
(2) 14 cm from side of cable	10	0.52
(3) 33 cm from side of cable	1	0.16
(4) 90 cm from side of cable	0.1	0.05
(c) Touching side of coaxial cable near the antenna patch panel	1	0.16
II. Feeder room in attic of transmitter building:		
(a) Touching hot spot on coaxial line, between floor and roof of attic, near head height	20	0.73
(b) 1 m below open-wire line for antenna 25 L, near head height	10	0.52
(c) Floor of attic, average field value	1	0.16
III. Outside of transmitter building, toward antenna number 2:		
(a) Touching coaxial cable on wooden pole at input to rhombic antenna, near the antenna matching transformer	2	0.23
(b) Directly beneath open-wire line at point where the line is about 4.5 m above ground:		
(1) 2.4 m above ground level	0.2	0.07
(2) head height	< 0.05	< 0.04
(c) Touching guy wire on final transmission line pole before rhombic antenna input, at head height	5	0.36
(d) Point B of antenna number 2, 15 cm above grounded end of terminating line	10	0.52
(e) Touching guy line of adjacent rhombic antenna pole, 1 m above ground	25	0.81
(f) Midway between points C & D of antenna 2:		
(1) 2.5 m above ground	0.1	0.05
(2) head height	0.05	0.04
(g) Point D of antenna 2, touching bottom end of counter-weight cable, 1.8 m above ground	5	0.36
(h) Point E, near bottom of vertical line at terminating end of rhombic antenna, which is about 1 m above ground:		
(1) 15 cm horizontally from line	50	1.15
(2) 30 cm horizontally from line	10	0.52
(3) 1 m horizontally from line	1	0.16
(4) 2 m horizontally from line	0.1	0.05

Figure 7-10. Magnetic field intensity near the transmitter, transmission line and antenna number 2, Long Island.